Universidade de Aveiro

Ano 2020

João António Abreu Pereira

Characterization of dental cements by computed tomography techniques

Caracterização de cimentos dentários através de técnicas de tomografia computadorizada

(1) 2021

Universidade de Aveiro

Ano 2020

João António Abreu Pereira

Characterization of dental cements by computed tomography techniques

Caracterização de cimentos dentários através de técnicas de tomografia computadorizada

Tese apresentada à Universidade de Aveiro para cumprimento dos requisites necessários à obtenção do grau de Mestre em Materiais e Dispositivos Biomédicos, realizada sob orientação científica da Professora Doutora Maria Helena Figueira Vaz Fernandes, Professora Associada do Departamento de Engenharia dos Materiais e Cerâmica, coorientação da Professora Doutora Maria Elizabete Jorge Vieira Costa, Professora Associada no Departamento de Engenharia dos Materiais e Cerâmica, orientação sob o programa Erasmus do Professor Doutor Håvard Jostein Haugen, Professor Associado no Instituto de Odontologia Clínica da Universidade de Oslo e coorientação sob o programa Erasmus do Doutor Liebert Parreiras Nogueira, Engenheiro Senior no Instituto de Odontologia Clínica da Universidade de Oslo.

Dedico esta dissertação aos meus avós, Manuel Abreu e Reisinanda Abreu, que perdi durante esta tão importante etapa da minha vida.

o júri

presidente

Prof. Doutor João André da Costa Tedim
professor Auxiliar em Regime Laboral da Universidade de Aveiro

Doutor Nuno André Fraga de Almeida
responsável de Laboratório, Valmet Portugal

Prof. Doutor Maria Helena Figueira Vaz Fernandes
professor associado da Universidade de Aveiro

agradecimentos / acknowledgments

Esta tese representa a conclusão de uma etapa muito importante na minha vida e uma viagem, em termos de conhecimento, que só foi exequível com o ajuda de todos os que me acompanham diariamente. Num ano como este, com tanto de estranho como de trabalhoso, o desafiante alcançar desta etapa torna-se muito mais saboroso. Assim, gostaria de agradecer a todos os que se cruzaram comigo durante esta etapa, em Aveiro e na Noruega, aonde deixo amigos e momentos que nunca vou esquecer.

-Às minhas orientadoras, a Professora Maria Helena Fernandes e a Professora Elizabete Costa, que durante todo este processo me apoiaram e me fizeram lutar contra todas as inquietudes que foram tornando a conclusão deste cada vez mais possível.
-To my supervisors in Norway, to Håvard J. Haugen and to Liebert J. Nogueira for all the support and all the knowledge that have been passed to me during my stay in Oslo.
-Aos meus pais, Manuel e Filomena, por sonharem comigo, por sofrerem comigo, por sorrirem comigo e por sempre acreditarem que os sonhos só são sonhos até ao dia em que o esforço e a dedicação os tornarem realidade. Obrigado especialmente por me ensinarem a nunca desistir, um ensinamento que levo para a vida e que aplico em tudo o que faço.
- Aos meus irmãos, Tatiana e Diogo, e ao meu outro irmão Telmo, obrigado pela vossa presença constante e por todos os ensinamentos que me foram passando ao longo destes 24 anos. Obrigado pela vossa amizade e companheirismo.
-Aos meus avós de quem tantas saudades tenho, um profundo e eterno obrigado pelo amor sem medida que sempre recebi.
-A toda a minha restante família, por todo o apoio que sempre me prestaram e por me fazerem sentir especial em vos ter.
-À Mari Carmen, por ter sido sempre um pilar fantástico durante esta etapa e por toda a calma e amor que trouxe à minha vida. Tornaste os meus dias melhores e muito mais fáceis. Um obrigado especial a ti.
-A todos os meus amigos, de Portugal, de Espanha, da Noruega e do mundo, um muito obrigado a todos por me relembrarem que mesmo nestas alturas, é importante sentir-vos, mesmo que à distância.

E por fim, e uma vez mais, a todos, um muito e sincero...

...Obrigado! Gracias! Thank you!

palavras-chave

nano-CT, micro-CT, cimentos, porosidade, silicato tricálcio, biovidro, nanopartículas de prata, obturação, odontologia.

resumo

Hoje em dia, os cimentos dentários fazem parte dos materiais fundamentais em diversos tratamentos dentários, com o intuito de resolver problemas geralmente relacionados com infeções bacterianas que ocorrem na dentição e que precisam de uma restauração adequada que consiga manter a integridade dessa mesma dentição. O cimento dentário é fundamental em tratamentos de canais radiculares (muitas vezes chamada de desvitalização dentária), e tem como objetivo principal impedir a ocorrência de uma segunda infeção. Desta forma, é necessário que os cimentos utilizados vedem todo o espaço entre o sistema de canais radiculares e os tecidos circundantes de maneira a não permitir a passagem de microorganismos. É também importante que os cimentos apresentem propriedades antimicrobianas. No entanto, esta capacidade dos materiais utilizados na produção dos cimentos acaba por se deteriorar com a passagem do tempo, tornando se difícil a tarefa de inibir uma infeção secundária. A porosidade dos cimentos está diretamente ligada à formação dos biofilmes; quanto mais reduzida esta for, menor será a possibilidade da entrada de bactérias no interior destes, o que torna relacionável a percentagem de porosidade com a probabilidade de formação de um biofilme bacteriano responsável por lesões como a periodontite apical pós-tratamento.

A micro-CT, uma tecnologia não-destrutiva (NDT), foi a técnica escolhida para a análise dos cimentos dentários através do Skyscan 2211, e permitiu um estudo cuidado da porosidade por todo o volume das amostras. Esta técnica tornou possível não só a análise da porosidade inerente em cada um dos cimentos dentários analisados, mas também disponibilizou informação de enorme relevo relativamente às dimensões dos poros presentes em cada amostra.

keywords nano-CT, micro-CT, cements, porosity, tricalcium silicate, silver nanoparticles, obturation, dentistry.

abstract Nowadays, dental cements are part of the fundamental materials in several dental treatments, in order to solve problems usually related to bacterial infections that occur in the dentition and that need an adequate restoration that can maintain the integrity of that same dentition. Dental cement is essential in root canal treatments (often called dental devitalization), and its main objective is to prevent the occurrence of a second infection, so it is necessary that the cements used seal the entire space between the canal system roots and the surrounding tissues so as not to allow the passage of microorganisms. It is also important that the cements have antimicrobial properties, however, this capacity of the materials used in the production of the cements ends up deteriorating with the passage of time, making the task of inhibiting a secondary infection difficult. The porosity of cements is directly linked to the formation of these biofilms, the smaller this is, the less the possibility of bacteria entering the interior, which makes the percentage of porosity related to the probability of formation of a bacterial biofilm responsible for injuries such as post-treatment apical periodontitis. Micro-CT, a non-destructive technology (NDT), was the technique chosen for the analysis of dental cements using Skyscan 2211 and allowed for a careful study of porosity throughout the sample volume. This technique made possible not only the analysis of the porosity inherent in each of the dental cements analyzed, but also provided information of enormous importance regarding the dimensions of the pores present in each sample.

Index

List of Figures

Fig.19 – Comparison of total porosities obtained on the surfaces and in the bulks of every type of samples after 1 day of maturation in FBS and in mQ water

Fig.20 – Comparison of total porosities obtained on the surfaces and in the bulks of every type of samples after 7 days of maturation in FBS and in mQ water

Fig.21 – Comparison of total porosities obtained on the surfaces and in the bulks of every type of samples after 28 days of maturation in FBS and in mQ water

Fig.22 - Image of a sample of BG10_FBS with the identification of the different volumes analyzed. All the samples were divided in these different volumes with the objective of understanding how porosity varies.

Fig.23 – Total porosities obtained on the base of the bulk of every type of samples for all the maturation periods (1 day, 7 days and 28 days)

Fig.24 – Total porosities in all the volumes analyzed in samples of BG10_FBS and BG10_W for maturation periods of 1 day, 7 days and 28 days. Sequentially, from left to right: surface porosities (shades of blue), average total porosity (shades of orange), base of bulk (shades of yellow), middle of the bulk (shades green) and final of bulk (shades of red).

Fig.25 – Total porosities in all the volumes analyzed in samples of BG20_FBS and BG20_W in for maturation periods of 1 day, 7 days and 28 days. Sequentially, from left to right: surface porosities (shades of blue), average total porosity (shades of orange), base of bulk (shades of yellow), middle of the bulk (shades green) and final of bulk (shades of red).

Fig.26 – Total porosities in all the volumes analyzed in samples of nAg0.50_FBS and nAg0.50_ for maturation periods of 1 day, 7 days and 28 days. Sequentially, from left to right: surface porosities (shades of blue), average total porosity (shades of orange), base of bulk (shades of yellow), middle of the bulk (shades green) and final of bulk (shades of red).

Fig.27 – Total porosities in all the volumes analyzed in samples of nAg1.00_FBS and nAg1.00_ for maturation periods of 1 day, 7 days and 28 days. Sequentially, from left to right: surface porosities (shades of blue), average total porosity (shades of orange), base of bulk (shades of yellow), middle of the bulk (shades green) and final of bulk (shades of red).

Fig.28 – Total porosities in all the volumes analyzed in samples of nAg2.00_FBS and nAg2.00_ for maturation periods of 1 day, 7 days and 28 days. Sequentially, from left to right: surface porosities (shades of blue), average total porosity (shades of orange), base of bulk (shades of yellow), middle of the bulk (shades green) and final of bulk (shades of red).

Fig.29 – Total porosities in all the volumes analyzed in samples of TCS_FBS and TCS_W for maturation periods of 1 day, 7 days and 28 days. Sequentially, from left to right: surface porosities (shades of blue), average total porosity (shades of orange), base of bulk (shades of yellow), middle of the bulk (shades green) and final of bulk (shades of red).

List of Tables

List of Abbreviations and Acronyms

- **OMD** Ordem dos Médicos Dentistas
- **CEJ** Cementoenamel Junction
- **DEJ** Dentinoenamel Junction
- **DH** Dental Hypersensivity
- **ASC** Adult Stem Cell
- **hDPSC** Human Dental Pulp Stem Cell
- **VRF** Vertical Root Fracture
- **AB** Acid Base
- **ZOE** Zinc Oxide Eugenol
- **ASPA** Aluminiosilicate Polyacrylic Acid
- **GIC** Glass Ionomer Cement
- **FAS** Fluoroaluminosilicate
- **RMGI** Resin Modified Glass Ionomers
- **MTA** Mineral Trioxide Agreggate
- **WMTA** White Mineral Trioxide Agreggate
- **TCS** Tricalcium silicate
- **AgNP** Silver Nanoparticle
- **BG** 45S5 Bioglass
- **DNA** Deoxyribonucleic Acid
- **IRM** Intermediate Restorative Material
- **2D** Two-Dimensional
- **3D** Three-Dimensional
- **Micro-CT** Microcomputed Tomography
- **Nano-CT** Nanocomputed Tomography
- **CAT** Computed Axial Tomography
- **NDT** Non-Destructive Technology
- **FDK** Feldkamp, Davis and Kemp Algorithm
- **ART** Algebric Reconstruction Technique
- **ILST** Interactive Least Squares Technique
- **SIRT** Simultaneus Iterative Reconstruction Technique
- **mQ water** Ultrapure Water
- **FBS** Fetal Bovine Serum
- **ROI** Region of Interest
- **SPSS** Statistical Package for Social Sciences
- **PC** Portland Cement
- **BSA** Bovine Serum Albumine

1. Introduction

According to the Oral Health Barometer published in 2019 by the Portuguese Dental Association (OMD)[1], it is estimated that over 30% of Portuguese never go to the dentist or just in case of emergency. Another scary data collected in this survey that highlights the lack of dental care is the fact that 10% of the Portuguese population has no natural teeth. These numbers are largely due to economic difficulties that are present in a significant percentage of the population and also to the fact that the participants say they do not need to go to dental appointments, thus placing oral health and hygiene in a secondary position. In 2016, a data collected by Eurostat[2] revealed that Portugal was the fifth European country with the highest number of dentists per 100,000 inhabitants, only surpassed by countries such as Lithuania, Cyprus, Bulgaria and Greece. The indifference to the prevention of oral diseases and the contrast evidenced by the number of dentists practicing in Portugal make these data catastrophic and alarming. The teeth play an important role in the performance of various tasks and are essential for humans. In addition to being important during chewing, teeth are directly involved in speech and play a preponderant role in aesthetics and are one of the cornerstones for a good self-esteem.

Oral health is extremely important and should not be left behind, in fact, it has been linked to major health issues like diabetes, respiratory disease and cardiovascular disease[3]. Another indicator of the importance of oral health is the relationship evidenced in some studies between missing teeth and difficulties in balance, which can often increase the risk of falling, especially in the elderly[4]. The dental anatomy is complex, and it is composed by diverse types of tissues with different functions. To protect the tooth homeostasis, it is important to preserve the oral tissues by maintaining a dental follow-up that must be essential for a good oral health.

2. State of the Art

2.1. Dental Anatomy

Dental anatomy is composed of several constituents with different functions, and its graphic representation is shown on Fig.1 a). However, all components perform important tasks in maintaining oral health. The teeth are essentially divided into two parts, are the crown and the root (Fig.1). The root is surrounded by a fibrous connective tissue structure called the periodontal ligament, which connects the root cementum to the alveolar bone, facilitating the fixation of the teeth on the alveolar bone and transmitting occlusal forces from the crown to the bone[5,6]. The crown is the seeable part of the tooth. This portion of the teeth is covered by enamel and it is separated from the root by the cementoenamel junction (CEJ), which is also called cervical line.[7] The CEJ constitutes the anatomical limit present between the root and the crown surface. This junction is defined as the area where it occurs the bonding between the cementum and enamel in the cervical region of the tooth and is an essential anatomical structure of the tooth with morphological variations.[8,9] There are several different CEJ relations between cementum and enamel that cause the morphologically distinction of the CEJ itself (Fig.1 b)). Although all of these relations can be found in the circumference of a single tooth [8], the most common relation is an overlapping of the cervical margin of the enamel by the cementum. However, there are still other, though less common, relationships such as the touch of the enamel margin with the cementum end and the dentin exposure due to the gap between cementum and enamel. The latter may lead to increased site sensitivity caused by root dentin exposure [10].

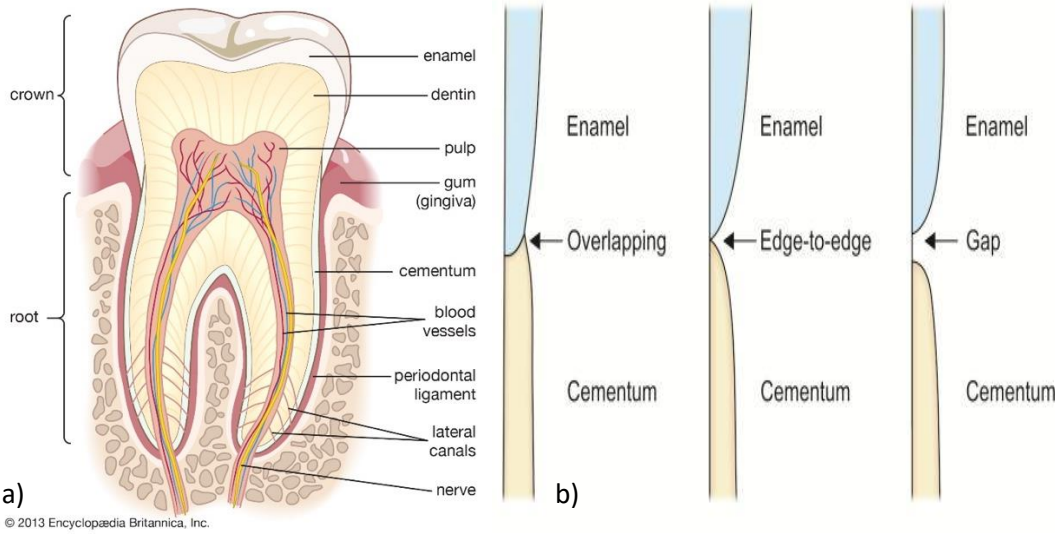

Fig.1- a) Human tooth anatomy and its constituents[11]; b) CEJ relations between cementum and enamel[12].

The enamel is the outer constituent of the tooth crown and has the function of protecting from wear the vulnerable area of the underlying tooth[13]. It is one of the most resistant tissues in the human body, as it is composed of hydroxyapatite, which makes it also one of the most mineralized tissues. The enamel is made just before the tooth eruption, and the ability to regenerate a new enamel in each tooth is lost after the tooth erupts completely[14]. Since dental enamel is extremely important for the maintenance of dental integrity, many studies have been carried out to restore or mimic this component.

Like the dental crown, the root also has a highly mineralized coating called cementum, that has the basic functions of anchoring the gum and the periodontal ligament fibers and also to protect the underlying dentin where cementum is firmly attached[15,16].Dental cementum is divided into two major parts which are both fundamental, although with distinct functions and different locations, the acellular and the cellular cementum. The acellular cementum is named like this due to the absence of cementocytes in its matrix. Its function is to anchor the main fibers of the periodontal ligament to the surface of the cervical root making it fundamental for the teeth fixation and periodontal function[16,17].

The cellular cementum includes in its matrix the presence of cementocytes and surrounds the apical portion of the root, which maintains a flexible role in sustaining the tooth in its occlusal position[16,18]. Due to its small size, cementum was the last of the three hard tissues present in human teeth to be discovered and further studied [16], while enamel and dentin layers were well known to researchers long before cementum was recognized.

There is another hard tissue that should be addressed when the focus is the anatomy of the tooth, the dentin. This is a sensitive tubular tissue primarily responsible for tooth color due to the transparency of enamel and, it is also responsible for supporting highly mineralized and fragile enamel. Thus, the dentin makes it resistant to occlusal and chewing forces without fracturing[19]. The composition of dentin can be divided in two different phases, the extracellular dentin and the functional dentin. The extracellular dentin consists of a fibrilled mineralized organic extracellular matrix which is composed of collagen fibers for the deposition of plate-like crystals of carbonate apatite[20]. On the other hand, the functional dentin includes predentin and dentin-forming cells known as odontoblasts, that with their cytoplasmic processes penetrate mineralized dentin and dentinal fluid. This penetration by the odontoblasts, is only possible due to the existence of dentin tubules in most of extension of the functional dentin[21]. These tubules form an essential network for nutrient supply extending from the dentinoenamel junction (DEJ) to the pulp expressing an S-shaped configuration that allows the migration of odontoblasts throughout this network. The different type of mineralization allow the distinction between the formation of two types of dentin, the intertubular dentin and the peritubular (or intratubular) dentin[22]. The tubules present in the dentin are coextensively surrounded by peritubular dentin, and the spaces between the tubules are occupied by intertubular dentin[21]. The intertubular dentin is essentially composed by type I collagen fibers reinforced with apatite crystals, and on the other hand, peritubular dentin is hypermineralized and is responsible for the formation of the dentin tubules walls[21] (Fig.2).

The dentin tubules are crucial for maintaining the vitality of the dentin and the tooth as a whole, since these contain inside cytoplasmic extensions of odontoblasts that once formed the dentin are responsible for their maintenance. This cruciality is, also, due to the fact that the dentin tubules work as a blood vessel, since they can carry out from the pulp chamber all the nutrients that are necessary for maintaining the vitality of the dentin. For this reason, it is essential the continuous fluid flow inside

of these structures [21]. Due to the permeability imposed by these tubules, when the dentin is exposed because of enamel damage, there is a high possibility of appearing dental hypersensitivity (DH) problems, that may be a result of attrition, abrasion, erosion, and/or abfraction (loss of tooth surface in the cervical areas of teeth) of the dentinal tubules. Dentinal exposure mainly occurs due to soft tissue (gingiva) recession along with the loss of cementum on the root surface[23], which makes gingiva recession the major responsible for DH. It remains to say that not all exposed dentins become sensitive. This can also be due to the presence of a layer of microcrystalline and organic particle debris as a result of grinding of enamel and dentin, that may be found on the surface of dentin tubules openings, forming the so called smear layer[24]. The smear layer is thinner in tooth with more sensitive dentin when compared to the smear layer in tooth with less sensibility in the dentin[23], being possible to correlate this argument with the presence of this type of pathology (DH).

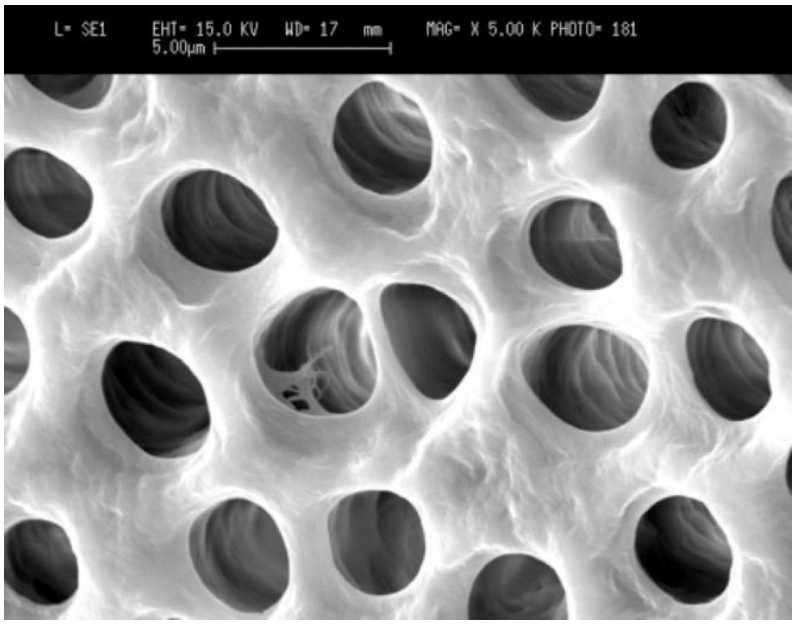

Fig.2 - Scanning Electron Microscopy (SEM) images of dentin tubules. Dimensions between 2.5 and 3 µm.[25]

2.2 Soft Tissues and Cellular Structures

Dental pulp is one of the most important soft tissues on the oral cavity, it is a vascularized vital tissue which provides a wide range of essential processes for the teeth like nutrition, protection, formation and restoration of teeth characteristics[26]. The vitality of the dental pulp considerably affects the tooth homeostasis as well as the proprioception therefore increasing its longevity. This soft tissue acts as biosensor to recognize pathogenic stimuli and also plays an essential role in the development of immature teeth. There are two principal factors that affect the vitality of dental pulp, the trauma and the bacterial infection. Pulp infections are, generally, irreversible due to the anatomical location of the pulp and also due to the restrained blood supply which generate an insufficient immune response leading to several adversities to counteract the bacterial invasion. The endodontic procedure that is used to remove the infected pulp and seal the root canal system is called root canal therapy and it is an extremely successful procedure (high success rate)[26]. However, this surgical technique can result in a physiologically nonvital state of the tooth and can also result in crown discoloration, mainly because of the staining effect resulting from root filling materials[27].

The knowledge acquired over the years about dental soft tissues and the cellular structures represented in them, is far from enough to overcome certain barriers that today are still problematic with regard to oral health. It is important to understand, for example, the soft tissue behavior during prosthetic implantation. For a successful implant restoration, the soft tissue that surrounds the dental implant should be healthy in order to ensure the establishment of its function, vigor and esthetics. In dental implantation, this happens during the healing process after implant placement, the only difference is that the surrounding soft tissue will have to deal with a foreign body (abutment of the implant)[28]. This issue will be preponderant for the success of dental implants, since it is essential to establish a barrier of soft tissues capable of harboring the underlying bone structures promoting osseointegration of the implant body.

Being aware of the importance of soft tissues for maintaining oral health, many researches have been carried out in order to find resolutions for problems related to the malfunction of these dental soft tissues. Tissue engineering has shown a great potential and is expected to have a huge impact in this area in the future. Particular combinations of scaffolds, stem cells and cytokines may be an asset in the treatment of soft tissues. Within these scaffolds, hydrogels may be an excellent option since they

can easily incorporate diverse types of cells and biological factors (e.g. growth factors) directly by mixing[29].

Some researchers have found that the particularities of stem cells could offer various advantages and new opportunities to deal with several diseases related with soft tissues. Among all stem cells, adult stem cells (ASCs) have shown great potential in the regeneration of blood cells, bone and cartilage[30]. Recently, some studies have been carried out using human dental pulp stem cells (hDPSCs) and have shown promising results since there is no or little practical limitations with regard to its harvesting and it is possible to obtain a significant number of hDPSCs per patient in a single tooth[29,31]. Also, these stem cells are capable of multilineage differentiation into adipocytic cells, neurogenic, odontoblastic, and other types of cells, making them a wise choice as a source of cells for tissue engineering[29].

2.3 Endodontic Treatment (or Endodontic therapy)

Endodontology has as its main basis the study of lesions and diseases of the dental pulp, as well as the peri radicular region. The study of the shape, function and health of this soft tissue is of great interest to the scientific community, since apical periodontitis, as the main disease associated with this tissue, still has many loose ends in relation to what is known today[32]. It is also important, when talking about endodontics, to associate the therapies used to solve certain problems. These therapies mainly involve root canal procedures and are designed to keep the dental pulp healthy or at least, part of it. However in many cases the solution is to remove the infected structures and the consequent obturation (filling) of the root canals[33]. This measure has as main objective to protect the tooth that has been decontaminated from a future bacterial invasion.

Microbial invasions are effectively the main responsible for lesions in the pulp and periapical tissues, but there are other causes, such as trauma or constant chemical irritation that, although less common, present an equal level of concern for oral health. When a microorganism enters the dental cavity, the immune system reacts immediately with a non-specific inflammatory reaction and through a specific immune response. The development of the lesion will depend profoundly on how it reacts, and the host's response will also depend on the type of microorganism that invaded the dental pulp

space[34]. An infectious disease is a response to the invasion of microbes in the tissues, in which its presence will produce clinical symptoms that will result from an immune system reaction to the presence of opportunistic pathogens. Periapical and pulp pathologies (periodontitis) are a succession that depends directly on the performance of these microbial organisms and their performance will come from the host's response. An endodontic infection develops as follows, occupation of the site (microbial invasion), multiplication of the pathogen and, finally, its activity[34,35]. The formation of biofilms is likely to worsen through the presence of bacteria that can resist through the endodontic treatment or bacteria that can access the dental pulp through some cracks[36]. This development results from the multiplication of different microbial species that give rise to a community, its adherence and its subsequent development in the oral cavity result in the appearance of periodontal diseases (periodontitis, periapical periodontitis and peri-implantitis) and dental caries that are some of the most widespread diseases that affect society in general, from the youngest to the oldest[37]. Biofilms formed in the oral cavity, also called oral biofilms, subsist in a wide alignment of microbes fixed with a consistent matrix of extracellular polymeric compounds, and are divided into three main phases, which begin with a pellicle formation (saliva-derived film), followed by bacterial colonization and ending with the maturation of the biofilm. This process, if not controlled, it will lead to the development of oral diseases[38–40].

When talking about root canal treatment, the objective associated with this therapy can be divided into three phases, all of which are preponderant for the elimination of an infection. The first stage is to remove, as much as possible, microorganisms from the root canal, followed by the sealing of the canal and, subsequently allow its cure[41]. When removing the pathogens, the dentist should be truly careful, since this procedure must be done without compromising the function of the tooth. The success of this treatment depends directly on the rate at which the healing occurs, and if it is fast enough, salivary microleakage can be avoided. If this does not occur with the desired rate, the saliva, which contains pathogens, chemicals and some toxins, will infiltrate the interface between the dentin and the cement applied to seal the channel, culminating in contamination and, subsequently, possible endodontic failure. Another detail that will directly influence the success of the process itself, is the apical extension in which the root filling takes place[41,42]. A recent paper from 2019, has concluded that procedures of root canal filling that close the root on the apical part of the tooth or beyond, were more related with cases of vertical root fracture (VRF's)[43], a situation that can easily lead to unwanted extraction.

2.4 Dental Cements – Their importance on the effectiveness of endodontic therapy

The success of a root canal treatment depends on several factors of extreme importance, from the beginning of the procedure until its end. The instrumentation used is one of these essential concepts, as well as the biomechanical preparation, and lastly, being more relevant to the development of this research, the filling and the materials used in it. Another factor that will be of great importance for the success of this therapy is the clinical case itself, and that will lead to each approach being done differently, specializing in the characteristics of the patient[43].

Proper filling will have the main ambition of eliminating pathogens and reducing, on a large scale, the chances of a second infection. In such a way, for this to happen it is necessary to be extremely careful during sealing, so that the possibilities of bacterial proliferation and subsequently a pathology, are practically zero. In order to avoid the occurrence of a serious pathology as much as possible, there is a huge concern with the filling material that is intended to be used in each case, which is the reason why endodontic cements have become so important for dentistry[43].

In restorative dentistry, dental cements have been used for a long time in view of two main points. One of these objectives, which will be preponderant for the development of this thesis, is the action of dental cement with filling material for temporary or permanent restorations when diseases that jeopardize the vitality of the tooth occur. Another basis for these compounds is to serve as a luting agent between the dental structure and a material manufactured to correct any loss of dental function, such as dental implants[44,45]. These cements turn out to be multifunctional, since they can also serve as a basis for the manufacture of restorative materials. A dental cement to be functional, more than just being biocompatible, it must meet certain fundamental mechanical and biological parameters. All of these cementing agents must be fluid enough so that it settles throughout the component to be filled, as well as its solidification must be effective and fast to allow the dental structure to resist functional forces, and, undoubtedly, it should not harm the soft and hard tissues that make up the tooth. Another important parameter of the dental cements that must be fulfilled by the used material is to not dissolve and maintain the sealing of the root [45,46].

2.5 Types of Cement - Looking at the past with a view to the future

Endodontic cements came into use in the late nineteenth century, having become a common choice in many clinical applications since the early twentieth century[47]. As previously written, these cements are often used as root canal filling materials. However, their function is not limited to this. Dental cements are also used as protective cavity coatings, they are used to connect prosthetic crowns to the dental structure and can also act as protective cavity linings[47].

The cements used today are practically all based on interaction between a powder (which acts as a base) that has the ability to release cations to an acidic solution, and a liquid (which acts as acid) that has the ability to release cations that allow the cement to form. This liquid also has acid anions that form stable complexes as soon as they react with the cations present in the solution, allowing the formation of a salt. In this way, cured cement is generally a matrix of salt hydrogel that is surrounded by a layer of powder that has not undergone a chemical reaction[47].

Cements formed through processes like this, are called AB (acid-base) cements. However, there is also an important range of cements used today, which are formed through a reaction of polymerization of macromolecules. These cements are commonly called resins[45].

The possible acid-base combinations are immense. This facility in the creation of new cements causes new types of biomaterials to be tested and implemented in the market almost every year. The evolution is constant, but the ideal dental cement is still awaited, which is due to the fact that much research that is done in the area of biomaterials, has not yet reached the desired level.

The acids used in the composition of dental cements are diverse, and they can be organic chelators, such as eugenol, they can be acid minerals, such as phosphoric acid, and they can be Lewis acids (atoms that constitute the chemical species, have deficiency), such as magnesium chloride. The bases used in these reactions are, like acids, quite diverse. These include simple metal oxides, such as zinc oxide, species resulting from the decomposition of glass, such as aluminosilicates, and also silicate minerals, such as wollastonite[47,48].

These cements have been used in the dental industry for over 150 years, both as filling materials and cementing agents. The first acid-based reaction cements to emerge were Sorel cements, in 1855, as filling materials are formed from the reaction between zinc oxide and zinc chloride. A decade later, zinc was replaced by magnesium in the manufacture of Sorel cements resulting in very similar properties, although this substitution has given rise to a stronger and more elastic cement than the previously designed cement[48,49]. The main objective of these cements at the time was not endodontology, rather they were created with other purposes more linked to the construction area.

Nevertheless, they ended up serving as inspiration for the creation of cements with a view to solving problems associated with this area of study, the endodontology, and in the late nineteenth century, zinc phosphate cements began to be manufactured and became the first luting cement to be used in dental filling[45]. These cements were formed from a reaction of zinc oxide, which acted as a base, and an aqueous solution of phosphoric acid[48]. These filling materials also proved to be highly successful in dental restorations (metal-ceramic, metals and porcelain). Their properties are excellent in terms of handling and fluidity and endow an adequate film thickness. Even so, zinc phosphate cements do not have an essential characteristic, which is anticariogenicity, which in other words means the ability to inhibit the formation of dental caries[44,45].

Other points that led to the incessant search for new solutions at the level of cementation, was the fact that they do not completely adhere to the dental structure and show a propensity for the occurrence of a slight dissolution, after a certain period of time. Also, taking into account their composition based on phosphoric acid, these cements do not provide proper protection to the dental pulp[44]. Even so, all cements developed afterwards are based on zinc phosphate cements, due to their high functionality[45].

A relevant handicap is that zinc phosphate cements do not have the necessary sensitivity for situations in which they have to be in contact with the pulp. Therefore, it was important to find a cement that was more biocompatible. In the late 1960s, Smith invented zinc polycarboxylate cement[47], a material that brought a resolution, not only for the biocompatibility required when contacting the dental pulp, but also for the problem of cement adhesion to the dental structure itself. The composition of these cements is primarily zinc oxide, the liquid in which the zinc oxide will react is a polyacrylic acid, and in some cases, it may also be a copolymer of that acid[44]. The pH of these cements is quite similar to the pH of zinc phosphate cements, but the biological properties of zinc polycarboxylate cement are

clearly superior. The fact that it has excellent biocompatibility, makes it extremely useful as a luting agent, especially when the dental filling needed, is close to the pulp[44].

At the time, the main objective of researchers in the manufacture of this innovative dental cement would be to reconcile the excellent physical properties (such as strength) of zinc phosphate cements with the exceptional biocompatibility and adhesion to the tooth structure of zinc oxide eugenol cements (ZOE cements used for temporary cementation)[46]. Therefore, zinc polycarboxylate cements were created, which showed excellent results, showing a chemical bond between liquid cement moments before its solidification, and the calcium present in the hydroxyapatite that forms the hard tissues present in the tooth, such as dentin and enamel more specifically. This chemical bond between the cement and the hard structure of the tooth allows the formation of a thin layer of organic debris and microcrystalline particles called the smear layer, previously mentioned in this dissertation. By way of comparison, these cements are not as strong as zinc phosphate cements, however, they are less harmful to dental pulp[44].

The tensile strength of zinc polycarboxylate cements is one third greater than that of zinc phosphate cements, however, the compressive strength is approximately half when compared to the same zinc phosphate cements. Its young module is three times less than that of zinc phosphate cements, which guarantees a plastic deformation of the cement when it occurs load on it. The intraoral solubilities in both types of cement are quite similar, leading to conditions of acidic oral pH that generate the possibility of cement erosion[44,46].

To conclude, the zinc polycarboxylate cement, despite having several benefits in its properties, shows a very reduced tensile strength and an almost zero release of fluorine[44]. This element, abundant in nature, is an important ally in the maintenance of enamel and also an essential component in the demineralization and mineralization processes that occur systematically in the oral cavity[50]. Thus, their poor release may be a problem in maintaining good oral health.

In view of the need to develop new cements, and mainly due to the imperative of developing a cement with plausible fluoride release values, in 1969, Wilson and Kent, developed a new cement that would be originally called aluminosilicate polyacrylic acid (ASPA), and was , like all cements developed up to that time, an AB cement[51].

Later, this cement came to be called glass ionomer cement (GIC), and it proved to be a promising material, since it showed good chemical adhesion to the teeth involved, caused by the chelation with calcium and phosphate present in the enamel and dentin, and also because it exhibits an excellent cariostatic potential since the release of fluorine occurs slowly and prolonged. These, and other reasons such as its admirable translucency, were the main reasons that led this cement to become an excellent alternative to previously developed cements[44,45].

Despite all the changes in chemical terms, all conventional GIC cements have polycarboxylic acid, water, tartaric acid and fluoroaluminosilicate (FAS) as fundamental components[46]. The substitution of phosphoric acid for polycarboxylic acid in the composition of these cements, greatly decreases the probabilities and susceptibility of GIC's to dissolution in the oral environment[50]. Tartaric acid, on the other hand, has very important functions directly connected with the proper functioning of this type of cement. Its addition operates as an accelerator that facilitates the extraction of ions from FAS glass, promoting their connection to the polyanion, causing the hardening after application of GIC cements to be significantly increased[46].

In terms of mechanical properties, GIC cements have properties very similar to the properties of zinc phosphate cements, but glass ionomer cements have a lower and much more advantageous oral solubility. The fact that they present this improvement, makes them a good choice for the implementation of orthodontic brackets and in metallic restorations. In comparative studies with zinc phosphate cements, antibacterial properties were found to improve slightly in GIC cements[44,45].

GIC's revealed a high young modulus and a low resistance to flexion, making them very weak and prone to fractures. Taking into account all these properties and knowing that GICs are excellent in preventing the appearance of tooth decay due to the constant release of fluorine and also excellent combatants of tooth demineralization, these also have factors that make it defective[50]. The fact that they have mediocre resistance properties was one of the reasons that led researchers to look for new solutions. Their application in places susceptible to high pressures would not be the most appropriate[45]. It is reported that after 24 months, the viscosity of the material increased, thus leading to the creation of many doubts regarding its expiration date and the search for new options for cases of dental restoration[52].

In order to improve the resistance of cements to dissolution and fracture, researchers began adding water-soluble polymers to conventional GIC's, creating in the early 1980s a new category of dental cements – the Resin-Modified Glass Ionomers (RMGI), also known in the industry as hybrid ionomers[46].

Its development started with the replacement of the aqueous component that constitutes the glass polyalkenoate cement through a mixture of water-hydroxymethylmethacrylate coupled with an activator/inhibitor for the resin that is added. These cements act through an electrostatic interaction of the hydroxyapatite present in the tooth's constitution with the polycarboxylate acid that is the main constituent of RMGI cements. This interaction allows to create a bond between cement and dentin and enamel[46]. This adhesion between the material and the tooth is due to the ionic bonding of the hydroxyapatite around the collagen and also to the fact that there is a micromechanical interlock that culminates in the hybridization of the dentin. This hybridization creates a greater fixation force as well as a greater resistance to fracture than that found in the use of GIC cements[46,53].

RMGIs are then a cement created to smooth some edges that the previously developed cements were not able to solve, however, even though there was a great evolution in this area, these cements continued to generate some concerns in researchers who are dedicated to this area. The fact that this cement, when applied, becomes very rigid, can lead to significant problems when its subsequent removal is necessary and can create lesions in the dental soft tissues[45,46]. Another Achilles' heel that has influenced researchers in the continuous search for new alternatives is the fact that RGMI's, like GIC's, are susceptible to shrinkage due to dehydration that may occur a few months after the application of these cements, leading to the possibility of fractures occurring due to stress at the tooth-cement interface. These fractures give rise to uncontrollable gaps between the cement and the tooth[45,54]. Also, the addition of resins that increase the hydrophilicity of these cements, causes the sorption of aqueous components leading to an impertinent volumetric expansion. All these factors mentioned above, raised some doubts regarding the stability and physical properties of RGMI cements[45].

Acid-base cements and resin cements, both types in the market, are mainly formed by polymers and fillers such as fluor and solidify through the polymerization of monomers of the main component,

resin[55]. In case of incomplete polymerization, unreacted constituent monomers may form which, besides being deeply toxic[55], may cause irritations in the dental pulp.

A new cement class - dental compomers – was introduced in the mid-1990s. Dental Compomers were designed to combine two different types of material, composites (comp) and ionomers (omer), with a view to a valuable development in aesthetic terms by using of traditional resins and also in terms of fluoride release and competent adhesion of cements to dental hard tissues, provided by the glass ionomer cements[56]. These compomers are also called polyacid-modified composite resins, as designated for the first time in 1994 by *John W. McLean et al.*[57]. These cements have, since then, been widely used because of their innovative properties and also , due to their cariogenic potential that makes them very suitable for dental restoration in teeth whose problem is associated with damage by dental caries[56].

The physical behavior provided by the compomers is similar to RGMI cements; however, they present a higher Young's module, which makes compomers more resistant when compared to RGMI that would be, at the date of this innovation, the ex-libris of dental cements[45,58].

These cements were initially produced assuming that the associated resins would allow an incessant absorption of water responsible for the reaction of the cement, regarding the fact that polyacid-modified composite resin cements are composed of ions leachable glass and polyalkenoic acid without traces of water. Its production also had in view the combination of the advantages of glass ionomer cements and composite resins in only one material, which was not achievable, since they are mainly composed of anhydrous resins[45]. This characteristic thus influences the inability of compomers to transport ions, making their release of fluorine insignificant and transient. Another detail that raised some doubts about their evolution capacity was the fact that adhesion to dental hard tissues is only conceived from the addition of a resin-bonding agent[58].

The most recent developments in dental cements are in the field of bioceramic materials, a class of biomaterials with numerous applications not only in dentistry, but also in medicine in general[59].

As bioceramics, bioactive cements have high biocompatibility since they have a fascinating ability to develop a layer of hydroxyapatite when they are in direct contact with tissues rich in calcium and phosphate, which allows them to be, in addition to biocompatible, excellent osteoconductors and osteoinductors and thus excellent sealers[60].

The first appearance of this type of bioactive cements goes back to the 90s with the creation of the mineral trioxide aggregate (MTA). These cements are also often called hydraulic cements, since they need a certain degree of hydration to occur their solidification, and after the occurrence of this change from liquid to solid state, these cements become invulnerable to further the dissolution [59]. MTA dental cements are the result of a mixture between Portland cement and bismuth oxide. Portland cement is well-known in the construction industry, since it is the main component of most of the concrete produced for the construction of buildings and has been used since the unfolding of the 19th century. It has in its composition, essentially, silica, synthesized trioxides of calcium and alumina[61]. Its second main component, bismuth oxide, is used to increase the levels of radiopacity for endodontic use, facilitating the utilization of X-ray radiation in certain dental exams[59].

These first-generation materials, such as MTA, have a wide range of dental applications that can go from dental filling to direct pulp cover. Although the development of these bioactive cements has facilitated the life of dentists, they continue to have certain limitations, the major of which is the fact that these types of cements, when in its pure form, do not present the ability to seal endodontics, derived from the high particle size (between 1.5 and 160 microns)[59].

To solve this problem, resins or other additives are often added in order to improve their fluidity. However, this addition creates a new complication, as it alters the biology and physical properties of the original material. Thus, even with these materials having an excellent biocompatibility, researchers keep insisting in new developments that would lead to the second generation of cements – the hydraulic cements [59,60].

This new generation of hydraulic cements is based on nanotechnological factors focused on the idea of minimizing the size of particles in nano and micro dimensions in order to facilitate its ability to flow[59]. These cements are essentially composed of pure calcium silicate, without the presence of heavy metals in its constitution, since these have been identified as a relevant cause of tooth discoloration[59].

The ability of these cements to form a layer of hydroxyapatite remains similar to that of cements from the previous generation (e.g. MTA), although in this generation the sealant becomes rigid through a hydration reaction that forms calcium hydroxide and also hydrate calcium silicate, which are mainly responsible for the formation of the hydroxyapatite layer when in contact with the tissue fluid. To increase the density of these cements, zirconia is often introduced. Besides being extremely

biocompatible, zirconia also acts as an opacifier[59]. The best known and most used material of this generation is white-MTA (WMTA), which differs from MTA, exactly because of its color. White MTA does not have iron oxide in its constitution, making it lighter than the original MTA and is more suitable in terms of aesthetic solutions [62]. However, some studies have shown that the WMTA does not completely solve the problem of tooth discoloration, and also has other problems such as the difficulty of handling, the high price and the difficulty in removing it after curing[63].

The last 150 years have been years of multiple developments in the field of endodontology and it is estimated that this evolution will continue at an amazing pace. The giant steps taken during this time were central to the development of new endodontic materials with different characteristics that solved several problems. However, despite all these improvements, the most used cements today, still have multiple gaps that make the research in search of a cement considered the holy grail of all these, be continuous and provide quantum leaps in this new era of research. In this way and taking into account this incessant and exponential evolution that has been observed up to the present, it is estimated that this will not slow down over the next few years, creating extremely high expectations about what is to come.

In conclusion, the future of dental cements is expected to be quite golden for all who come in the dental industry and research, an extremely interesting object of study with prospection for colossal improvements.

2.6 Tricalcium silicate (TCS)

The tricalcium silicate (TCS) has been used, regularly, as a bone cement since it has shown a reasonable bioactivity and biocompatibility. In some cement developments, the addition of calcium fluoride enhances the capacity of forming apatite, and also additions of calcium and sodium carbonate, as well as additions of monocalcium phosphate monohydrate and calcium sulphate hemihydrate had shown improvements in the physical properties of the cement[64]. In the presence of physiological fluids, the tricalcium silicate hydrates into calcium hydroxide and calcium silicate hydrate and, subsequently generates hydroxyapatite especially at the surface of the TCS paste. In dental cements, the biocompatibility is crucial and the paste of tricalcium silicate presents this singular particularity that

induces the differentiation of important soft tissues cells, particularly the human dental pulp cells. An extremely huge number of dental materials based on the tricalcium silicate has been developed, being one of the most well known in the dentistry community is the Biodentine.

The composition of the Biodentine consists in tricalcium silicate as a main component, calcium oxide and dicalcium silicate as a second main components, calcium carbonate as a filler material and zirconium oxide as a radiopacifer. The incorporation of zirconium oxide (ZrO_2) in this cement, as radiopacifier, allows the absorption of x-rays, facilitating the obtention of radiological image, sometimes essential for detecting anomalies after the implementation of dental cement.

In the production of this dental cement, a hydrosoluble polymer is added to the cement powder in order to facilitate the good flowability and when the cement is implemented, an uptake of calcium and silica is evidenced in the root canal dentin when a physiological solution is present. The addition of ZrO_2 has additionally shown in some previous studies the effectiveness in controlling the calcium (Ca) release, with a slower and more prolonged release rate. It was also concluded that the inclusion of ZrO2 in dental cements reduce the cytotoxicity and does not affect the mechanical properties of the dental cement [65].

This cement can be used in situations where there is a need of restoration of radicular and deep cervical lesions, pulp capping and pulpotomy, root-end obturation in endodontic surgery, apexification and also, for restoration of deep and large lesions related with coronal caries.

2.7 Silver Nanoparticles (AgNP)

Silver nanoparticles (AgNPs) have excellent physical, biological and chemical properties and so have been applied in dental cements in order to avoid or, leastways, reduce the microbial colonization in dental materials, exponentiating the levels of oral health and improving, concomitantly, life quality. These nanoparticles have been subject of study due to their optimistic particularities, being already used in areas such as endodontics, implantology and restorative dentistry.

Particles of silver in small dimensions are used in some calcium silicate cements as an alternative radiopacifier. Also, the addition of silver in TCS cements, has shown an enhancement of the

physicochemical properties like setting time, which reduces with the incorporation of AgNPs. These nanoparticles have also presented antibiofilm activity and anti-adhesion properties and showed noncytotoxic effect in the bone cells[66]. The inclusion of AgNPs has shown positive results in the endodontic treatment where the principal cause of endodontic treatment failure is the prevalence of bacterial species, in which the most common is the *Enterococcus faecalis*. When these microorganisms organize themselves, they form a bacterial biofilm that can be truly problematic for the oral health, making it difficult to maintain the oral homeostasis. The presence of silver nanoparticles on the dental cements, decreases the possibilities of *E. faecalis* biofilm formation and organization, since AgNPs demonstrated that affects the biofilm structural integrity. Not all dimensions of silver particles are positive to the dental cements. Particles with less than 10 nanometers are the most useful since they can directly interact with the bacteria due to their really small dimensions, allowing them to connect with the bacterial membrane. This interaction between the silver particles and the bacterial membrane affects the permeability and consequently, facilitates the influence of the silver particles in the internal components through the release of ions resulting from the chemical action of dental cement with AgNPs, with the oral environment. In this way, the AgNPs will act to prevent the DNA replication of the bacterial flora[67]. Relatively to AgNPs, it is possible to understand in the literature that the smaller the particles, the greater the bacterial effect. It is also possible to determine which large silver particles may suggest undesired levels of cytotoxicity and in this way, the antibacterial effect will be greatly reduced[68].

Another advantage coupled with the inclusion of silver nanoparticles in dental cements is the fact that, when in extremely small dimensions (4-11 nanometers), they penetrate the pores of the cements, providing an acceleration in the hydration of the silicates and thus, enabling a shorter setting time [67]. In this way, it will also be possible to reflect on the possibility of acquiring dental cements with reduced porosities when incorporating AgNPs.

2.8 Bioactive Glass 45S5

The bioactive glass 45S5 has in its composition 45 wt% SiO_2, 24.5 wt% CaO, 24.5 wt% Na_2O, and 6.0 wt% P_2O_5, and has been used in dentistry since the late 1990s due to its excellent properties and

antibacterial activity. Furthermore, the bioactive glass is also known for inducing dentin remineralization and eliminating enzymatic degradation at the dentin interface, causing it to present extremely important effects in endodontics[69]. The 45S5 bioglass is often included in dental cements, as it has several characteristics that may be essential for maintaining a healthy oral environment and may facilitate recovery. In addition, this material is osteoconductive and osteoinductive, facilitating the healing of dental interventions that include the bone. The fact of improving cell adhesion to cement is another characteristic that makes 45S5 bioglass extremely interesting for the dental industry. This compound is also associated to an important therapeutic relief by means of occlusion of the dentinal tubes through their connection to the collagen fibers and later, after inducing the formation of hydroxyapatite (HA) together with other components, causes the deposit of this HA between the tissue and the material[70].

The addition of 45S5 bioglass to dental cements has to be done in controlled quantities since it can induce some cytotoxicity due to the increase of pH as a result of the high rate of degradation directly coupled to the presence of a high level of Na^+ and Ca^{2+} ions. The increased cytotoxicity may result in a foreign-body reaction leading posteriorly to the formation of a fibrous capsule, particularity dangerous when it is applied together with a prothesis. In this situation the appearance of micromovements may occur and subsequently an eventual failure of the prothesis.

2.9 Oral Biofilms – How the nanoparticles are used to control them?

Oral Biofilms consists of a matrix of organic polymers that is originated through bacteria and saliva. The bacteria start agglomerating in this matrix leading to form a dense arrangement[71]. There is an incessant search by the scientific community for methods of controlling the formation of oral biofilms, and among many hypotheses and methods, nanomaterials are, today, the bet that is most promising. Since the 1980s, nanomaterials have revolutionized the concept of material, having been highlighted in the most diverse scientific areas including dentistry[39,72]. There is a long range of nanomaterials that can be of high efficiency when it comes to controlling oral biofilms. Some of the most important these days are graphene, silver, gold, titanium oxide, copper oxide and zinc oxide nanoparticles[39,73]. Metal nanoparticles have been showing excellent antimicrobial and anti-adhesive properties, especially silver

and gold, having been applied to other materials already used in the industry such as PMMA and hydrogels[73]. Nanoparticles, as a result of their small size, are also extremely influential in the biomedical field due to their improved biocompatibility. Thus, they can be used directly as bactericides, or in other cases, they can serve to increase the solubility in aqueous medium of a given drug[74].

In addition, and taking into account their ease of manipulation, nanoparticles are easily tailored by several factors, such as their size, surface charge, chemical composition and other properties, making them exceptionally flexible for transporting and releasing important drugs, at the time and place where they are most needed. Another point of high importance in the use of these nanomaterials, is the fact that microorganisms, such as bacteria, are less susceptible in the acquisition of resistance against them, especially if we talk about metal nanoparticles, such as silver, gold and copper, the most studied materials in this area over the past 40 years[73,74]. However, even having some relevant information related to the biocompatibility of these nanoparticles, an even more in-depth study is needed regarding their toxicity mechanisms. Information on absorption and excretion of these components is quite necessary, since their accumulation within the human body will be inevitable when used. In such a way, it will be relevant to draw a safety profile according to the nanoparticles used in each case. Finally, as previously mentioned, in these materials of reduced dimensions, the inherent surface chemistry is often modifiable, which opens their range of applications in biomedicine, as well as in dentistry[73].

It is essential to study the dental composition with the aim of detect problems that could be happening in the structure of the teeth. There is some methods to evaluate the condition of the tissues that compose the tooth, but most of them are complex, time-consuming and can induce distortions in the internal anatomy of the specimens analyzed [75]. Micro and Nano-CT has gained some growing significance in the study of the dental hard tissues, since it is a non-destructive technology (NDT) and it gives very detailed cross-section images, that can be reconstructed forming the 3D image of the specimen that wants to be observed [75].

2.10 Micro and Nano-CT in 3D Porous Structure Characterization

Microcomputed tomography (micro-CT) has become a crucial technique for quantification of structure-function relationships structure-function and also to assess disease progression. This technique has smoothed the way for numerous scientific and bioengineering advancements since the 80s[76]. The increased use of this NDT in research and industrial applications is currently in its best development opportunities, especially the high-resolution X-ray applications.

The micro-CT is a sophisticated equipment that grants the digitized three-dimensional scan of a x-radiated sample [77]. Actually, it can be described as a non-destructive 3D microscope, whose spatial resolution is a few micrometers, typically in the range between 1–100 µm. Micro-CT scanners capture a series of 2D planar X-ray images and recreate the data into 2D cross-sectional slices. These slices can be further prepared into 3D models and may give rise to 3D physical objects for analysis (Fig.3). With 2D X-ray systems it is possible to see through an object, but with the power of 3D micro-CT systems become possible to analyze and observe inside the object and reveal its internal features, providing non-destructive volumetric information about the microstructure of the sample[78]. Particular attention has been paid to the fundamental and operation principles of micro-CT as well as micro-CT approaches, especially for quantitative evaluation of bone and cartilage, making it a very important tool for other biological structures such as teeth.

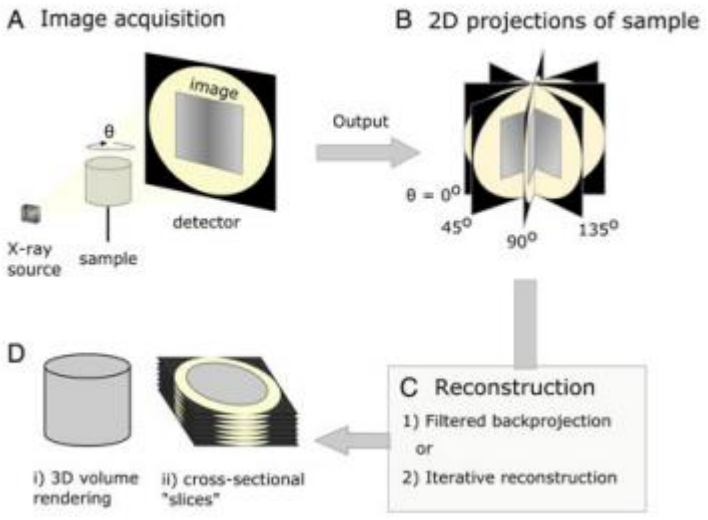

Fig.3 - Diagrammatic representation of X-ray micro-computed tomography workflow[79]

X-rays are based on the balance between penetration of, and attenuation by, the sample, so that sufficient contrast can permit the differentiation of internal features of interest. The contrast results from the differential attenuation of X-rays, as determined by the attenuation coefficient of the constituent materials[80]. If a material includes heavy elements i.e. if a material is dense, more X-rays will be attenuated, and transmittance will be reduced.

The MicroCT equipment, also called microcomputed tomography, has an extremely improved resolution when compared to CAT (Computed Axial Tomography) systems, with the size of the pixels being as small as 100 micrometers and the possibility of analyzing objects reaching dimensions of 200mm in diameter. The working principle is also similar to that of the Nano-CT, however, in the latter the resolution is even higher, more detailed and more precise. As a result of the continuous technological advancements in the development of CT systems ultra-high spatial resolution devices have become available in the recent years[81]. Nano-CT represents an emerging technical advancement of the established micro-CT technology developed in the early 80s.

In nano-computed tomography (Nano-CT), the resolution capacity can exceed that of micro-CT systems, due to the fact that the focal spot size can be decreased to less than 500 nm making possible to achieve a superior spatial resolution up to 400nm when using specific detectors and examination protocols (geometric enlargement, angular scanning, noise reduction by repetitive image acquisition)[82]. These systems allow clear visualization of cellular structures as well as inner ultrastructure of bone trabeculae and also submicron hard tissue cracks[81], making it extremely relevant for research in restorative dentistry and oral implantology, though not much explored yet. The precise rotation that is characteristic of these devices makes the data acquisition process very stable and also very fast obtaining scans of the sample, which is another advantage when compared with micro-CT devices[81].

Nowadays, nano-CT provides new applications in endodontics, due to the high spatial image resolution provided by these tomographic devices. In the future this technique will be able to provide reliable and novel information on details of dentinal tubules of the root dentine, on pathological changes in the root and their reparative processes, pulp tissue engineering and so on[81]. A relevant limitation is in the sample size, which makes all its handling very thorough and that may cause some crucial errors that can affect the reliability of the obtained data[81,83].

The Skyscan 2211 X-Ray nano-CT system (Fig.4) that will be used throughout this research at the University of Oslo, Department of Biomaterials, employs an X-ray source using new technology to acquire a spot size of 500 nanometers, combined with an extremely high precision sample manipulator and a highly sensitive camera[84].

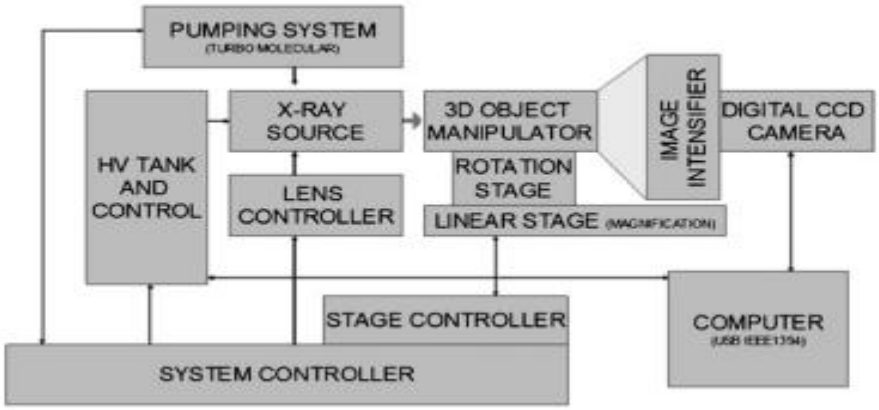

Fig.4 - Schematic representation of the Skyscan 2211 X-ray nano-CT system[85].

2.11 Principle of computed tomographic imaging

In CT imaging devices, an x-ray beam is produced by the target made of, generally, by tungsten or copper, and it is scanned in direction of the patient and a radiation detector is placed on the opposite side of the patient. With a monoenergetic beam, the transmission of X-rays through the subject is [79]:

$$I = I_0 e^{-\mu x}$$

Intercepted by two regions with attenuation coefficients μ_1 and μ_2 and thicknesses x_1 and x_2, the x-ray transmission is[79]

$$I = I_0 e^{-(\mu_1 x_1 + \mu_2 x_2)}$$

If many (n) regions with different linear attenuation coefficients occur along the path of X-rays, the transmission is[79]

$$I = I_0 e^{-\sum_{i=1}^{n} \mu_i x_i}$$

With a unique transmission measurement, the separate attenuation coefficients cannot be determined, due to the fact that there are too many unknown values of μi in the equation.

However, with numerous transmission measurements in the equivalent plane but at different orientations of the x-ray source and detector, the coefficients can be separated so that a cross-sectional display of attenuation coefficients is obtained across the plane of transmission measurements[79]. Different ranges of attenuation coefficients coincide with different grey levels, and on this way, an image can be produced with the representation of different structures on the subject analyzed (Fig. 5).

Fig.5 - MicroCT vertical cross-section of a human tooth showing the different contrasts of the different hard tissues[86]

The grayscale provided by this technique is extremely important in dentistry, since it can supply important information about the densities of the different tissues that are present in the tooth, clarifying the disparities between hard tissues (enamel, dentine and cementum). It can also be utilized

for soft tissues when a marker is used, since in soft tissues the x-ray attenuation is significantly low which creates the need to use staining methods[87].

2.12 The process of acquiring a CT scanning

The process of using CT scanning equipment has as its main objective obtaining relevant images for researchers and can be divided into four essential steps:

I. Production of X-rays

II. X-ray absorption through the sample

III. Rotation of the sample to acquire a series of projection images

IV. Reconstruction of the projection images into virtual slices

I. Production of X-rays

X-rays are generated by directing electrons produced in a cathode at a target which can be made of tungsten, copper, iodine, etc. Posteriorly, the target emits X-rays which are then transmitted to the sample. The emitted X-rays form a cone (cone-beam) where the origination point is a spot on the target and the emitted beam diverges out in a conical shape (Fig.6). A cone-beam allows the acquisition of a larger volume of the sample during a single scan rotation.

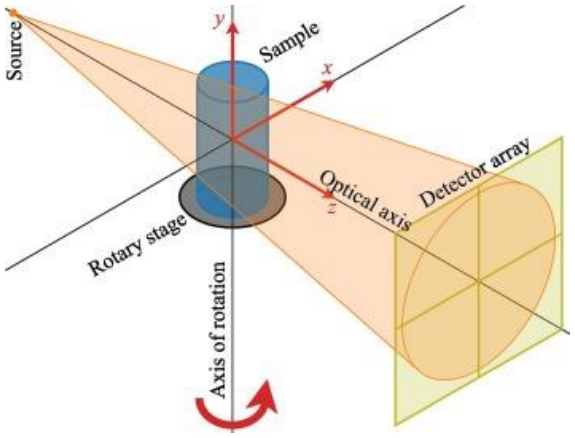

Fig.6 - Illustration from a Cone-Beam tomography setup[88].

II. X-ray absorption through the sample

CT scanning requires that there is both (a) partial absorption, meaning that some X-ray photons are absorbed in the material while others are transmitted to the detector, and (b) differential absorption, defining that the different materials that compose the object have distinct absorption characteristics to, subsequently, give contrast. If there are no differences in the absorption, the sample result comes out as a homogeneous gray level.

If samples atoms have a great atomic number, the x-rays will not have enough power to pass through it and reach the detector. For example, lead stops X-ray and so it is used as a shielding material for the systems, but it is not useful to scan more than a millimeter of lead. Also, the sample has to have some density to stop some X-rays, otherwise it will be transparent. Materials with a low average of Z (atomic number) such as pure Beryllium and soft tissues like gingiva can be difficult to image due to their low attenuation rates[89].

III. Rotation of the sample to acquire a series of projection images

After a projection image is taken, the sample is rotated a fraction of a degree, typically 0.5 degrees or less. A new projection image is taken at each of these steps. This is done throughout the 360-degree

rotation[90]. To reduce the time of scan, 180 degrees can be used as the projection images. From 0-180 degrees we find the mirror images of the project images from 180-360 degrees. Normally, if the chosen step sizes are thinner, the resulting cross section will be correspondingly thinner.

IV. Reconstruction of the projection images into virtual slices

The reconstruction of cross-sections is known as the process of assembling the internal and structural information from projection images. Feldkamp, Davis and Kemp (FDK) algorithm is the most productive cone beam reconstruction and it is a form of filtered backprojection. These cross-sections are used to have a sight about the internal features. These 2D images may be analyzed and reconstructed into virtual 3D models. It can be also used to generate movies, 3D models and more.

2.13 Algorithms for image reconstruction

The mathematical basis behind the reconstruction of images acquired using a CT technique is the reconstruction algorithm, which can be one of four types.

Simple backprojection

In this method, each X-ray transmission path through the sample is divided into equally spaced elements. Every element is assumed to contribute equally to the total attenuation along the X-ray path. By summing the attenuation for each element over all X-ray paths that intersect the element at different angular orientations, a final summed attenuation coefficient is determined for each element[79]. To obtain an image composed with the different attenuation coefficients, all of the different coefficients are summed generating a specific coefficient for all the other components of the anatomical section that was scanned by the incident X-rays. Despite being this approach straightforward, some of the images of the object appear blurred, even when the object presents sharp features.

Filtered backprojection

The filtered backprojection often referred to as the convolution method, uses a one-dimensional integral equation for the reconstruction of a two-dimensional image. In this convolution method, the transmission of X-rays is combined with a deblurring function to remove nearly most of the blurring before the data are back projected. The most common deblurring function is the use of a filter which main role is removing the frequency components of the X-ray transmission data that are responsible for most of the blurring in the composite image. The convolution method of image reconstruction has as its main advantage the fact that the image can be constructed at the same time as the collection of X-ray transmission data.

Fourier transform

On the Fourier transform, the X-ray attenuation pattern, at each angular orientation, is divided into frequency segments of disparate amplitudes. Taking into account these frequency components, the completed image is created in "frequency state" giving rise to a spatially correct image, being then reconstructed by filtered backprojection, an inverse Fourier transform process.

Series expansion

In this technique, variations of which are known as ART (algebraic reconstruction technique), ILST (interactive least-squares technique), and SIRT (simultaneous iterative reconstruction technique), X-ray attenuation data at one angular orientation are divided into equally spaced elements along each of several rays [91]. These data is posteriorly compared with the acquired data in different angular moments. The differences evidenced by the different X-ray attenuation in two distinct orientations are added uniformly to the appropriate elements. This procedure is replicated in all the different angular orientations, and to ensure the consolidation of the reconstruction data a reduced fraction of the attenuation discrepancies is added. In this method, all X-ray attenuation data must be available before reconstruction can begin[79].

2.14 X-Ray sources

The choice of X-ray source is strongly important since it affects micro or nano-CT system performance. This particularity is due to the tradeoff between thermal loading of the source's metallic anode and the focal spot size. Most X-ray tubes with micro-focus tubes (focal spot diameter <~50µm) operate with very low photon output (in the order of 100-times lower) compared to the high-power tubes used in clinical scanners. This fact explains the increase in the average scan time required in micro-CT compared with clinical scans[92]. The most used X-ray sources for micro-CT are micro-focus, fixed tungsten anode tubes operating in continuous mode, with voltages in the range of 20-100 kV and anode currents in the range of 50-1000µA[92].

2.15 X-Ray detectors

X-ray detectors can exist in two ways, in gas-filled ionization chambers or in solid-state detectors. These are selected according to the operating stability, due to their efficiency in detecting X-rays and also due to the short response time. In the case of solid-state detectors, these may include bismuth germanate (BGO) or cadmium tungstate ($CdWO_4$). They should also include scintillation crystals, usually composed of sodium iodide (NaL) and calcium fluoride (CaF), as well as ceramic materials. All of these components are chosen due to their high detection efficiency and the short fluorescence decay time. In the case of ionization chambers loaded with gas, pressurized xenon (25 atm) is the most used since it improves the efficiency of X-ray detection [79].

The stability of response from one transmission measurement to the next with any detector, is essential for production of images free of artifacts. The geometry and the rotational source generate some instability on the detector, causing the formation of ring-shaped artifacts on the acquired image. Minimum energy dependence presented on the detectors and expressed over the energy range of the X-ray beam is also crucial, especially if corrections for beam hardening are in need to be applicable to all samples size and configuration.

Micro-CT analysis has proven to be useful in a wide variety of applications. It can provide high-resolution images as well as both qualitative and quantitative analysis of human tissues, although the average scan time required in micro-CT is increased when compared to larger CT operating systems.

2.16 Reduction of Images Artefacts

Due to geometrical accuracy and also limited resolution present in Micro and nano-CT, the major problems related to these techniques are measurement artefacts. Image artefacts are unnatural structures in the resulting scans which do not correlate with the real sample feature, however, and due to the facilities provided by the analyzing softwares, it is possible to correct the images by suppressing the artifacts in the reconstructed CT slices efficiently (Fig.7 a)). These artificial structures are a result of image discrepancy that cannot be explained by transmission or by noise properties and can result in problems with dimensional accuracy and measurement interpretation. There are a lot of types of images artefacts, and the most common are cupping artefacts derived from beam hardening and are represented on the Fig.7 c). This cupping effect is produced by operating a polychromatic X-ray spectrum released by the tube and the strong vulnerability of the attenuation coefficient of the interconnected material on the photon energy. When an object is penetrated, the radiation of the beam corresponding to low energies is vigorously absorbed with intensified penetration depth and only the radiation corresponding to high energies penetrates the object and supplies information for image generation. Moreover, the efficiency of the detector is a function of the corresponding photon energy and these regions have low contrast values in the reconstructed dataset as a result. For materials composed by atoms with a high Z (atomic number), these artifacts distort the resulting image and can be reduced by filtering X-ray spectrum with titanium, copper and aluminum filters, consequently removing low energy photons previous to the input of x-rays in the object[93].

For materials with only one component a widely used rectifying procedure is linearisation[94]. This principle is based on transforming the measured values of polychromatic projection into monochromatic values. Effectively, it is determined a non-linear and characteristic correction curve considering the projection values of reference samples with familiar geometries. This correction curve serves as a pre-processing step before reconstruction begins[93]. Another typical artefact type is the ring artefacts, usually caused by an insufficient calibration of the detector, and for micro-CT is a

considerable issue since it disturbs the quality of acquired images either as rings (in transversal slices) or also transformed as line structures (in sagittal and coronal views). Previous studies have shown that these artifacts were responsible for inhomogeneity and the increased noise in CT images, becoming likely the reduction of low contrast resolution[93,95]. There are already some ring artifact correction methods that make it possible to alleviate this problem.

Other important artefacts are listed below [93]:

- Motion artefacts: When an object is being analyzed, it is important that the object does not change its position (do not move), not only the object but also the CT device. Otherwise, the result will be the production of motion artefacts, as it is observed on the Fig. 7 b).

- Reconstruction artefacts: this type of artifacts normally result from the approximation features of computing operations. The filtered backprojection is used to try to decrease the number of reconstruction artefacts.

- Partial volume artefacts: an object usually has a very sharp edge. This edge, generally, is not located at the boundary of different detector elements, mostly due to the narrow resolution of the detector. Therefore, the intensity of the X-ray on the analyzed element will be measured taking into account the average of the width of the detector and the object will be blurred. A solution to this problem may be to reduce the size of the voxel, thus reducing this effect.

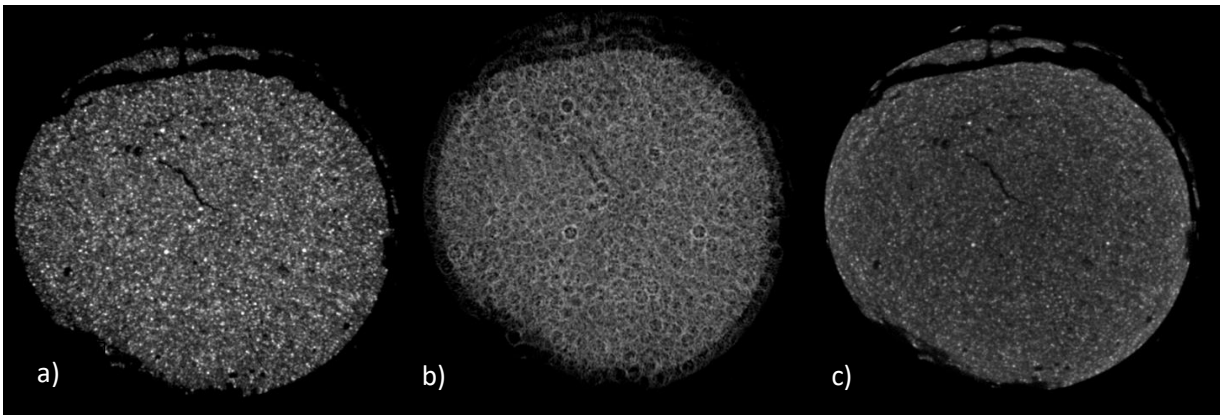

Fig.7 – Slice Representation of a BG10_FBS immersed for 7 days. a) Corrected slice; b) Slice without misalignment compensation (motion artefacts); c) Slice without beam hardening correction

3. Objectives

The health of the teeth is important for the preservation of the oral health and for the well-being in general, and the maintenance of the natural denture must be encouraged with oral hygiene and accompanying measures such as periodic visits to dental health technicians. The dental obturations are the most performed procedures on the clinical dentistry, and its function passes through removal of infected or damaged tissues present on the inner part of the tooth without extracting it and, thus, preserving the natural dentition.

In addition to the need of making a proper follow up of the oral health by monitoring the natural denture, today, researchers in the field of dentistry are facing problems that do not always have a simple solution. Diseases such as periodontitis, dental hypersensitivity and peri-implantitis are, perhaps, the biggest puzzles that they have in their hands.

Periodontitis is one of the biggest concerns for the researchers working on this area and It is commonly caused by residual bacteria that starts accumulating on the soft tissues of the teeth. This infection can cause inflammatory reactions in gums and in, in some cases, it can affect also the dental pulp, causing apical periodontitis. The apical periodontitis is an acute inflammatory injury caused by the entrance of bacteria in the pulp canal system, and is usually the result of untreated dental caries [96]. The root canal therapy is an effective treatment for this lesion, and this approach avoids tooth removal, since this therapy consists in eliminating the infection and protecting the tooth, already decontaminated, from future microbial invasions by filling (obturation) it with a certain dental cement[97]. However, the dental cements used has been shown to deteriorate over time and thus lose the ability to properly protect the tooth from a second microbial invasion. For this reason, there is a need to develop cements with longer antibacterial activity, and also less porous, in order to make it difficult for bacteria to pass through the dental cements.

In view of this problem, there was then a need to develop cements in which, in their inclusion, they involve materials with prolonged antibacterial activity. Some materials that represent a lot of interest were bioactive glass and tricalcium silicate, since they exhibit a very intense bactericidal effect. This bactericidal effect inherent to these materials, is due to the diffusion of leachable components and, above all, silicon oxide. The inclusion of nanoscopic-sized compounds, such as silver nanoparticles

treated in this study, effectively eliminates bacterial biofilms acquired inside dentinal tubules. These nanoparticles can also be responsible for the transformation of the material's surface characteristics, since they alter wettability and surface charge. In this way, the potential of these compounds must be taken into account in order to understand the properties of the materials, such as physical, chemical and biological properties.

Given the importance of the dental cements in these dental applications, the aim of this research will be to characterize them by using advanced techniques such as micro and nano-CT. The use of this techniques will allow a more detailed knowledge that, in the future and ideally, will provide a better understanding of the dental cements. The better understanding of this materials pass by the idea of how the porosity varies over time, having in mind the improvement of the compositions of dental fillings, in order to avoid a secondary infection.

4. Experimental Section

The dental cements were developed and provided by the University of Oslo within a scientific collaboration between research groups. The dental cements have as main components, materials that have already shown, in previous studies, to be extremely beneficial when included in dental cements. The constituent materials studied were, in particular, silver nanoparticles (nAg), 45S5 bioglass and tricalcium silicate (TCS). The latter was present in all samples, although with a varied concentration, since certain amounts of cement were replaced by the other two materials. All cements also included 20% zirconia oxide, an extremely useful radiopacifier that facilitates the observation of cements in X-ray analysis of silver that were added in the cements through the replacement of certain percentages of TCS.

4.1. Test Materials

The materials used in this study were as follows:

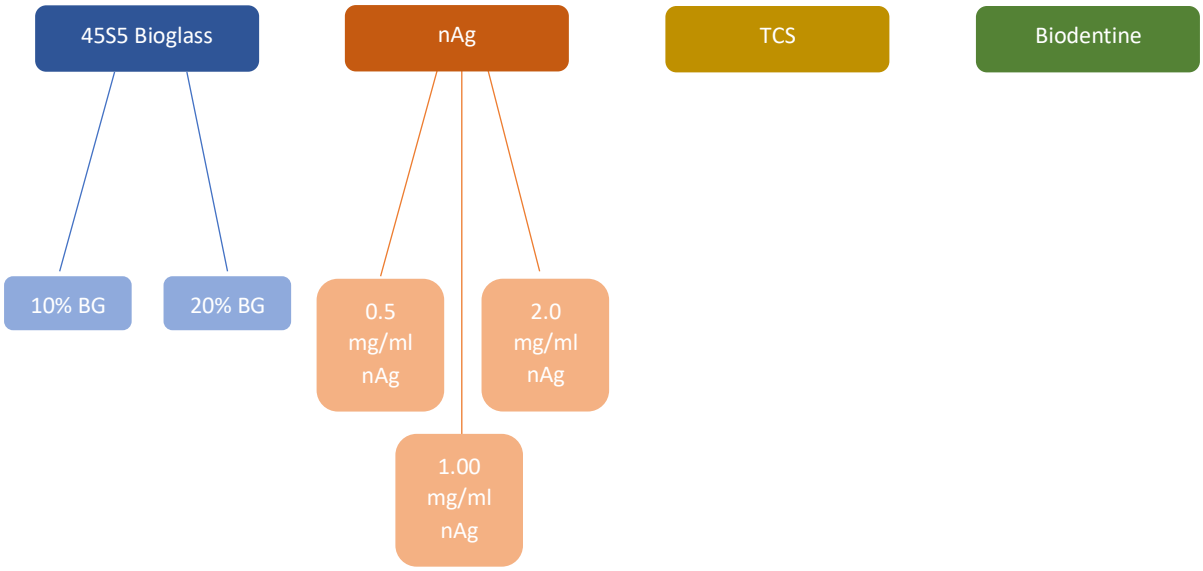

The samples of 45S5 Bioglass and nAg had their TCS/ZO replaced/added by specified quantities presented on the diagram above. On the 45S5 Bioglass samples, the replacement was made by taking out 10%/20% of TCS, and posteriorly adding the same percentage of 45S5 Bioglass. On the nAg samples, different quantities of silver nanoparticles (nAg) were added to the TCS/ZO. The TCS samples were composed only by TCS with 20% of zirconium oxide and finally, it was analyzed also a commercial dental cement called Biodentine that would mainly serve as a control material. These cements were then immersed into two distinct mediums: FBS and mQ water. The first of which had as its main objective the mimicry of the environment achieved in the oral cavity, in order to enable the study of the behavior of these cements at the time of their application since their properties are similar to the properties of tissue fluids. MQ water, on the other hand, as a conveniently inert solution, will not react after immersing the cements, making these media chemically non-reactive.

4.2. Sample Preparation for Analysis

Prototype materials were hand-spatulated with mQ water using a water/power ratio prototype of 0.35 ml/gr and commercial materials were handled and mixed according to the manufacturer instructions. The cements prepared were compacted by uniaxial pressing inside teflon moulds (3 mm

thickness, 4 mm diameter) which were placed upon glass microscope slides in order to create a macroscopically flat surface; this surface corresponds to the denominated ‘’surface of the sample’’ and it is the opposite surface to that where the pressure was applied. Subsequently, the samples were covered with a wet gauze and were allowed to set for 24 h at 37 °C in an incubator. After this period, the material pellets were taken out of the discs and were immersed in 4 ml mQ water or Fetal Bovine Serum (FBS F9665; Merck KGaA, Darmstadt, Germany). The samples were incubated for 1, 7 or 28 days at 37 °C, and the immersion liquid was replaced with a fresh one every 7 days.

All the samples were prepared in a research center of the Institute of Clinical Dentistry in the University of Oslo and were provided for microstructural studies by computed tomography techniques.

4.3. Assessment of Porosity with computed tomography scanner

For the microstructural studies, the following parameters were assessed by nano-CT: a) The volume of voids, b) the volumetric percentage of voids, c) the volumetric percentage of material. This information allowed to understand the relationship between porosity and incubation time.

4.3.1. Scanning of samples with Nano-CT

The samples were prepared in pieces of normal single-use straws made of PVC, and were placed in the system (Fig.8) with the technical features that are detailed below:

Fig.8 - Skyscan 2211 X-ray nano-CT system

4.3.2. System

The scanner utilized during nano-CT analysis was the SkyScan2211, with software version 2.5.0. The SkyScan 2211 was calibrated so that the images were as sharp and expressive as possible. This calibration went through the correction of the artifacts, the choice of the most suitable lens for these small samples and also the type of source of X-ray used. All of these steps were crucial for the slices acquired by the equipment to be able to provide as much information as could be useful for further analysis. The camera utilized for taking the 2D images corresponding to each slice of the sample was the flat panel sensor, and the pixel size of the camera 74.800 um, which gives a high level of details that will be essential for the interpretation of the samples content. The following table (Table 1) presents the relevant information about the system used through this analysis.

Table 1 – System information of Skyscan 2211 (X-ray Nano-CT)

Scanner	SkyScan2211
Software	2.5.0
Source Type	Xray-Worx
Camera	Flat Panel Sensor
Camera Pixel Size	74.800 um
Camera X/Y Ratio	1.0000

4.3.3. Acquisition

The acquisition of the images was programmed so that all the data acquired was as wide and relevant as possible. A certain voltage and current were chosen in order to exponentialize the quality of the resulting image taking into account its density. The partial width was defined in order to obtain complete sections of the sample, and an image was acquired every 7 μm of thickness of the sample. A 0.5 mm Ti filter was used to improve the contrast of the cross sections, make it easier to analyze the porosity and reduce the presence of artifacts. The following table (Table 2) shows the parameters used for making the acquisition in the most useful way.

Table 2 – Optimization parameters for acquisition of images by Skyscan 2211

Source Voltage	70 kV
Source Current	70 uA
Source focus mode	High power
Source target type	HighResDiamond
Partial Width	58%
Image Rotation	-0.0380
Exposure	300 ms
Image Pixel Size	7.00 um
Scaled Image Pixel Size	7.00 um
Object to Source	26.557 mm
Filter	0.5 mm Ti
Rotation Step	0.670 deg

Use 360 Rotation	Yes
Flat Field Correction	On
Scanning Trajectory	Round
Type of Motion	Step and Shoot
Type of Scan	Flat-Panel

4.3.4. Reconstruction

The reconstruction of the cross-sections was made by using the program NRecon (Fig.9 a)) with the version 1.7.4.6. The engine used was GPUReconServer with the version 1.7.4. The images came from the scanning made by SkyScan 2211 and were manipulated in such a way that its entire portion could be observed during further analysis. A region of interest (ROI) was defined with dimensions larger than the sample, including specially the base of the samples and the bulk. The reconstructions were carefully analyzed, and some features were added in order to reduce the image artefacts (Fig.9 b)). The reconstructed images were saved in the specific folders with the name of the sample, facilitating their organization. The table presented below (Table 3) shows the parameters used for the reconstruction of the cross-sections and the specifications used to reduce the presence of image artefacts.

Table 3 – Relevant reconstruction parameters with software NRecon

Reconstruction duration per slice	0.042411 s
Result Image Width	796 pixels
Result Image Height	796 pixels
Pixel Size	7.00000 um
Reconstruction Angular Range	360.46
Angular Step	0.6700 deg
Smoothing	0
Ring Artifact Correction	6
Reconstruction from ROI	ON_ROUND
Filter type description	Hamming (Alpha=0.54)
Beam Hardening Correction	60%
Cone-beam Angle Horizontal	16.689785 deg
Cone-beam Angle Vertical	22.887764 deg

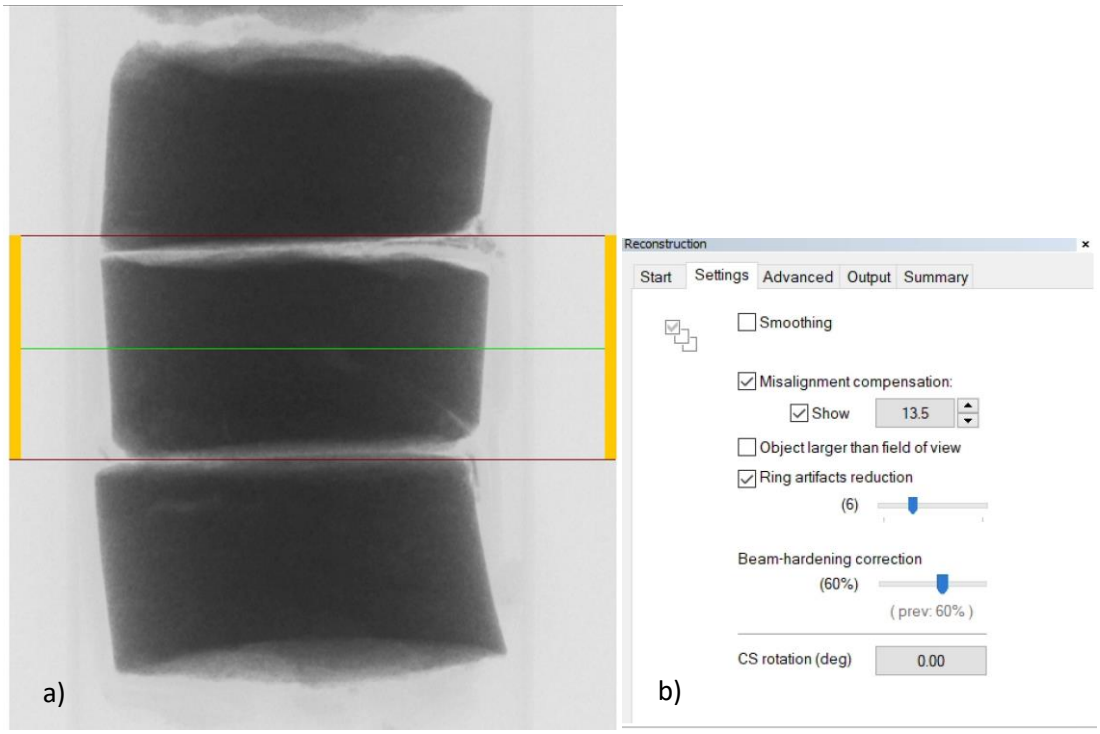

Fig.9 – a) BG10 samples before reconstruction with NRecon; b) Parameters used to optimizate the images and remove artifacts after the image acquisition.

4.3.5. Analysis of the cross-sections of the samples using CTAn

To prepare the analysis on CTAn, the samples were divided in surfaces and bulks, with a region of interest (ROI) of 3801.004 x 3801.004 μm (Fig.10). The first four slices of every sample counted from the base, which is the part of the sample that was placed upon glass microscope slides in order to create a macroscopically flat surface, are analyzed as the surface.

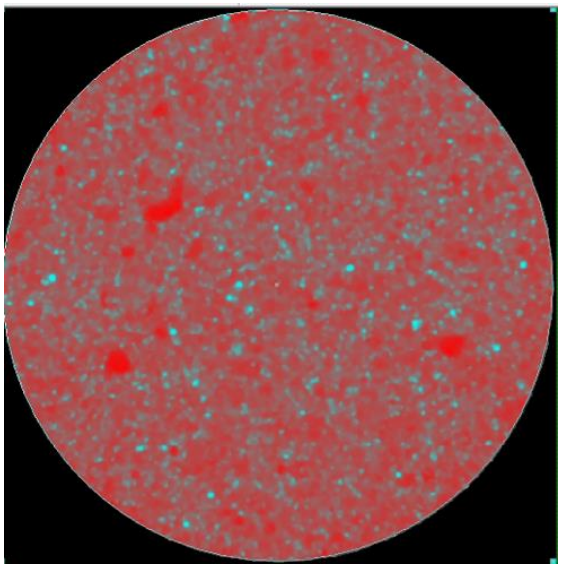

Fig.10 – ROI of a BG10 sample immersed in water for 1 day (Skyscan 2211)

Subsequently, the analysis of the bulk was made with, most of the times, 200 slices present in the middle of the specimen. In some cases, due to the reduced dimensions of some samples that had significantly less slices in total, the number of slices used was shortened. Then a filtering was applied consisting of an anisotropic diffusion that favored the wide regions, with 8 iterations and a gradient threshold of 8.

4.3.5.1. Surfaces

To analyze the surfaces, firstly an appropriate thresholding was chosen for each sample, in order to find the most adequate grayscale index that shows all the structures that are understood like pores. The step of choosing the satisfactory grayscale index is a critical one, in order to don't miss any pores. In the fig 11 a), we can see a CTAn image of a slice from the surface of a Biodentine sample immersed on FBS for 1 day with the respective pores and with some different types of greyscale indexes that could be used, and that would have a great influence in the total porosity of the samples. If the greyscale index used, is smaller than the adequate, the number of accounted pores will be smaller than the number of existent pores present on the slice (Fig.11 b)); also, if the greyscale index used is higher than the acceptable, the number of accounted pores will be much higher, since the software will count the presented noise as pores (Fig.11 c)). Taking this into account, it is crucial for the operator to choose

the ideal thresholding by comparing the image of the obtained slice with the binary image. When this comparison is being done, the voids presented in the slice, must be represented on the binary image with the exact same dimensions and this process must be very careful to not result in biased data. After choosing the adequate thresholding (Fig.11 d)), the operation was followed by a custom processing that includes the respective thresholding chosen, two different despeckles, and a 3D analysis in order to obtain the most reliable porosity value and the least possible voids. The first despeckle (Sweep) it was used to remove all the other objects presented on the image except the largest object. The second despeckle was used to remove black objects below 40 voxels that escaped from the thresholding. The 3D analysis preformed after the thresholding and the despeckles initiates a 3D image analysis of the selected objects (white colour) inside of the volume of interest (VOI) of the sample. By analyzing the objects inside of the VOI, we can find the porosities inherent in which sample.

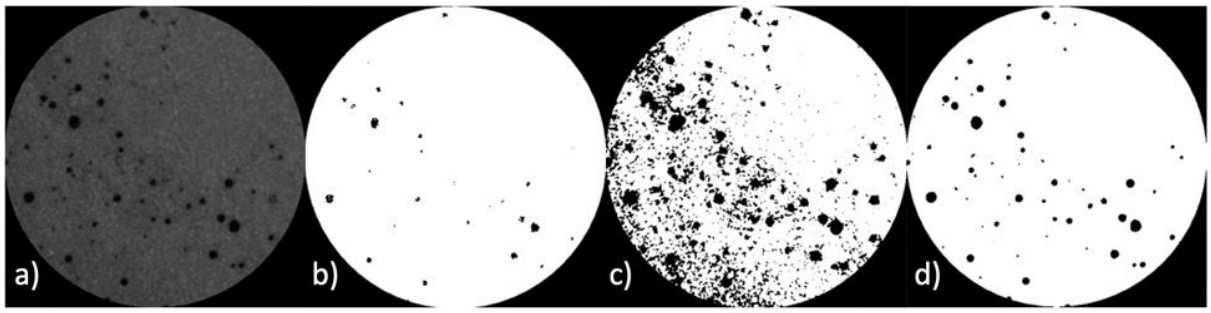

Fig.11- a) 2D image of a Biodentine obtained by CTAn; b) Low thresholding, not showing all the pores that the image contains; c) High thresholding, showing the pores contained in the image and noise artifacts; d) Correct thresholding, showing only the pores

Table 4 shows the task list applied to the surfaces (Fig. 12) of the samples.

Table 4 – CTAn task list applied to the surfaces of the samples

Thresholding	o Defining the Greyscale Indexes (Between 1 and 255)
Despecke 1	o Sweep (3D space) o Remove: All except the largest object o Apply to: Image
Despeckle 2	o Remove black speckles (3D space) o Volume: Less than 40 voxels o Apply to: Image
3D Analysis	• Basic Values (Total VOI volume, Object volume, Percent object volume, Total VOI surface, Object surface, Intersection surface…) • Additional values (Structure thickness, Structure separation and number of objects)

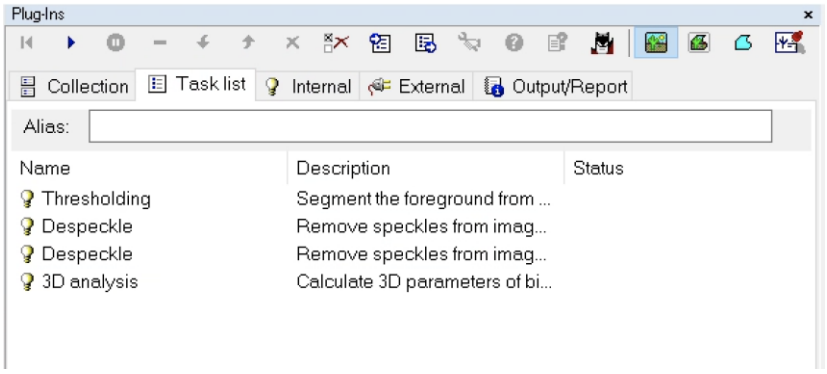

Fig.12 – Task list for surface analysis (CTAn)

4.3.5.2. Bulks

The analysis of the bulk consisted also in choosing the most appropriate thresholding for each sample, followed by a more complex custom processing that includes the respective thresholding, two different despeckles, 2D analysis, 3D analysis. On the analysis of the bulk, some different parameters were used. The 2D analysis was applied to the bulk, in order to understand how the size of the pores vary from the different zones of the bulk, by giving the 2D analysis of all images of a dataset inside the region of interest. On the bulks, after the 2D and the 3D analysis, the open dataset was reloaded without deleting the selected ROI on the creation of the task list. After the reload, a different thresholding was defined by adding 4 units to the previous thresholding, in order to define the error. Posteriorly, the same two despeckles were add to the process and, finally the 3D analysis was the last process to be add on the task list, with the goal of understanding how the values of porosity changed with the error defined on the thresholding.

The table below shows the task list applied to the bulks (Fig. 13) of the samples containing the following features:

Table 5 - CTAn task list applied for the bulks of the samples

Thresholding	○ Defining the Greyscale Indexes (Between 1 and 255)
Despeckle 1	○ Sweep (3D space) ○ Remove: All except the largest object
Despeckle 2	○ Remove black speckles (3D space) ○ Volume: Less than 40 voxels ○ Apply to: Image
2D Analysis	○ With all the results
3D Analysis	○ Basic Values (Total VOI volume, Object volume, Percent object volume, Total VOI surface, Object surface, Intersection surface…)

	○ Additional values ((Structure thickness, Structure separation and number of objects)
Reload	○ Apply to: Image (reloading the image without deleting the ROI created)
Thresholding	○ Defining the greyscale indexes by adding 4 units to the thresholding used on the beginning of the process
Despeckle 1	○ Sweep (3D space) ○ Remove: All except the largest object
Despeckle 2	○ Remove black speckles (3D space) ○ Volume: Less than 40 voxels ○ Apply to: Image
3D Analysis	○ Basic Values (Total VOI volume, Object volume, Percent object volume, Total VOI surface, Object surface, Intersection surface…) ○ Additional values ((Structure thickness, Structure separation and number of objects)

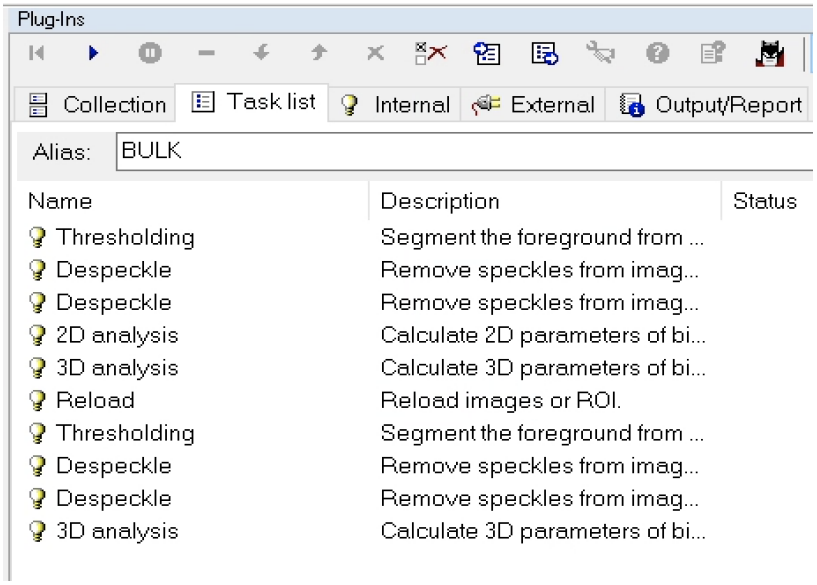

Fig.13 – Task list for bulk analysis (CTAn)

After this analysis, we obtain Microsoft Excel files with information corresponding to information of every sample. The 2D and 3D analysis gave some information about the different types of porosities (open, closed and total porosity) and also the number of pores in each slide of each sample. Structure thickness and structure separation had also a great importance in this analysis, since they provide essential information about the sample's porosity. The structure thickness gives an insight into the thickness distribution of the walls that make up the pores, basically it is defined as the diameter correspondent to the largest sphere that encloses the pore within the structure, and the structure separation gives information about the structural matrix, being interpreted as the distance between two parts of the same structure [98].These two parameters allow the visualization of the results in a three-dimensional way through the use of rendering software called CTVox (Fig. 14).

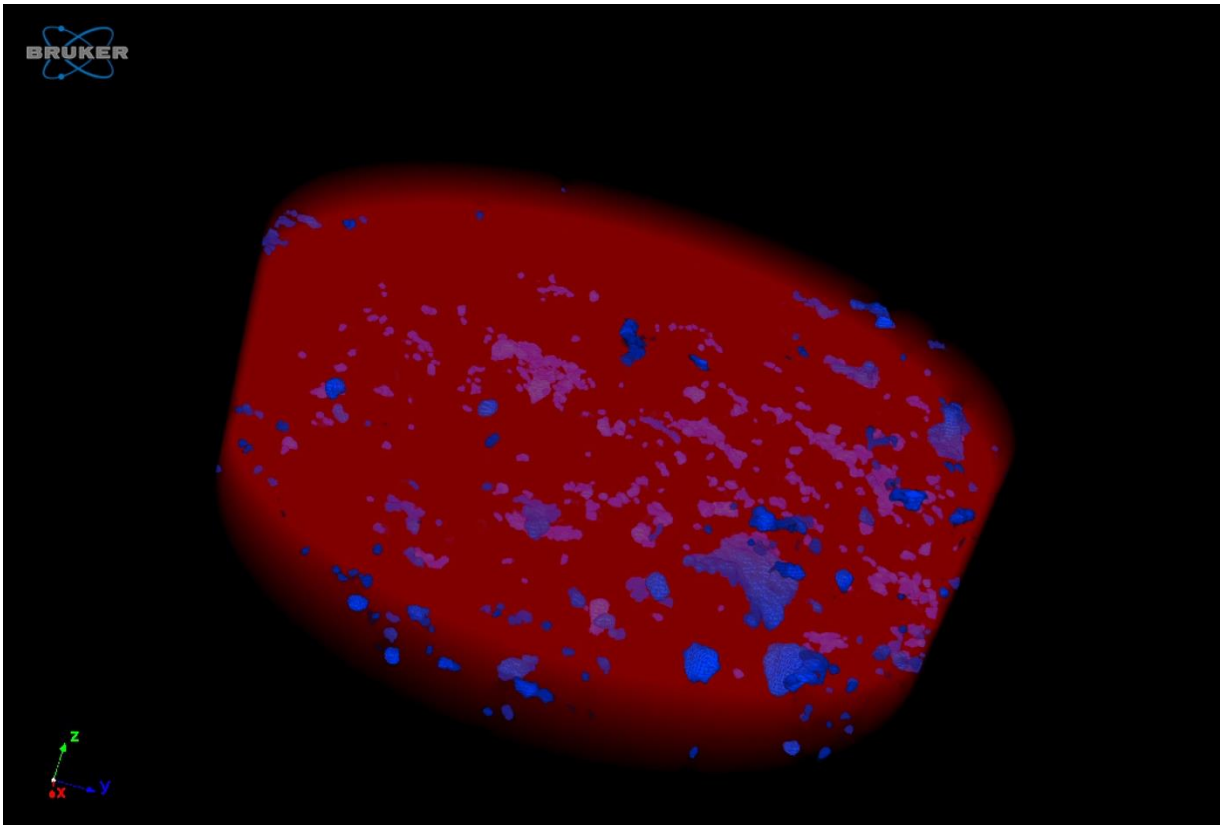

Fig.14 – 3D image of BG10_W sample. In red the dental cement structure. In blue the porosity

4.4. SPSS – The fundamental tool for the interpretation of the results

After data acquisition through nano-CT, a more detailed analysis of the results obtained would be necessary to pragmatically make conclusions. The data collected after the reconstruction by the NRecon software, gave rise to sets of 200 slices for all samples, with some exceptions in which the sample proportion was, either greater or less, depending on the dimensions of the manufactured cement samples.

The slices, which correspond to 2D images acquired after the incidence of x-rays in the sample during acquisition, all have different porosity values, as well as different areas of the different types of pores (closed and open). Therefore, it was necessary to use statistical analysis methods in order to make possible a certain organization of the data. The software used was SPSS, which related the

acquired data in a way that its reading was, thus, possible. The tests carried out using this software were varied, and had as main focus, the comparison between the samples relating their variables, especially the material that composes the dental cements, the time of immersion and the medium where the samples were immersed.

The materials used in this study were then analyzed taking into account the medium (FBS or mQ water) and the three different maturation times. 9 samples of each material were manufactured, divided by the three maturation times (3 samples for 1 day of maturation, 3 samples for 7 days of maturation and 3 samples for 28 days of maturation), making a total of 126 samples analyzed and scanned by Nano-CT. Some of them ended up being discarded due to problems during their manufacture that gave rise to broken samples and that would lead to skewed results and therefore were not analyzed. There were 8 samples not analyzed, including one on the first day (n1.00_W) (Fig.16), one on the seventh day (n1.00_W) and six on the twenty-eighth day (one of n0.5_FBS, one of n0.5_W, one of n1 .00_W, two of n2.00_FBS and one of TCS_FBS), the reason for not analyzing these samples was constant in all of them, all of them showed cracks that would induce an increase in porosity levels after analysis by CTAn, since this software counts all the void as pores and, in these cases, the porosities would be influenced giving rise to false and extremely high values.

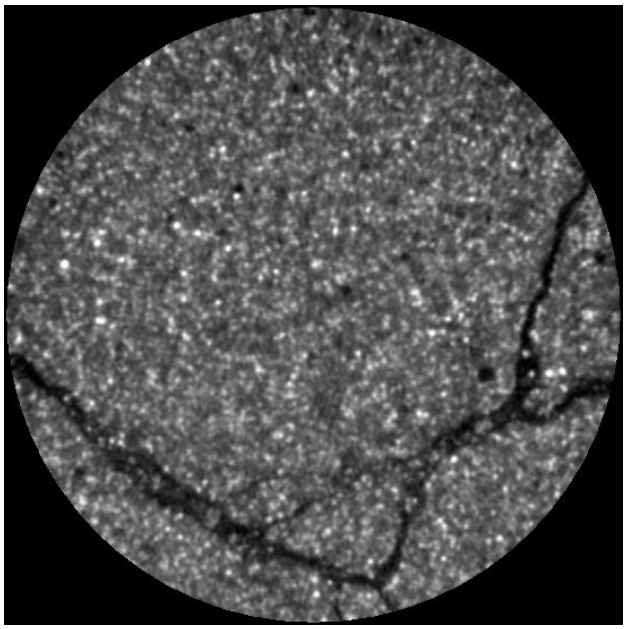

Fig.15 - CTAn image of nAg1.00_W acquired by Skyscan 2211, a broken sample that was not analyzed due to the observed fractures

All viable samples were analyzed and the data for each one was transferred to an Excel document, so that it was easier to identify possible differences in the level of porosity among them, always taking into account the different variables associated with each of the sample (maturation time, maturation medium, type of material, etc.).

5. Results and Discussion

As mentioned before, one of the objectives of this project was to examine the microstructure of dental cements samples using computed tomography techniques and optimize the operational parameters of the equipment aiming the output of adequate 3D images of the surface and bulk of the samples. An important microstructural parameter is porosity since it affects not only mechanical properties (closed porosity) but also the possibility of penetration of different oral fluids and bacteria potentially harmful for the unprotected dentin (open porosity)[99]. A second objective of this project was to evaluate and understand how porosity changes with maturation time (1 day, 7 days and 28 days of incubation were tested).

To facilitate the execution of a statistical analysis, the open and closed porosity values were analyzed together, giving rise to final porosity values. These final porosity values were estimated for different cements and for different maturation times.

5.1. Nano-CT and its relevance in the study of the porosity

The samples were received after maturation and were analyzed according to their maturation time. The first samples to be analyzed corresponded to 1 day of maturation and were first analyzed in MicroCT (SkyScan 1172). However, due to the small dimensions of the samples (3 mm thickness, 4 mm diameter), the cements did not reveal the intended results, since it was impossible to identify the corresponding porosity levels for each sample with a high degree of certainty. It was then necessary to scan the samples by Skyscan 2211, which is a multiscale CT equipment since allows the micro and the nano resolution. This equipment was then used due to its greater power, allowing a greater flow of X-rays at the same time which reduces the acquisition time. Besides that, the X-ray detector used on the Skyscan 2211, has a much larger active area, making possible the acquisition of 3 samples simultaneously in each image. Taking into account that the resolution used for these samples was 7 μm, it was used micro-CT to evaluate the porosity of the several samples, however the equipment used could reach higher resolution that were not necessary for this study. On these scans, the identification of the pores corresponding to each cement becomes easier, as well as to distinguish the pores from the artifacts associated with the use of this technique. The micro-CT technique and the nano-CT technique differ only in the resolution range of each. The nano-CT device used, Skyscan 2211, in

addition to being a very valuable equipment, the sensitivity coupled with its use, requires a lot of expertise and extreme care when using it. Thus, the use of micro-CT device, Skyscan 1172 was, no doubt, a fundamental step, not only to acquire the perception that the samples needed a more rigorous 3D acquisition, but also to acquire the necessary expertise to handle this complex equipment and so useful for the analysis of small samples. We can thus refer to the Skyscan 1172, as the introductory stage of a porosity study whose main objective is to elucidate about the evolution of porosity during the maturation of these dental cements in periods of 1, 7 and 28 days.

After analyzing some samples with 1 day of maturation with Skyscan 1172, it was then possible to conclude that the scanning of the samples was taking high periods of time in order to achieve the ideal level of detail, leading to the need of all samples being analyzed using the nano-CT device.

The nano-CT device proved to be the most efficient and time-saving technique as it allowed to identify both open and closed pores and the acquisition of the images takes less time, due to the increased flow of X-rays. Its interpretation was only possible due to the level of detail provided by this nondestructive technique. Another detail that proved to be crucial was the inclusion of zirconium oxide in all samples, since as a radiopacifier, it increases the inherent radiodensity of each cement, allowing its visualization during the analysis.

After the reconstruction of all slices in each sample, the segmentation continued to be necessary. In the analysis performed with the CTAn, it was necessary to calibrate the software in order to define a gray scale corresponding to the 2D images of each slice (Fig.15). This interpretation was established according to the colors of the voids (pores) and cement, so that they could be distinguished. Each sample required a rigorous interpretation, so that it was possible to verify what would be a pore and what would be cement. In these cases, and even after the correction of the artifacts, it may happen that some of the pores counted are related to artifacts that were not detected in the correction performed in each sample.

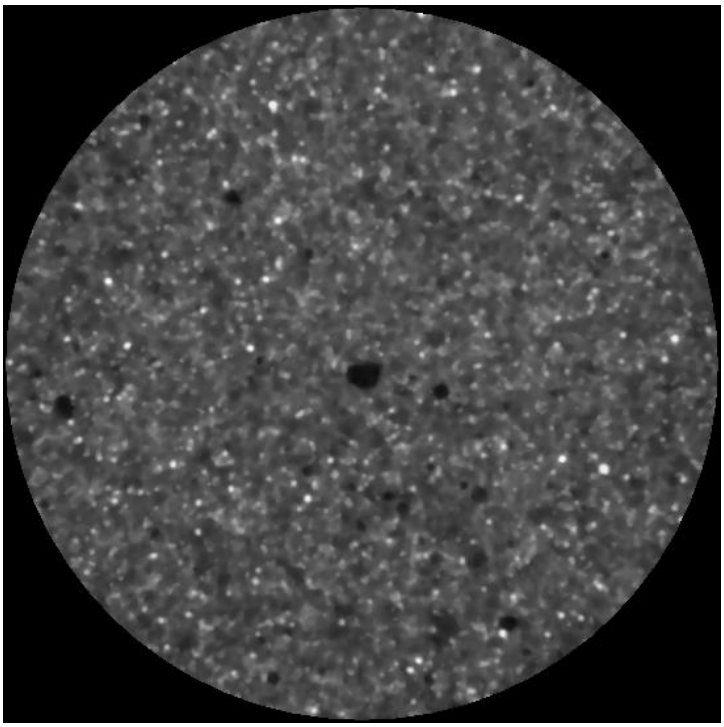

Fig.16 – CTAn image of BG10_FBS (Slice number 140) acquired by Skyscan 2211. The black voids represent the pores, while in grey and white correspond to the materials that composes the cement

5.2. Surface Porosity

There are two principal objectives related with the analysis of the total porosity in the surfaces; the first is to understand how the porosity behaves in the volume of the sample and the second main objective is to compare the surfaces of all of them and understands how it differs. Also, the comparison between the total porosity in the surfaces with the porosity obtained in other volumes of the samples (the base, the middle, the final of the bulk and the entire bulk itself) is of great interest, since it shows us how the porosity varies between them. On the Fig.17, we can see the total porosity in the surface of the samples, which has as its maximum on nAg0.50 immersed for 1 day in mQ water with 7.26%, and its minimum on the Biodentine samples immersed on FBS for 28 days with 0.25%, making the average of the total porosities in all the samples in both mediums and for the three maturation periods as 1.86%.

The first information to be acquired was the data corresponding to the surfaces of the cement samples, consisting of 4 slices, which total thickness corresponds to 28 μm. The main objective was to

compare total porosities in the different zones of the cement samples. The time evolution of the total porosity at the surface for all the samples obtained by SPSS is shown in Fig.17. It is observed that, in most types of the samples, the surface porosity for that treated for one day was higher than that after longer maturation periods (7 days and 28 days). However, in 4 of the 12 types of samples, the highest porosities were recorded after 28 days (BG10_W, BG20_FBS, n0.50_FBS and n2.00_FBS) and only in the Biodentine samples (Biodentine_FBS and Biodentine_W) after 7 days. In 10 of the 14 types of cements and maturation mediums analyzed, the lowest surface porosity was found at the end of 7 days of maturation. It should be noted that the referred surface porosities are only and always open pores, since closed pores are not found at the surface.

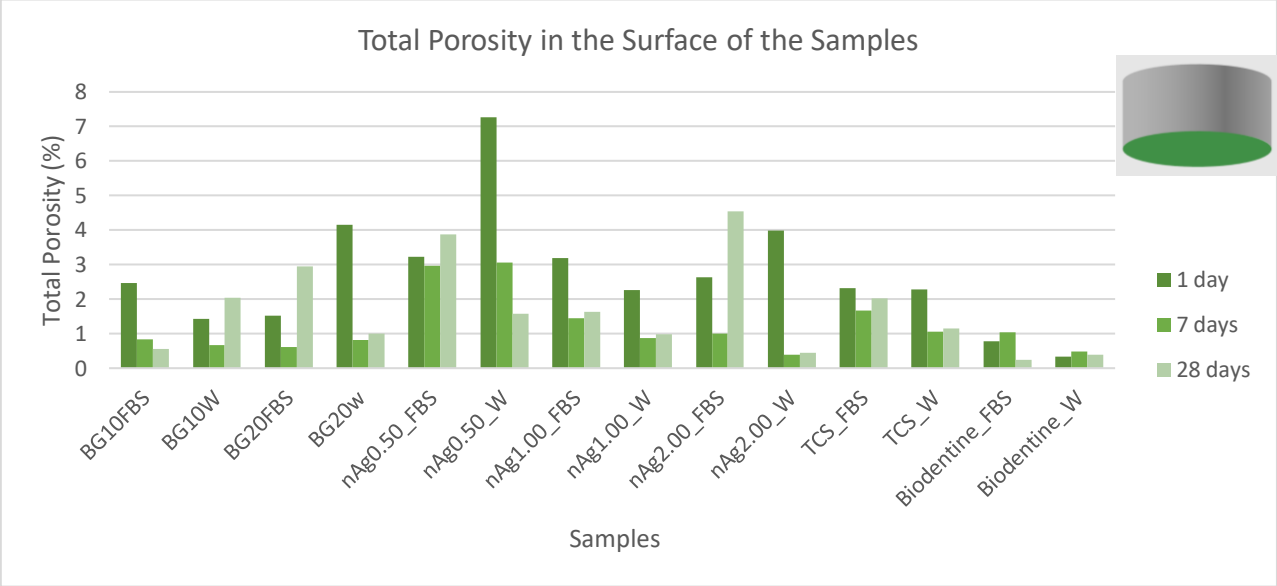

Fig.17 – Total porosities (open pores) obtained on the surfaces of every type of samples immersed in FBS and in mQ water.

5.3. Bulk Porosity – How is the porosity levels on the bulk of the samples?

After analyzing the sample surfaces, the next step was to analyze the bulks of all of them in order to understand how the different materials, the different maturation media, and the different maturation times influence the total porosity (open and closed) of the bulks of each sample. Initially, the bulks were analyzed as a whole, that is, all the slices that make up the bulk were taken into account.

As all of these bulks are mainly made up of 200 slices, the results obtained through this analysis do not show the eventual differences in porosity between the beginning (the base of the bulk), the middle and the end of the bulk, but refer to the averages of all slices.

As shown in the bar chart represented on Fig. 18, the porosities remain relatively constant in all materials, that is, there are no abrupt differences between most of the different types of cements, with porosities being relatively similar among them. It is also notable the difference between the porosity values on the bulk of the samples (Fig.18) when compared with the total porosity present on the surface of the samples (Fig.17), being the average total porosity value on the bulks 0.73% and the average total porosity on the surfaces 1.86%, revealing a much lower total porosity on the bulks. The highest total porosity found in the bulks is related to the nAg0.50 samples immersed in FBS for a 28-days period with a total porosity of 4.78%. On the other hand, the lowest total porosity found on the bulks refers to the Biodentine samples immersed on mQ water for a 7-days period with 0.03%. Also, on Fig.18, it was also possible to observe a significant difference between the porosities of samples of nAg 0.50 and nAg 1.00 matured in fetal bovine serum (FBS) for 28 days as compared to that of the remaining samples as the total porosities (open and closed pores) of nAg 0.50 and nAg1.00 samples are much higher than in the other samples in the third maturation period when immersed in FBS.

On the same graph it can be seen that, not all the samples show a decrease in their total porosity when increasing maturation time. As observed the porosity of the samples matured in mQ water tend to decrease with the increasing maturation time whereas samples matured in FBS do not follow this pattern, since only three among the seven samples matured in FBS have the lowest levels of porosity after 28 days of maturation. It is also possible observe by analyzing the figure that the porosity of the bulks of the Biodentine samples are much lower when compared to that of the other samples, thus showing a difference between this commercial cement (Biodentine) and the prototype cements (BG,nAg and TCS).

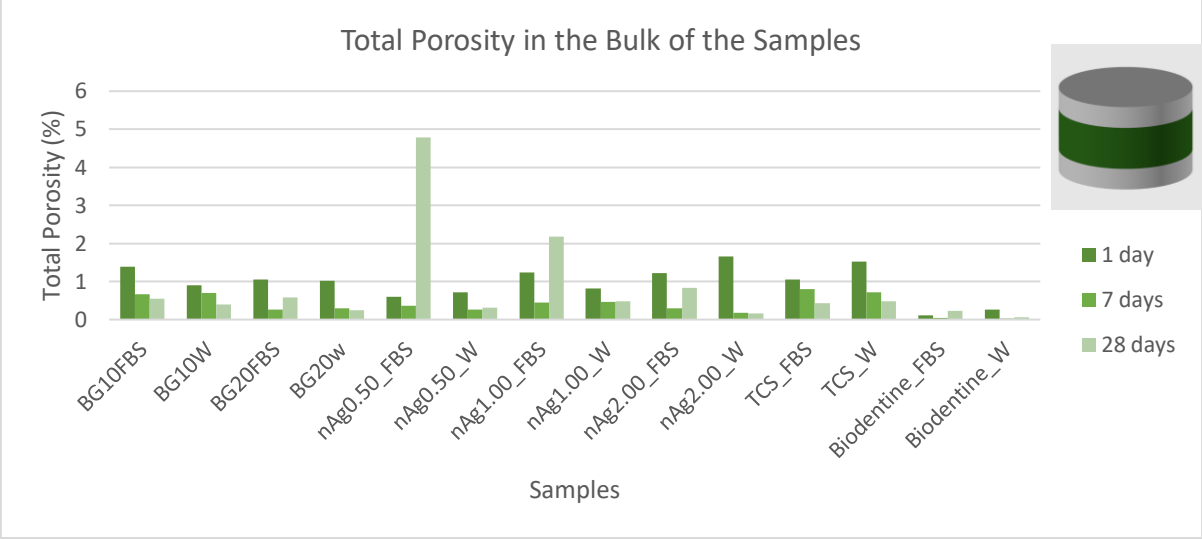

Fig.18 –Total porosities obtained on the bulks of every type of samples immersed in FBS and mQ water

This analysis allows some comparisons that are of great interest and that can help us understand certain differences between the types of viable sample analysis. One of the comparisons that would be relevant at this point in the study is the comparison between the porosities of bulks and surfaces.

5.4. Surface Porosity vs Bulk Porosity

Fig.19 compares the total porosities on surfaces and bulks at the end of 1 day of maturation, both represented in Fig.17 and Fig.18, respectively. In none of the samples the total porosity is higher in the bulk region, which reveals that surfaces are more susceptible to develop pores than the bulk in each sample. It is also concluded that the nAg0.50 samples, immersed in mQ water, show the greatest discrepancies between their surfaces and their bulks. It is also concluded that nAg0.50 samples, immersed in mQ water, evidence the highest difference between surface and bulks porosities: as their surface porosity has the highest values and their bulks have the lowest one when compared to the other non-commercial samples for equivalent maturation times, the delta of porosity is thus

maximized. The Biodentine samples showed again the lowest porosities, not only on the surface, but also in the average of the 200 slices (bulk), which makes them the less porous analyzed material.

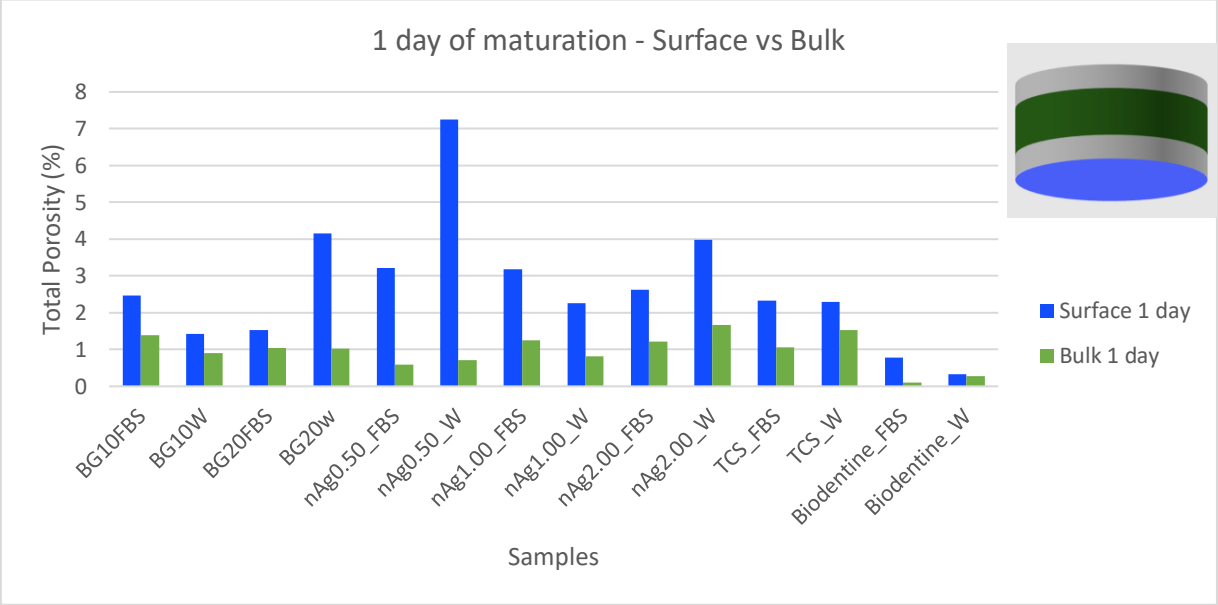

Fig.19 – Comparison of total porosities obtained on the surfaces and in the bulks of every type of samples after 1 day of maturation in FBS and in mQ water

For maturation periods of 7 days, the results revealed that the total porosity decreased substantially as compared to samples in which the maturation period was only 1 day. Although, this decrease can be observed both on the surfaces and on the bulks, the greatest discrepancy in porosity values remains between the surfaces and the bulks of nAg0.50 samples.

The total porosity of nAg0.50 samples is about 10 times larger on surfaces than on bulks, which may indicate some difficulty existing during the preparation of these samples, thus suggesting some heterogeneity in the porosity distribution throughout the sample. This may account for the different porosity values in nAg0.50 samples. The bar graph of Fig.20 also shows that there is a type of sample in which the bulk porosity was found to be superior than the total porosity found on the surface, these samples are the BG10_W, and even though this difference is very small, it may be an indication that these samples are quite homogeneous in content, since they have relatively close levels of porosities throughout their length, these means that both densities in the bulk and surface of BG10 samples

immersed in mQ water have similar values. This same type of samples, but matured in FBS, also presented small differences between bulk and surface porosities, which may indicate that BG10 are relatively homogeneous samples, with low and constant porosity throughout the sample.

By observing the Fig.20, where it is compared the total porosities on the surfaces and on the bulks of the samples, it is also notable that, apart the nAg0.50 samples, the biggest difference between the porosities found on the bulk and on the surface are present in the Biodentine samples, where the values of the surface porosity revealed to be not so much different from the prototype cements, however, it can be noted that the bulk porosity of Biodentine samples after 7 days of immersion are the lowest compared with all of the other cements.

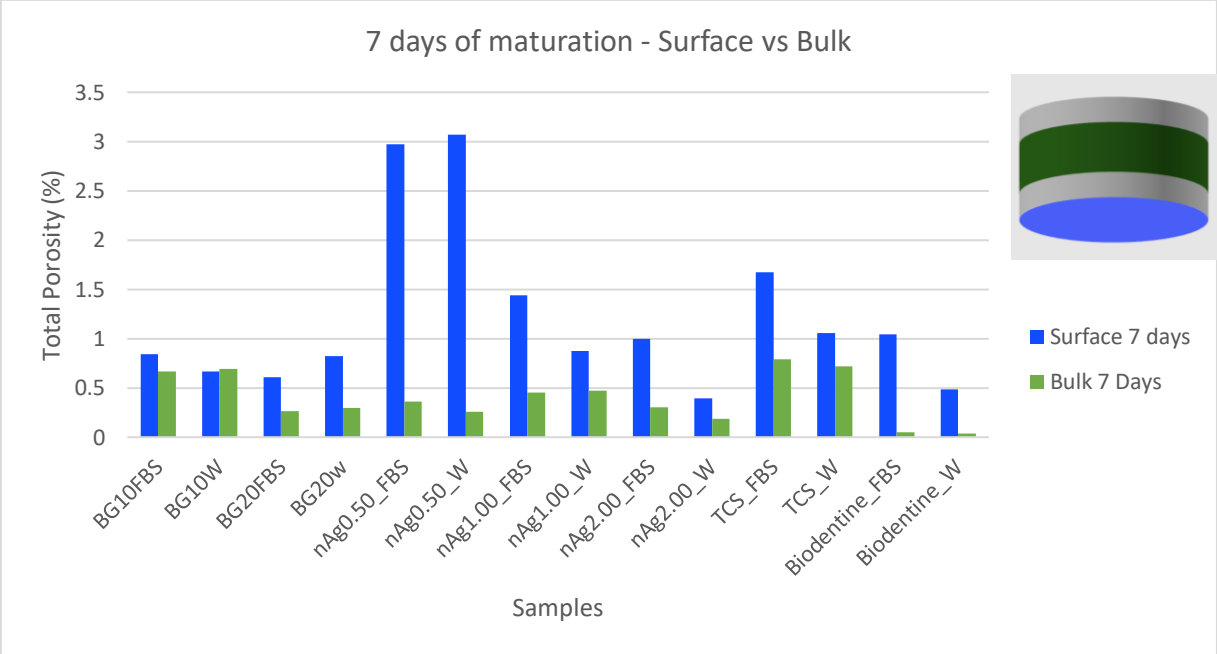

Fig.20 – Comparison of total porosities obtained on the surfaces and in the bulks of every type of samples after 7 days of maturation in FBS and in mQ water

Samples matured in FBS and mQ water in periods of 28 days (Fig. 21) yielded higher porosity values when compared to samples matured in 7 days in most of the types of dental cements analyzed. However, this evidence is not common to all types of samples: the bulks of samples matured in mQ water at the end of 28 days have very low porosities when compared to samples matured in FBS during

the same maturation time. Samples matured in mQ water at maturation times of seven and 28 days are quite similar, with no substantial differences with increasing maturation time.

Nonetheless, the surface porosities present, in almost all samples, higher values at the end of 28 days when compared to the surface porosities acquired at the end of seven days, being the exceptions BG10_FBS, nAg0.50_W and the Biodentine samples, both immersed and FBS and mQ water.

These results may be an indication that the samples are sufficiently aged at the end of seven days, this being the pivotal period in which the cements should be perfectly monitored, since they are more likely to generate changes in the levels of porosity during this period of time.

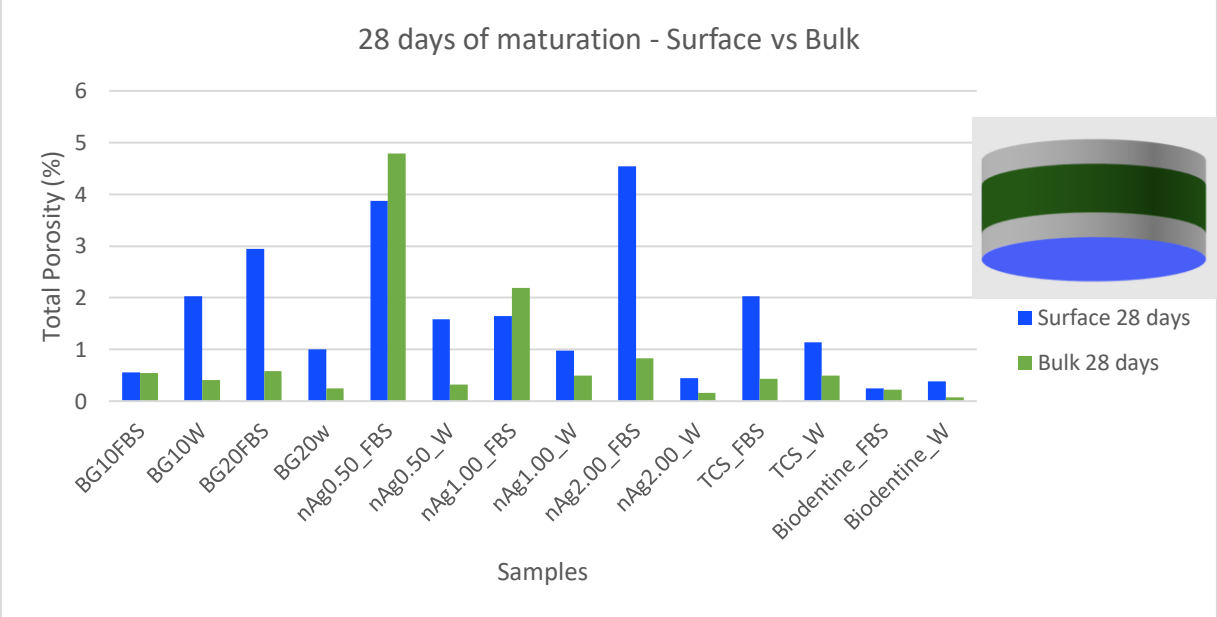

Fig.21 – Comparison of total porosities obtained on the surfaces and in the bulks of every type of samples after 28 days of maturation in FBS and in mQ water

Taking into account the data provided by the Fig.21, even though the analysis shows some important information about the way in which the porosities vary between the surface and the bulk of each kind of samples, the analysis should be more detailed, and should go through the bulk of the contents. The bulks have large dimensions (between 100 and 300 slices), and it is not possible to see if

the total porosity varies throughout its length, as the information acquired is the average of all slices included in the bulk.

This comparative analysis proved to be inconclusive, since all the relationships found have their exceptions, meaning that each cement behaves differently even taking into account the same variables. In fact, besides the different materials in the cements, they include different relative contents and above all the various cements were prepared under uncontrolled pressing conditions which does not assure similar procedure. Despite this limitation, the study of the different samples and the exploration of all parameters associated with the acquisition of data in the nano-CT equipment was very enriching and allowed to understand how to manipulate and take advantage of one of the most powerful technologies presently available for microstructural studies.

5.5. Bulk of the samples – Base, middle and final slices

As mentioned earlier, the number of slices in each bulk was too high and did not allow a rigorous assessment of the total porosity of the bulks, since the values acquired as total porosity were, simply, the average of all the slices that constitute the bulk of the samples. Thus, and in order to make the whole analysis more rigorous, each bulk was divided into three distinct segments, the base, the middle and the end of the bulk, each of these segments with 20 slices each, and it is represented on the Fig.22.

The basis of the bulk was defined as the first 20 slices that follow the 4 slices that make up the surface of each sample; the middle of the bulk was established as the 20 slices that are exactly in the middle of the bulk and the end of the bulk was determined as the final 20 slices that correspond to the end opposite the bulk base. In this more detailed analysis, it was expected to find the lowest porosity values in the 20 slices included in the middle of the bulk, since it is in the most inclusive areas of dental cement that the greatest homogeneity of materials is found, so the amount of void would be quite reduced when compared to other sections of cement. This was the initial hypothesis generated before performing this analysis, however it would be important consider that the sample bulks are made up of a large number of slices, however, they do not constitute the entire cement.

The samples, when scanned, generated an extremely high number of slices that had to be selected so that they could be analyzed later, that is, from the totality of slices, four slices were selected that

would correspond to the surface of each sample and about 120-300 slices (depending on the sample) that would correspond to the bulk, with the rest of the sample being neglected. This rest, in some samples, may even be higher than the volume considered for analysis, but it was estimated that the cement microstructure remained similar in remaining volume, thus not needing to be subjected to a detailed analysis.

Hence, the 20 slices corresponding to the end of the bulk, may present porosities very similar to the 20 slices corresponding to the middle of the bulk, since both may correspond to the central part of the dental cement thus exhibiting very similar degrees of homogeneity.

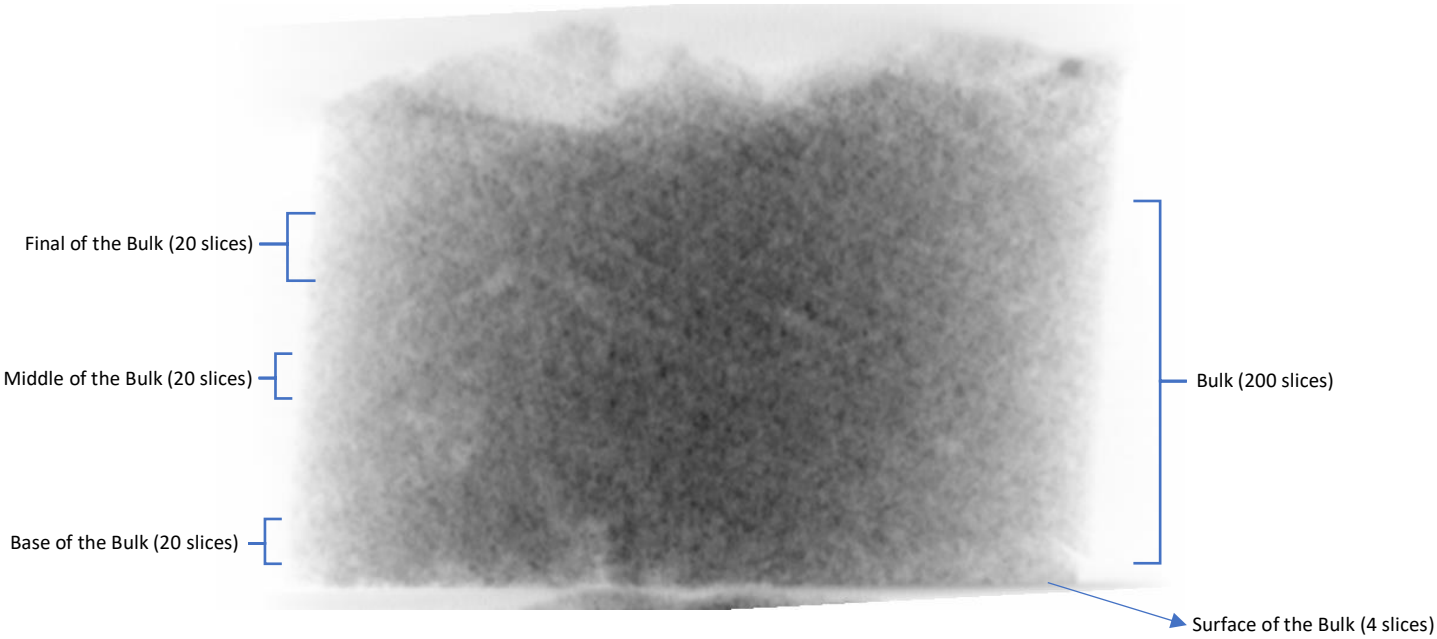

Fig.22- Image of a sample of BG10_FBS with the identification of the different volumes analyzed. All the samples were divided into these different volumes with the objective of understanding how porosity varies.

5.6. The 20 slices corresponding to the base of the bulk

The porosities in the 20 slices that are immediately after the four slices of the bulk, have total porosities relatively similar to the slices corresponding to the sample surfaces. However, in general the porosities are more reduced, which shows a decrease that will easily be related to the homogeneity of

the materials in the samples throughout their volume. Fig.23 shows the comparison between the bases of the bulk of the samples for the different maturation periods, in which it is possible to identify that the samples do not show a uniform trend in reducing the total porosity, as expected. This could be due to the fact that each sample was hand spatulated, involving different pressures, on this way, it was impossible to have every sample with the same behavior in terms of porosity in the base of the bulk, which explains the variable trend on the percentages of total porosity in each sample, regardless of the variables (time of maturation, medium of maturation, material, etc.).

As in the slices of surfaces and bulks, there is an evident reduction in porosity between the first and the seventh day of maturation. However, there are exceptions to the rule, where the total porosity was larger at the end of the seven-day period of maturation as is in the case of the BG10_FBS samples. On these samples, the total porosity increased at the end of the seventh day of maturation and decreased again when they are matured in the respective media (FBS) for 28 days. In the samples referring to the cements nAg0.50, nAg1.00 and nAg2.00, only nAg1.00 and nAg2.00, both matured in mQ water showed a decrease over time. All the other samples including silver nanoparticles in their constitution, showed a decrease in porosity at the end of 7 days and a substantial increase at the end of 28 days of maturation that proves to be far larger than the porosities found in samples after 1 day of maturation.

The nAg2.00 cements presented high porosities when matured for 1 day, but in the other two maturation periods, the samples presented very low total porosities in the two different media. And it can even be said that they exhibit the lowest porosities throughout the study of the bases of the bulk of the prototype materials, thus making it possible to deduce that nAg2.00 samples have some stability after a period of 7 days.

The cements with inclusion of Bioglass (BG10 and BG20), revealed different behaviors. However, only one in the four types of samples analyzed (BG10FBS, BG10W, BG20FBS and BG20W) showed a decrease of the total porosity between 7 and 28 days of immersion, this type of sample was the BG10FBS and also presents its higher porosity at the end of a 7-day immersion when compared with the other two maturation times.

The base of the bulk of the Biodentine samples, revealed, once again, the best results. Having on the 7-day, the lowest percentage of total porosity (0.108%-Biodentine_FBS;0.0585%-Biodentine_W).

These were also the lowest porosities analyzed on the bases of the bulk of all samples, revealing that this commercial cement presents a really low number of pores when compared with the protoype materials analyzed. However, at the end of an immersion of 28 days, it is possible to visualize that there are some prototype cements which reveal really similar porosities when compared with the Biodentine samples, both in FBS and mQ water. These samples are the BG20_W and nAg2.00_W and nAg2.00_FBS.

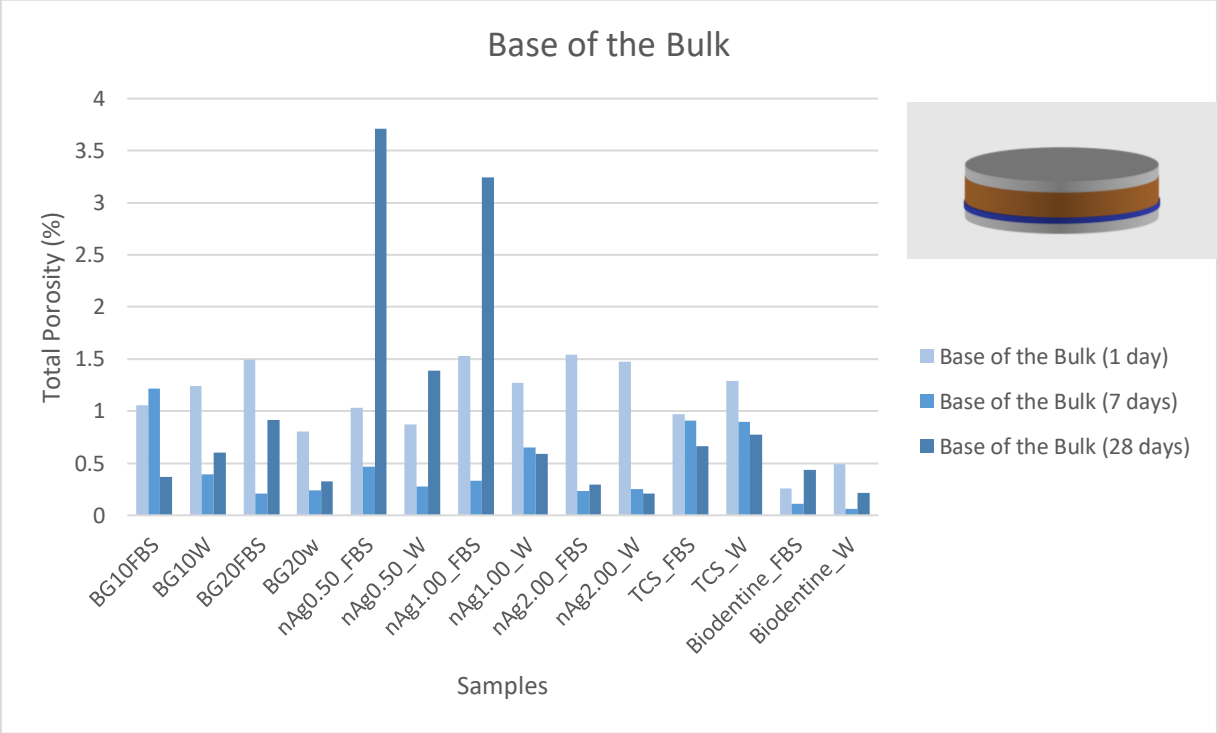

Fig.23 – Total porosities obtained on the base of the bulk of every type of samples for all the maturation periods (1 day, 7 days and 28 days)

The comparison between the total porosity on the surface and the total porosity of the 20 slices that makes up the base of the bulk and other analysis that were also made in order to understand how the porosity varies between the 20 slices corresponding to the middle of the bulk and the 20 slices that makes up the final of the bulk are presented on the annex A and annex B.

5.7. FBS vs mQ Water: How the mediums affect the different dental cements?

During this study, besides the four types of samples to be studied, two different maturation media were used as well.

The mediums used were the fetal bovine serum (FBS) and mQ water, the first of which had as its main objective the mimic of the environment achieved in the oral cavity, in order to enable the study of the behavior of these cements at the time of their application since their properties are similar to the properties of tissue fluids. MQ water, on the other hand, as a conveniently inert solution, will not react after immersing the cements, making these media chemically non-reactive.

Fig.24 to 30 represent the compilation of all the results corresponding to the 100 samples studied. In each bar chart, sequentially and from left to the right, are presented the surface porosities (shades of blue), the average total porosity (shades of orange), the bases of bulk (shades of yellow), the middle of the bulk (shades of green) and, finally, the final of bulk (shades of red) for the three maturation periods (1, 7 and 28 days). In each figure, left bar chart corresponds to the maturation carried out in FBS and the chart on the right to mQ water.

In general, the total porosities of the samples that were matured in mQ water tend to be lower than those matured in FBS. The reason accounting for this difference may be due to the fact that the medium composed of mQ water, as an inert solution, will not react with the dental cements, making these medium chemically non-reactive to the cements, and on this way does not increase the porosity of the samples over time.

Furthermore, the charts also show that, in most of the analyzed cements, there is a tendency for the decrease of porosity with the increase in the maturation time. Additionally, it is also noticed that the total porosity tends to decrease as we move from the surface layer down into the bulk of the samples. Among the 6 different types of samples, it is noticeable that some cements present lower total porosities in both media when compared with the others (BG10, TCS and Biodentine. Among all the various types, BG10 samples are the ones presenting values of total porosity with a relatively regular time variation. As observed, the evolution of the total porosity of BG10 over the three maturation periods shows a uniform decrease with the increase in immersion time, which is a promising result because when applied on the teeth, the decrease of porosity over time indicates a smaller

probability of bacterial biofilm formation and, on instance, closer to what would be ideal for a dental cement, i.e decrease of surface porosities over time, strong antibacterial activity, high biocompatibility with the oral cavity, etc.

Other types of samples are also worthy of notice. For example, BG20, shows the lowest porosity values when compared with the other prototype materials. Also, nAg2.00 showed promising results: the samples of nAg2.00 showed, in comparison with all the others, very low porosities after 7 and 28 days of maturation. However, revealed somewhat labyrinthic details related with the surface porosity, such as its increase after 28 days immersed on FBS and this may be due to the reaction between the medium and the samples since all of them present in its composition tricalcium silicate (TCS) which reacts with animal proteins present on the FBS. This detail is common to most of the samples, being the only exception the BG10 and Biodentine samples.

Despite the general trends of porosity evolution with maturation time commented above, we observe that some samples, in particular the samples nAg0.50 and nAg1.00 matured in FBS, exhibit a minimum of porosity at the seventh day followed by a noticeable maximum on the twenty-eighth day. The manufacture of these two types of samples probably suffered some biases, since the total porosities present extremely high values when compared to those of the same samples matured in mQ water or during different immersion times (1 day and 7 days). These biases are provoked by some small and undetected cracks present on the samples and it is reflected in the high total porosity values.

As a commercial cement, the Biodentine was used since it is a dental cement that is well-established on the market and could be a good comparative term between the prototype cements analyzed. Biodentine cement revealed the lowest porosities among all the samples analyze. This condition of low porosity maybe very advantageous for hindering the formation of a bacterial biofilm: its reduced porosity makes it difficult to bacteria to access the interior of dental cement.

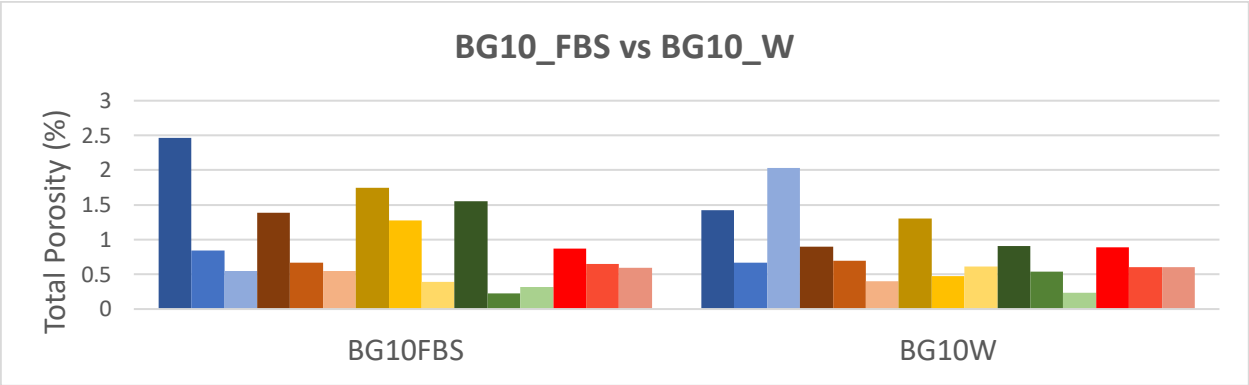

Fig.24 – Total porosities in all the volumes analyzed in samples of BG10_FBS and BG10_W for maturation periods of 1 day, 7 days and 28 days. Sequentially, from left to right: surface porosities (shades of blue), average total porosity (shades of orange), base of bulk (shades of yellow), middle of the bulk (shades green) and final of bulk (shades of red).

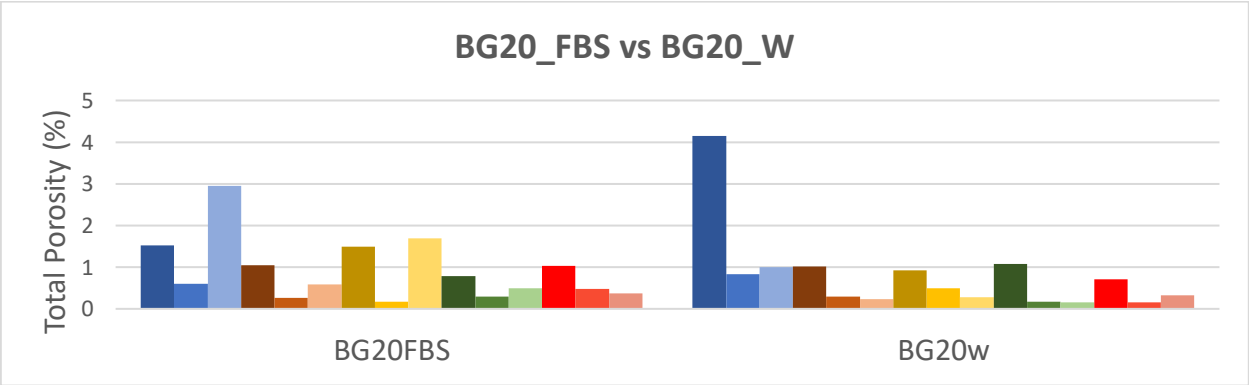

Fig.25 – Total porosities in all the volumes analyzed in samples of BG20_FBS and BG20_W in for maturation periods of 1 day, 7 days and 28 days. Sequentially, from left to right: surface porosities (shades of blue), average total porosity (shades of orange), base of bulk (shades of yellow), middle of the bulk (shades green) and final of bulk (shades of red).

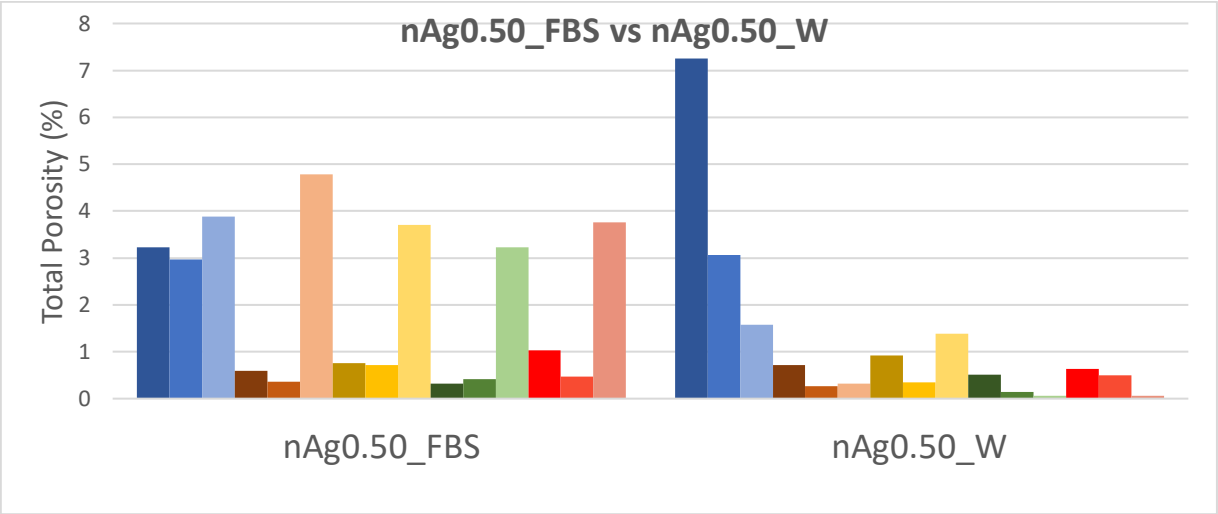

Fig.26 – Total porosities in all the volumes analyzed in samples of nAg0.50_FBS and nAg0.50_ for maturation periods of 1 day, 7 days and 28 days. Sequentially, from left to right: surface porosities (shades of blue), average total porosity (shades of orange), base of bulk (shades of yellow), middle of the bulk (shades green) and final of bulk (shades of red).

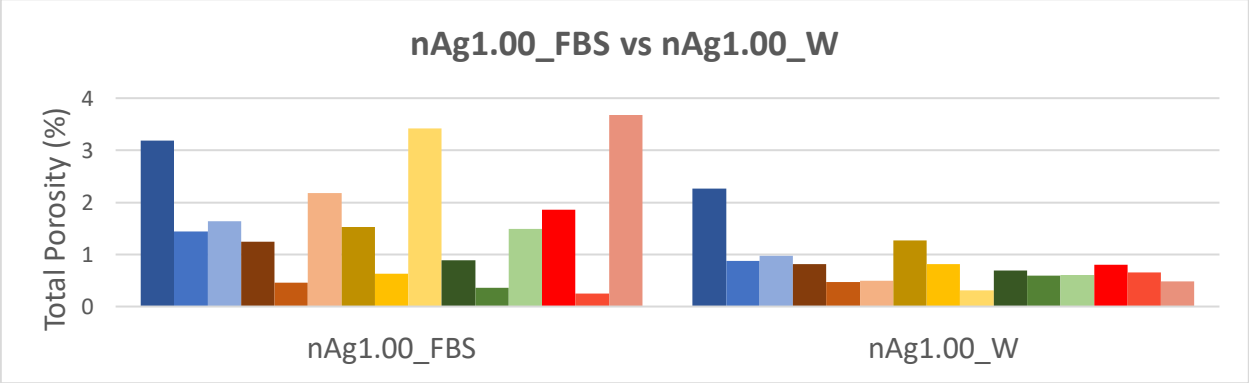

Fig.27 – Total porosities in all the volumes analyzed in samples of nAg1.00_FBS and nAg1.00_W for maturation periods of 1 day, 7 days and 28 days. Sequentially, from left to right: surface porosities (shades of blue), average total porosity (shades of orange), base of bulk (shades of yellow), middle of the bulk (shades green) and final of bulk (shades of red).

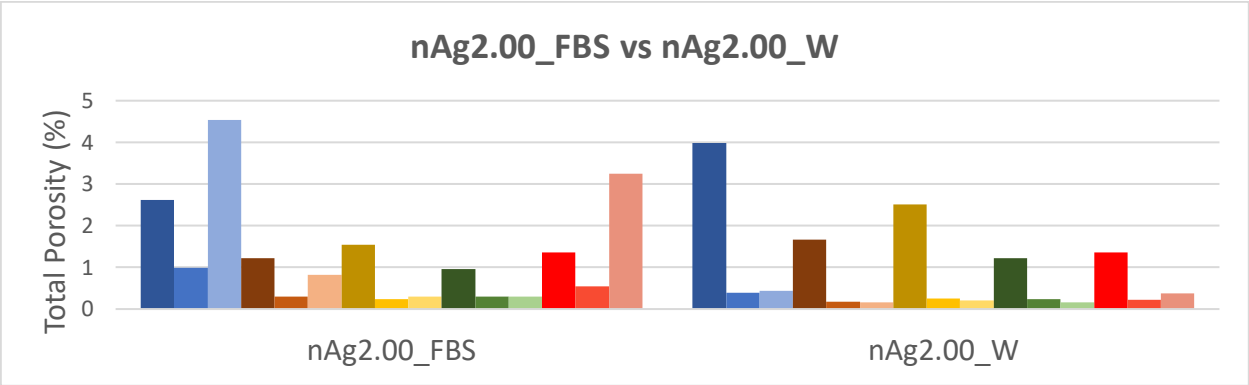

Fig.28 – Total porosities in all the volumes analyzed in samples of nAg2.00_FBS and nAg2.00_W for maturation periods of 1 day, 7 days and 28 days. Sequentially, from left to right: surface porosities (shades of blue), average total porosity (shades of orange), base of bulk (shades of yellow), middle of the bulk (shades green) and final of bulk (shades of red).

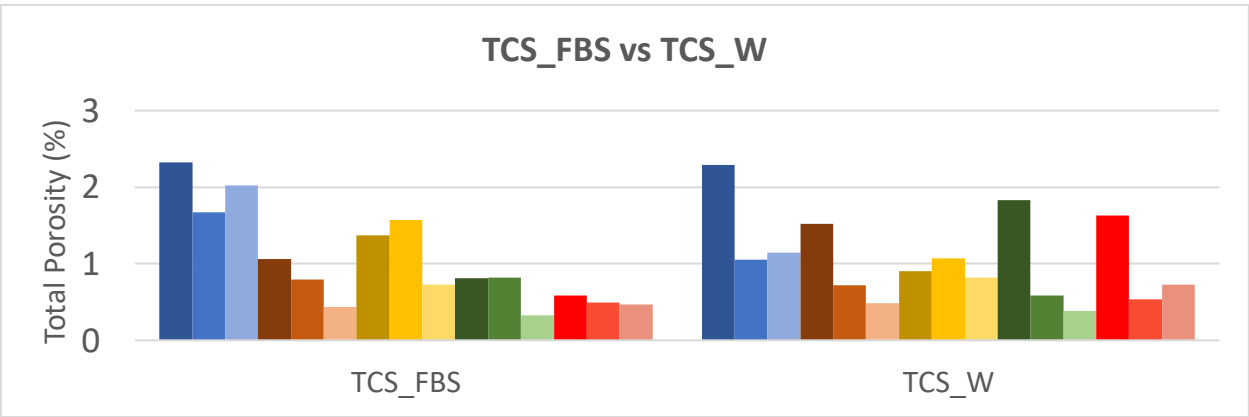

Fig.29 – Total porosities in all the volumes analyzed in samples of TCS_FBS and TCS_W for maturation periods of 1 day, 7 days and 28 days. Sequentially, from left to right: surface porosities (shades of blue), average total porosity (shades of orange), base of bulk (shades of yellow), middle of the bulk (shades green) and final of bulk (shades of red).

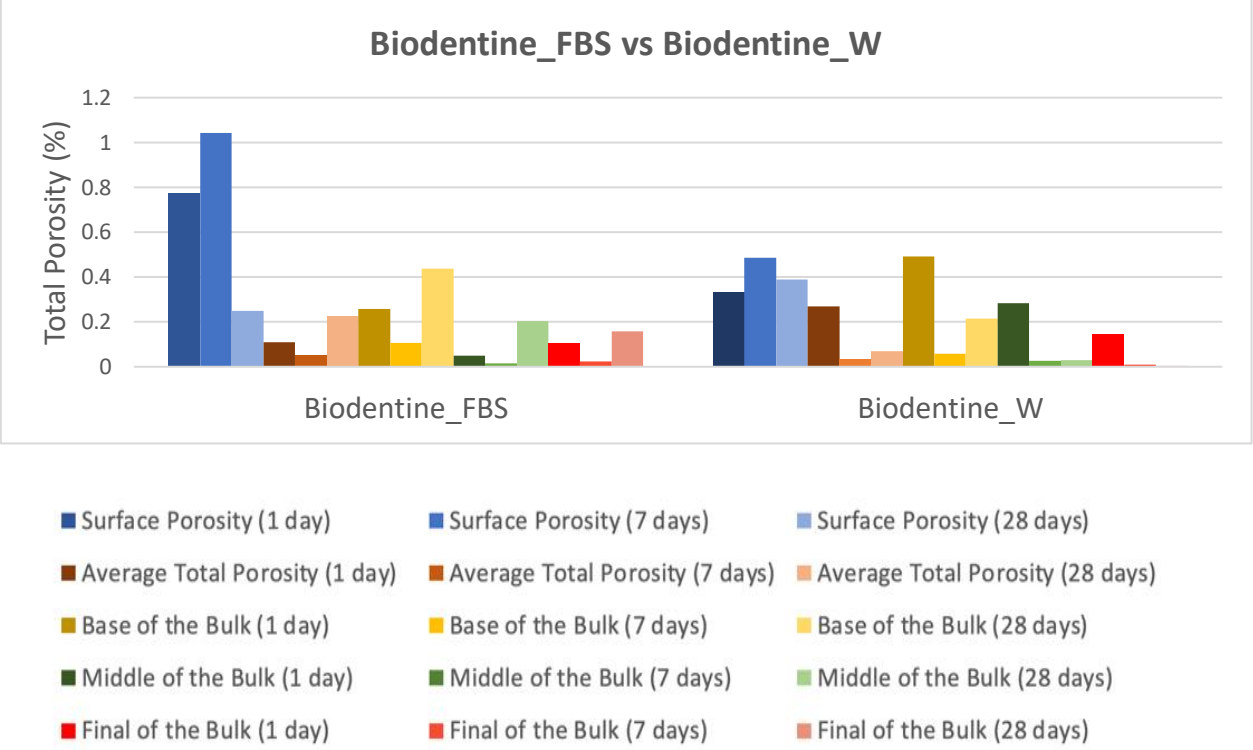

Fig.30 – Total porosities in all the volumes analyzed in samples of Biodentine_FBS and Biodentine_W for maturation periods of 1 day, 7 days and 28 days and the legend of the bars corresponding to each volume.

Taking into account all the materials analyzed, the nAg1.00 samples were discussed in more depth, once the total porosities revealed justifiable trends related with the making process (Uniaxial pressing), the maturation periods and related also with the immersion media.

5.8. nAg1.00 Samples – Effects of the Uniaxial Pressing

All the samples were produced by uniaxial pressing, and as the literature indicates, this method is of high simplicity and of very low cost. This pressing causes a marked friction between the particles of the mixture and the wall surface of the mold in which the samples were pressed. This process results in a cement with different density gradients, as described by *G. Bukvic et al* [100]. In all the samples analyzed, it is possible to identify density gradients throughout the analyzed length of the cements, being all the surfaces more porous (with lower density) than the bulk of the samples, for the same

maturation time condition. In the samples immersed in both media (FBS and mQ water) containing tricalcium silicate (TCS) with 20% incorporation of zirconium oxide (ZO) and with the addition of 1.00mg/ml silver nanoparticles (Fig.39 and Fig.40), it is possible to observe that the porosity found on the surface of samples immersed for 1 day is higher than for any of the other sections (base of the bulk, middle of the bulk and final of the bulk) for the same maturation period; the same behavior occurs for the surface porosity of the samples immersed for 7 days. It is reported in the literature, that density assumes higher values on the upper part of a sample uniaxially pressed than its bottom part; also, this density gradient decreases continuously from the surface to the center of the sample [101]. Accordingly, and contrarily to the results commented above, it was expected that the higher porosity would be found on the middle of the samples. Nevertheless, for the nAg1.00 samples, the middle of the bulks showed the lowest values of porosity in almost every immersion period, not being the lowest in two cases (nAg1.00_FBS immersed for 7 days and nAg1.00_W for 28 days) but with very similar values of total porosity. The observed decrease in the values of total porosity, from the surface until the middle of nAg1.00 samples, can be due to the very small dimensions of the silver nanoparticles incorporated in this tricalcium silicate (TCS) cements, which may facilitate the packing of the particles in the cement sample before reaching the setting point [67].

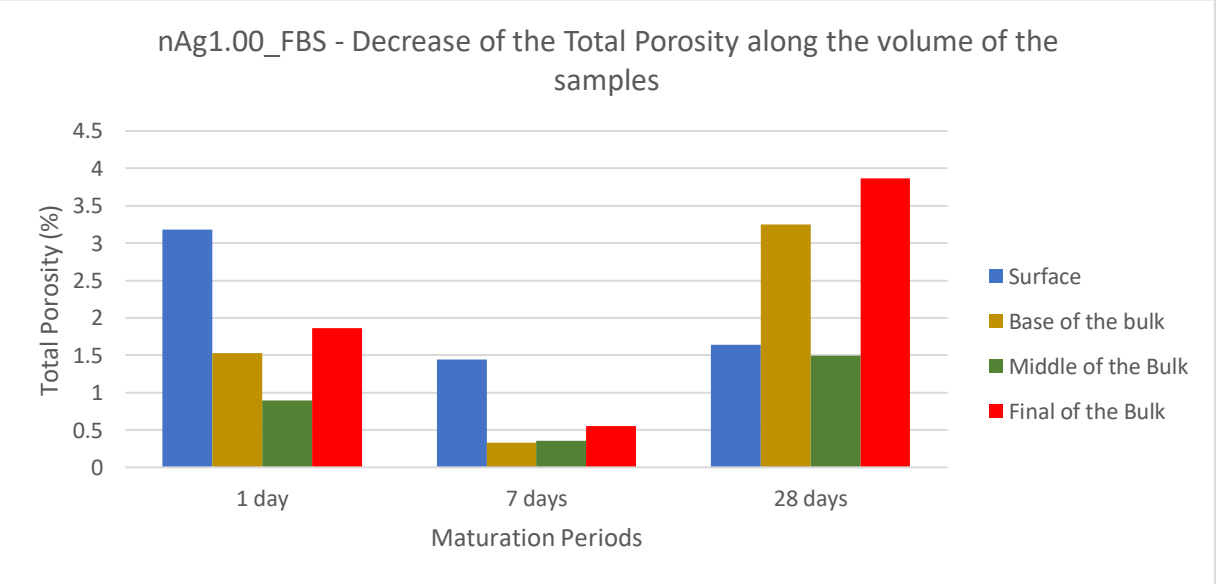

Fig.31 – Total porosities in all the volumes analyzed, except the average bulk values, in samples of nAg1.00_FBS for immersion periods of 1 day, 7 days and 28 days

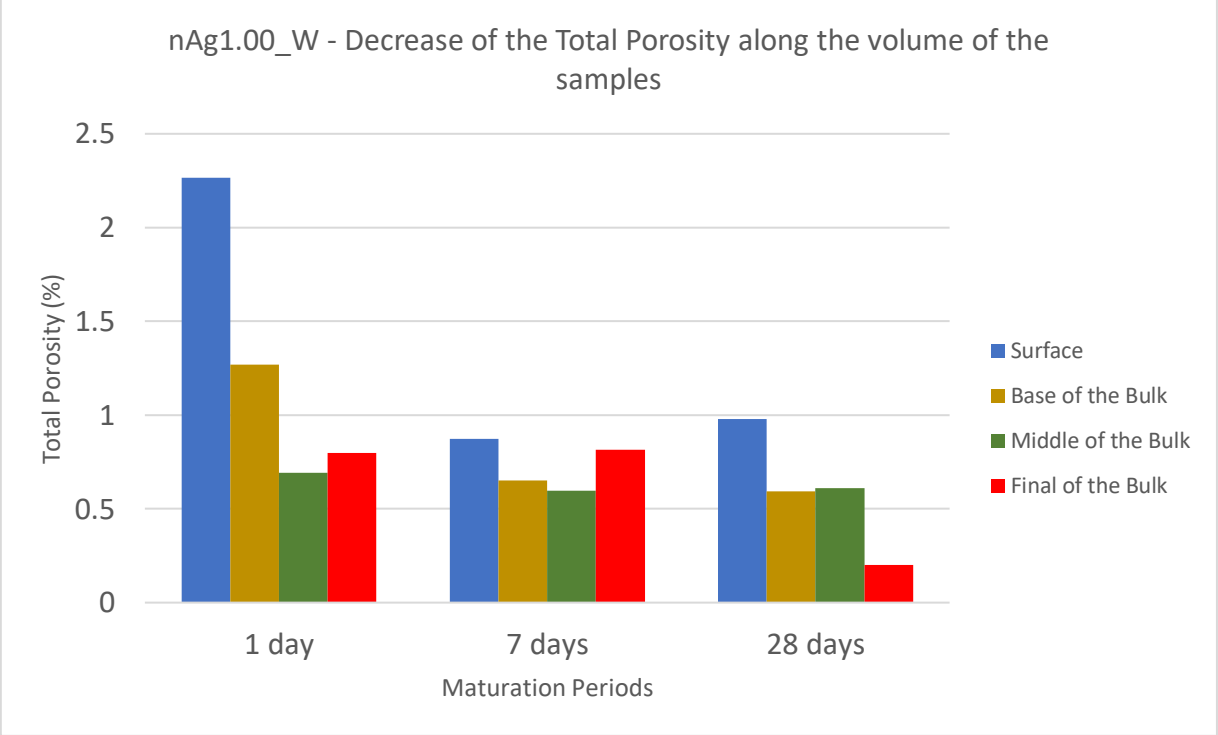

Fig.32 – Total porosities in all the volumes analyzed, except the average bulk values, in samples of nAg1.00_W for immersion periods of 1 day, 7 days and 28 days

5.9. nAg1.00 Samples – Hydration and Dissolution of the cements

The variation of the porosity values during the maturation of the nAg1.00 samples result in a change of the consolidation of the material, and this process lasts for several weeks (+ 4 weeks), where the hydration processes take the lead, resulting in the decrease of the porosity and a subsequent increase of the mechanical resistance of the dental cement [102]. The hydration process happens due to the fact that tricalcium silicate-based cements react with water, making them hydraulic cements [103]. This hydration process comes along with the dissolution and re-precipitation of calcium components (1) and these are the main causes for the decrease of total porosity along the different time periods in nAg1.00 samples immersed in water during the three different maturation periods. This dissolution re-precipitation process consists basically on the reaction between the calcium-silicate components and mQ water, which result in the chemical bonding with water molecules, originating calcium silicate hydrate and calcium hydroxide (2), both responsible for remineralizing effects [103, 104]. These products

of the hydration process are here suggested to be the main responsible for the decrease of the porosity in the nAg1.00 samples along the different periods of immersion.

$$Ca_3SiO_5 + 3H_2O \rightarrow 3Ca^{2+} + 4OH + H_2SiO_2^{-4} \text{ (dissolution phase) (1)}$$

$$2Ca_3SiO_5 + 7H_2O \rightarrow 3CaO{\cdot}SiO_2{\cdot}4H_2O + 3Ca(OH)_2 \text{ (overall reaction) (2)}$$

Samples of nAg1.00 immersed in FBS showed a different behavior in terms of porosity, revealing a decrease of total porosity from 1 to 7 days of immersion in FBS followed by an increase in all the volumes between the seventh and the twenty-eighth days of maturation. This porosity increase can be related to the composition of FBS, since the animal proteins present in the fetal bovine serum (FBS) have already shown to decrease the compressive strength of tricalcium silicate-based cements, and this decrease is affected by the total porosity present on the dental cement [105]. *Remadnia, A*. *et al* have described the influence of the animal proteins in the Portland cement (PC) showing a decrease of 54.41% of the compressive strength in cements immersed in a mixture containing hemoglobin[106]. Another study developed by *Nekoofar, M. H., Stone, D. F. et al* [107] showed that the MTA (tricalcium silicate-based cement) contaminated with blood had presented a significantly lower microhardness when compared with the samples of MTA without blood contamination. It is known that the main components of the FBS are bovine serum albumin (BSA) and hemoglobin, and its dimensions are, approximately 66 kDa and 64 kDa [108]. Assuming that these proteins are circular, and taking into account the table presented by *Erickson, Harold P*, the molecular weight of both proteins might correspond to ~6nm each one [109]. Knowing the dimensions of the main proteins that compose the FBS and taking into account the Table 6 with the dimension of the pores, it is possible to assume that even being the pores extremely small, they are still much bigger than these proteins. On this way, the animal proteins that are present on the FBS may enter on the open pores of the surface and act as a foaming agent increasing the size of the pores. However, these increase on the pore size on nAg1.00 immersed in FBS can just be noted after 28 days of immersion, at this time, it is possible to see that the percentage of smaller pores (7-21μm) reduced when compared with the percentage in samples immersed for 7 days. Also, it is possible to read from the Table 6, that the percentage of smaller pores is much higher in

nAg1.00 samples immersed in mQ water (2.55%) than in the same samples immersed in FBS (0.22%). Knowing that the mediums are replaced for fresh ones every 7 days, it is possible to deduce that the increase in terms of total porosity after 28 days may be due to the fact that the samples immersed in FBS for a 28-days period have their medium replaced three times causing the animal proteins to accumulate on the open pores at the surface. In the other hand, in the samples immersed in FBS for a 7-days period, the medium is not replaced thus there is no accumulation of proteins within the open pores, hence reducing the role of foaming agent of animal proteins. Also, the increase of the total porosity after 28 days of immersion in FBS, may be due to the degradation of the samples since over time it is possible that samples to be eroded and cracked which contributes for enhancing the volume of pores.

Table 6 presents the pore thickness which can be also defined as the mean pore diameter in nAg1.00 samples for the three maturation periods, and in both medias. As it is represented on the table 6, the size of the pores presented on the surface have two different ranges, from 7.0 until 21.0 μm, and from 21.0 to 35.0μm. For each pore size range, it is also indicated the percentage in volume. From the detailed analysis of this table, we can observe the time evolution of the pore dimensions at the surfaces of the nAg1.00 immersed both in FBS and in mQ water: the dimensions of the pores in nAg1.00 samples matured in mQ water have decrease substantially, as the percentage of pores with size between 7-21μm increased from 0.08% (day 1) to 0.27% (day 7) and finally 2.55% (day 28) when immersed on mQ water. This increase in the number of smaller pores can be related with the decrease of porosity in the surface of samples maturated for 7 days, although, as we can observe on the Fig.31, the surface porosity does not decrease between day 7 and day 28 - there is even a small increase. This small increase can be explained by the high increase of the smaller pores (7-21μm) between these two maturation periods. nAg1.00 samples immersed in FBS show a different porosity variation when compared with the one evidenced in mQ water: the smaller pores do not change significantly between the day 1 and the day 7 whereas between day 7 and day 28, it is noticeable a decrease in the size of small pores (from 1.04% to 0.22%). When analyzing the Fig.31, it is possible to understand that this decrease of the smaller pores is disguised by the presence of bigger pores, since the surface porosity at the end of 28 days of immersion (1.64%) is higher as compared to that corresponding to 7 days of immersion in FBS (1.44%). This means that there is a larger number of bigger pores, which makes the cement less dense and less strong.

Table 6 – Surfaces pore size on nAg1.00 samples along the three immersion periods and between the two used immersion mediums

		Pore Thickness (Por.Th) Distribution					
		1 day		7 days		28 days	
	Pore size / Parameters	*7.0 - 21.0 μm*	*21.0 - 35.0 μm*	*7.0 - 21.0 μm*	*21.0 - 35.0 μm*	*7.0 - 21.0 μm*	*21.0 - 35.0 μm*
nAg1.00_FBS	*Volume (μm^3)*	3.25×10^5	3.12×10^8	3.21×10^6	3.05×10^8	7.02×10^5	3.13×10^8
	Percentage volume in range (%)	0.1	99.9	1.04	98.9	0.22	99.8
nAg1.00_W	*Volume (μm^3)*	2.52×10^5	3.15×10^8	8.44×10^5	3.11×10^8	8.01×10^6	3.06×10^8
	Percentage volume in range (%)	0.08	99.9	0.27	99.7	2.55	97.4

6. Overall Conclusions

During the development of this thesis several dental cements were analyzed all tricalcium silicate-based. In some of them, 45S5 Bioglass was used to replace part of TCS (10% or 20%) and in some formulations silver nanoparticles were added in different quantities per milliliter of the preparation solution (0.5 mg/ml, 1.0 mg/ml and 2.0 mg/ml). The other cements were the tricalcium silicate without any addition (TCS) and a commercial cement called Biodentine. All the samples were submitted to two different mediums, one with mQ water and another one with FBS in which they were matured for different times up to 28 days.

The analysis of all specimens was performed by using the nano-CT equipment, a powerful non-destructive technology that allows to obtain relevant information on microstructure. A deep learning of the nano-CT technique was made in order to understand its potential. In terms of possible parameters to evaluate, versatility of the supporting software and possibility of extending the use of the technique to many other fronts beyond dentistry. The study of the cement microstructure was based on a particular parameter - the total porosity of the samples. The pores and the way that they are distributed in the samples were studied by having into account the different volumes of the cement specimens (surface, base of the bulk, middle of the bulk and final of the bulk).

The analyzed samples were provided by a research group in the University of Oslo and were produced by manual pressing mimicking the typical cement preparation in a dental clinical environment. The fact that the processing of the samples was not controlled made it difficult to find consistent trends in the behavior of the studied parameters. However, it was possible to identify groups of samples in which the observed variation in total porosity enabled some discussion of the obtained results. This was the case of nAg1.00 samples exposed to two different mediums (mQ water and FBS) during different maturation periods. When immersing the nAg samples in mQ water, it was possible to conclude that there was a decrease in the total porosity level from 1-day period to the 7-days period, and no significant variation from the 7^{th} to the 28^{th} day. Although not confirmed, this behavior may be related to hydration of the cement and associated dissolution-reprecipitation reactions. After immersion of the nAg samples in FBS it was found that the total porosity decreased between the 1-day period and the 7-days period, reaching the minimum total porosity on every layers of the sliced volume after 7 days. However, between the 7-days period and the 28-days period there was an increase in the

total porosity on every volume of the samples, probably attributed to a chemical reaction with the FBS or to the degradation of the samples, particularly evident after four weeks soaking.

The overall conclusion of the work carried out in this project was that the nano-CT device can provide very valuable indications on the microstructure of biological architectures at the microscale. Allowing to follow the changes produced in these architectures by different effects. It became clear as well that it is of utmost importance the careful design of the experimental plan for the preparation of the specimens to analyze and close monitoring of the samples manufacturing.

7. Future Research

Having acquired the adequate know-how to operate the nano-CT equipment available at the Institute of Clinical Dentistry of the University of Oslo, it would be interesting to perform the same study on samples produced under controlled conditions, in particular with respect to the pressures used during their preparation. Spatulation by hand may be a difficult task to reproduce and was probably responsible for the variability found in the porosity values obtained in more than 100 samples analyzed.

Monitoring the behavior of the TCS-based cements when immersed in different liquids showed to be relevant for the understanding of their in-vivo performance. Future studies on the effect of maturation periods should include a fourth intermediate time between the period of 7 and the period of 28 days, since cement stabilization is expected to occur during these periods.

Further studies are also needed to understand the hydration reactions and ion exchanges between the dental cements analyzed and the soaking mediums. Degradation profiles of the different cements on the selected mediums would be very helpful to follow the variation of ionic concentrations in the soaking liquids and to understand the cements durability and draw their stabilization curves.

8. References

(1) Dentistas, O. dos M. Barómetro de Saúde Oral https://www.omd.pt/observatorio/barometro/ (accessed Dec 2, 2019).

(2) Eurostat. Dentists, pharmacists and physiotherapists… https://ec.europa.eu/eurostat/web/products-eurostat-news/-/DDN-20190111-1?inheritRedirect=true&redirect=%2Feurostat%2Fnews%2Fwhats-new (accessed Dec 2, 2019).

(3) Kuo, L. C.; Polson, A. M.; Kang, T. Associations between Periodontal Diseases and Systemic Diseases: A Review of the Inter-Relationships and Interactions with Diabetes, Respiratory Diseases, Cardiovascular Diseases and Osteoporosis. Public Health 2008, 122 (4), 417–433. https://doi.org/10.1016/j.puhe.2007.07.004.

(4) Mochida, Y.; Yamamoto, T. et al. Does Poor Oral Health Status Increase the Risk of Falls?: The JAGES Project Longitudinal Study. PLoS One 2018, 13 (2), e0192251. https://doi.org/10.1371/journal.pone.0192251.

(5) Seo, H. et al. Regulation of Root Patterns in Mammalian Teeth. Sci. Rep. 2017, 7 (1). https://doi.org/10.1038/s41598-017-12745-1.

(6) Li, J.; Parada, C.; Chai, Y. Cellular and Molecular Mechanisms of Tooth Root Development. Development (Cambridge). Company of Biologists Ltd February 1, 2017, pp 374–384. https://doi.org/10.1242/dev.137216.

(7) Nelson, S. J. Wheeler's Dental Anatomy Physiology and Occlusion; Elsevier - Health Science, 2013.

(8) Vandana, K.; Haneet, R. Cementoenamel Junction: An Insight. Journal of Indian Society of Periodontology. Medknow Publications September 1, 2014, pp 549–554. https://doi.org/10.4103/0972-124X.142437.

(9) Stošić, N.; Dačić, S.; Dačić Simonović, D. Morphological Variations of the Cemento-Enamel Junction in Permanent Dentition ACTA FACULTATIS MEDICAE NAISSENSIS. Naissensis 2015, 32 (3), 209–214. https://doi.org/10.1515/afmnai-2015-0021.

(10) Nanci, A. Ten Cate's Oral Histology - E-Book: Development, Structure, and Function, 9th editio.; 2018.

(11) Britannica, T. E. of E. "Tooth." Encyclopaedia Britannica https://www.britannica.com/science/tooth-anatomy (accessed Jan 23, 2020).

(12) Bathla, S. Chapter 03 - Cementum. In Textbook of Periodontics; Jaypee Brothers Medical Publishers (P) Ltd., 2017; pp 28–28. https://doi.org/10.5005/jp/books/13037_4.

(13) Abbadent, D. & I. Why is Tooth Enamel Important? https://www.abbadent.com/blog/tooth-enamel-important/ (accessed Nov 26, 2019).

(14) Pandya, M.; Diekwisch, T. G. H. Enamel Biomimetics-Fiction or Future of Dentistry. International journal of oral science. NLM (Medline) January 5, 2019, p 8. https://doi.org/10.1038/s41368-018-0038-6.

(15) Bosshardt, D. D.; Selvig, K. A. Dental Cementum: The Dynamic Tissue Covering of the Root. Periodontol. 2000 1997, 13 (1), 41–75. https://doi.org/10.1111/j.1600-0757.1997.tb00095.x.

(16) Foster, B. L. On the Discovery of Cementum. Journal of Periodontal Research. Blackwell Munksgaard August 1, 2017, pp 666–685. https://doi.org/10.1111/jre.12444.

(17) Yamamoto, H. et al. Diversity of Acellular and Cellular Cementum Distribution in Human Permanent Teeth. J. Hard Tissue Biol. 2009, 18 (1), 40–44. https://doi.org/10.2485/jhtb.18.40.

(18) P. Schatten, G. Current Topics in Developmental Biology ; 2007; pp 65–70.

(19) Tjäderhane, L. et al. Dentin Basic Structure and Composition-an Overview. Endod. Top. 2009, 20 (1), 3–29. https://doi.org/10.1111/j.1601-1546.2012.00269.x.

(20) Butler, W. T.; Ritchie, H. The Nature and Functional Significance of Dentin Extracellular Matrix Proteins. Int. J. Dev. Biol. 1995, 39 (1), 169–179. https://doi.org/10.1387/ijdb.7626404.

(21) Giacaman, R. A.; Perez, V. A.; Carrera, C. A. Mineralization Processes in Hard Tissues: Teeth. In Biomineralization and Biomaterials: Fundamentals and Applications; Elsevier Inc., 2016; pp 147–185. https://doi.org/10.1016/B978-1-78242-338-6.00006-5.

(22) Goldberg, M.; Kulkarni, A. B. et al. Dentin: Structure, Composition and Mineralization. Front.

Biosci. - Elit. 2011, 3 E (2), 711–735. https://doi.org/10.2741/e281.

(23) Davari, A.; Ataei, E.; Assarzadeh, H. Dentin Hypersensitivity: Etiology, Diagnosis and Treatment; A Literature Review; 2013; Vol. 14.

(24) Mjör, I. A. Dentin Permeability: The Basis for Understanding Pulp Reactions and Adhesive Technology. Braz Dent J 2009, 20 (1), 3–16.

(25) Parirokh, M. et al. Effect of 808nm Diode Laser Irradiation on Root Canal Walls after Smear Layer Removal: A Scanning Electron Microscope Study. Iran. Endod. J. 2007, 2 (2), 37–42.

(26) Omidi, M. et al. Characterization of Biomaterials. In Biomaterials for Oral and Dental Tissue Engineering; Elsevier Inc., 2017; pp 97–115. https://doi.org/10.1016/B978-0-08-100961-1.00007-4.

(27) Lenherr, P. et al. Tooth Discoloration Induced by Endodontic Materials: A Laboratory Study. Int. Endod. J. 2012, 45 (10), 942–949. https://doi.org/10.1111/j.1365-2591.2012.02053.x.

(28) Geurs, N. C.; Vassilopoulos, P. J.; Reddy, M. S. Soft Tissue Considerations in Implant Site Development. Oral and Maxillofacial Surgery Clinics of North America. August 2010, pp 387–405. https://doi.org/10.1016/j.coms.2010.04.001.

(29) Jang, J. Y. et al. In Vivo Osteogenic Differentiation of Human Dental Pulp Stem Cells Embedded in an Injectable In Vivo-Forming Hydrogel. Macromol. Biosci. 2016, 1158–1169. https://doi.org/10.1002/mabi.201600001.

(30) Pessina, A.; Gribaldo, L. The Key Role of Adult Stem Cells: Therapeutic Perspectives. Current Medical Research and Opinion. November 2006, pp 2287–2300. https://doi.org/10.1185/030079906X148517.

(31) Tsukamoto, J. et al. Efficacy of a Self-Assembling Peptide Hydrogel, Spg-178-Gel, for Bone Regeneration and Three-Dimensional Osteogenic Induction of Dental Pulp Stem Cells. Tissue Eng. - Part A 2017, 23 (23–24), 1394–1402. https://doi.org/10.1089/ten.tea.2017.0025.

(32) De Moor, R. et al. Undergraduate Curriculum Guidelines for Endodontology. Int. Endod. J. 2013, 46 (12), 1105–1114. https://doi.org/10.1111/iej.12186.

(33) Berman, L.; Hargreaves, K. Cohen's Pathways of the Pulp Expert Consult - 11th Edition, 11th ed.; 2015.

(34) Ingle, J. I. Ingle's Endodontics 6, 6th ed.; Bindner, P., Ed.; BC Decker Inc: Hamilton, Ontario, 2008.

(35) Sundqvist, G.; Bloom, G. D.; Enberg, K.; Johansson, E. Phagocytosis of Bacteroides Melaninogenicus and Bacteroides Gingivalis in Vitro by Human Neutrophils. J. Periodontal Res. 1982, 17 (2), 113–121. https://doi.org/10.1111/j.1600-0765.1982.tb01137.x.

(36) Shrestha, A.; Kishen, A. Antibacterial Nanoparticles in Endodontics: A Review. Journal of Endodontics. Elsevier Inc. October 1, 2016, pp 1417–1426. https://doi.org/10.1016/j.joen.2016.05.021.

(37) Allaker, R. P. Critical Review in Oral Biology & Medicine: The Use of Nanoparticles to Control Oral Biofilm Formation. J. Dent. Res. 2010, 89 (11), 1175–1186. https://doi.org/10.1177/0022034510377794.

(38) Leung, K. P. et al. Control of Oral Biofilm Formation by an Antimicrobial Decapeptide. J. Dent. Res. 2005, 84 (12), 1172–1177. https://doi.org/10.1177/154405910508401215.

(39) Kuang, X.; Chen, V.; Xu, X. Novel Approaches to the Control of Oral Microbial Biofilms. BioMed Research International. Hindawi Limited 2018. https://doi.org/10.1155/2018/6498932.

(40) Berger, D.; Rakhamimova, A. et al. Oral Biofilms: Development, Control, and Analysis. High-throughput 2018, 7 (3). https://doi.org/10.3390/ht7030024.

(41) Saunders, W. Latest Concepts in Root Canal Treatment. In British Dental Journal; 2005; Vol. 198, pp 515–516. https://doi.org/10.1038/sj.bdj.4812297.

(42) Nakamura, D. H.; Garcia, R. B. et al. Sealing Ability of Cements in Root Canals Prepared for Intraradicular Posts. J. Appl. Oral Sci. 2006, 14 (4), 224–227. https://doi.org/10.1590/S1678-77572006000400002.

(43) PradeepKumar, A. et al. Impact of Apical Extent of Root Canal Filling on Vertical Root Fracture: A Case–Control Study. Int. Endod. J. 2019, 52 (9), 1283–1289. https://doi.org/10.1111/iej.13134.

(44) Moore, B. K. Dental Materials. In McDonald and Avery Dentistry for the Child and Adolescent; Elsevier Inc., 2011; pp 296–312. https://doi.org/10.1016/B978-0-323-05724-0.50020-5.

(45) Hill, E. E. Dental Cements for Definitive Luting: A Review and Practical Clinical Considerations. Dental Clinics of North America. July 2007, pp 643–658. https://doi.org/10.1016/j.cden.2007.04.002.

(46) Wingo, K. A Review of Dental Cements. Journal of Veterinary Dentistry. SAGE Publications Ltd March 27, 2018, pp 18–27. https://doi.org/10.1177/0898756418755339.

(47) Ishikawa, K.; Matsuya, S. et al. Bioceramics. In Comprehensive Structural Integrity; Elsevier Ltd, 2007; Vol. 9, pp 169–214. https://doi.org/10.1016/B0-08-043749-4/09146-1.

(48) Prosser, H. J.; Wilson, A. D. Development of Materials Based on Acid-Base Reaction Cements. Mater. Des. 1986, 7 (5), 262–266. https://doi.org/10.1016/0261-3069(86)90052-X.

(49) Chevalier, M. M. Rapports Du Jury International; 1868.

(50) Kanduti, D.; Sterbenk, P.; Artnik, B. Fluoride: A Review of Use and Effects on Health. Mater. Socio Medica 2016, 28 (2), 133. https://doi.org/10.5455/msm.2016.28.133-137.

(51) Wilson, A. D.; Kent, B. E. The Glass-Ionomer Cement, a New Translucent Dental Filling Material. J. Appl. Chem. Biotechnol. 2007, 21 (11), 313–313. https://doi.org/10.1002/jctb.5020211101.

(52) de la Macorra, J. C.; Pradíes, G. Conventional and Adhesive Luting Cements. Clinical oral investigations. December 1, 2002, pp 198–204. https://doi.org/10.1007/s00784-002-0184-1.

(53) Coutinho, E. et al. Gel Phase Formation at Resin-Modified Glass-Ionomer/Tooth Interfaces. J. Dent. Res. 2007, 86 (7), 656–661. https://doi.org/10.1177/154405910708600714.

(54) Diaz-Arnold, A. M.; Vargas, M. A.; Haselton, D. R. Current Status of Luting Agents for Fixed Prosthodontics. J. Prosthet. Dent. 1999, 81 (2), 135–141. https://doi.org/10.1016/S0022-3913(99)70240-4.

(55) Shelton, R. Biocompatibility of Dental Biomaterials. In Biocompatibility of Dental Biomaterials; Elsevier Inc., 2017; pp 77–94. https://doi.org/10.1016/c2014-0-03003-1.

(56) Nicholson, J. W. Polyacid-Modified Composite Resins (“compomers”) and Their Use in Clinical Dentistry. Dental Materials. April 2007, pp 615–622. https://doi.org/10.1016/j.dental.2006.05.002.

(57) Mclean, J. W.; Nicholson, W.; Wilson, A. D. Guest Editorial Proposed Nomenclature for Glass-Ionomer Dental Cements and Related Materials.

(58) Mount, G. J.; Martin, L. : An Atlas of Glass-Ionomer Cements: A Clinician’s Guide, 3rd ed.; London, 2002; Vol. 193.

(59) Kohli, M. R.; Karabucak, B. Bioceramic Usage in Endodontics | American Association of Endodontists. Bioceramics. July 8, 2019.

(60) F. G. Xavier, V. et al. Bioceramic Cements in Endodontics. In Oral Diseases; IntechOpen, 2020. https://doi.org/10.5772/intechopen.89015.

(61) Hall, C. On the History of Portland Cement after 150 Years. Journal of Chemical Education. April 1976, pp 222–223. https://doi.org/10.1021/ed053p222.

(62) Patel, N. Comparing Gray and White Mineral Trioxide Aggregate as a Repair Material for Furcation Perforation: An in Vitro Dye Extraction Study. J. Clin. DIAGNOSTIC Res. 2014. https://doi.org/10.7860/jcdr/2014/9517.5046.

(63) Parirokh, M.; Torabinejad, M. Mineral Trioxide Aggregate: A Comprehensive Literature Review-Part I: Chemical, Physical, and Antibacterial Properties. Journal of Endodontics. January 2010, pp 16–27. https://doi.org/10.1016/j.joen.2009.09.006.

(64) Camilleri, J.; Sorrentino, F.; Damidot, D. Investigation of the Hydration and Bioactivity of Radiopacified Tricalcium Silicate Cement, Biodentine and MTA Angelus. Dent. Mater. 2013, 29 (5), 580–593. https://doi.org/10.1016/j.dental.2013.03.007.

(65) Li, X. et al. Modified Tricalcium Silicate Cement Formulations with Added Zirconium Oxide. Clin. Oral Investig. 2017, 21 (3), 895–905. https://doi.org/10.1007/s00784-016-1843-y.

(66) Corrêa, J. M. et al. Silver Nanoparticles in Dental Biomaterials. International Journal of Biomaterials. Hindawi Publishing Corporation January 15, 2015. https://doi.org/10.1155/2015/485275.

(67) Vazquez-Garcia, F. et al. Effect of Silver Nanoparticles on Physicochemical and Antibacterial Properties of Calcium Silicate Cements. Braz. Dent. J. 2016, 27 (5), 508–514. https://doi.org/10.1590/0103-6440201600689.

(68) Magalhães, A. P. R. et al. Nanosilver Application in Dental Cements. ISRN Nanotechnol. 2012, 2012, 1–6. https://doi.org/10.5402/2012/365438.

(69) Skallevold, H. E.; Rokaya, D. et al. Bioactive Glass Applications in Dentistry. International Journal of Molecular Sciences. MDPI AG December 1, 2019, p 5960. https://doi.org/10.3390/ijms20235960.

(70) Heid, S. et al. Incorporation of Particulate Bioactive Glasses into a Dental Root Canal Sealer. In Biomedical Glasses; Walter de Gruyter GmbH, 2016; Vol. 2, pp 29–37. https://doi.org/10.1515/bglass-2016-0004.

(71) Yiru Y., O.; Zhao S., I. et al. Dental Biofilm and Laboratory Microbial Culture Models for Cariology Research. Dent. J. 2017, 5 (2), 21. https://doi.org/10.3390/dj5020021.

(72) Benoit, D. S. W.; Sims, K. R.; Fraser, D. Nanoparticles for Oral Biofilm Treatments. ACS Nano 2019, 13 (5), 4869–4875. https://doi.org/10.1021/acsnano.9b02816.

(73) Allaker, R. P.; Memarzadeh, K. Nanoparticles and the Control of Oral Infections. International Journal of Antimicrobial Agents. Elsevier B.V. February 2014, pp 95–104. https://doi.org/10.1016/j.ijantimicag.2013.11.002.

(74) Hamouda, I. M. Current Perspectives of Nanoparticles in Medical and Dental Biomaterials. Journal of Biomedical Research. May 30, 2012, pp 143–151. https://doi.org/10.7555/JBR.26.20120027.

(75) Grande, N. M. et al. Present and Future in the Use of Micro-CT Scanner 3D Analysis for the Study of Dental and Root Canal Morphology. Ann. Ist. Super. Sanita 2012, 48 (1), 26–34. https://doi.org/10.4415/ann_12_01_05.

(76) Swain, M. V.; Xue, J. State of the Art of Micro-CT Applications in Dental Research. International journal of oral science. 2009, pp 177–188. https://doi.org/10.4248/IJOS09031.

(77) Santini, M. Fundamentals and Recent Advances in X-Ray Micro Computed Tomography

(MicroCT) Applied on Thermal-Fluid Dynamics and Multiphase Flows. In Journal of Physics: Conference Series; Institute of Physics Publishing, 2015; Vol. 655. https://doi.org/10.1088/1742-6596/655/1/012004.

(78) Marciano, M. A. et al. Applications of Micro-Computed Tomography in Endodontic Research; 2012.

(79) Hendee, W. R.; Ritenour, E. R. Medical Imaging Physics; Wiley-Liss, 2002; p 512.

(80) O'Sullivan, J. D. B. et al. X-Ray Micro-Computed Tomography (MCT): An Emerging Opportunity in Parasite Imaging. Parasitology. Cambridge University Press June 1, 2018, pp 848–854. https://doi.org/10.1017/S0031182017002074.

(81) Ahmed, H. M. A. Nano-Computed Tomography: Current and Future Perspectives. Restor. Dent. Endod. 2016, 41 (3), 236. https://doi.org/10.5395/rde.2016.41.3.236.

(82) Kampschulte, M. et al. Nano-Computed Tomography: Technique and Applications. RoFo Fortschritte auf dem Gebiet der Rontgenstrahlen und der Bildgeb. Verfahren 2016, 188 (2), 146–154. https://doi.org/10.1055/s-0041-106541.

(83) Mavridou, A. M.; Pyka, G.; Kerckhofs, G.; Wevers, M.; Bergmans, L.; Gunst, V.; Huybrechts, B.; Schepers, E.; Hauben, E.; Lambrechts, P. A Novel Multimodular Methodology to Investigate External Cervical Tooth Resorption. Int. Endod. J. 2016, 49 (3), 287–300. https://doi.org/10.1111/iej.12450.

(84) Salmon, P. L.; Sasov, A. Y. Application of Nano-CT and High-Resolution Micro-CT to Study Bone Quality and Ultrastructure, Scaffold Biomaterials and Vascular Networks. In Advanced Bioimaging Technologies in Assessment of the Quality of Bone and Scaffold Materials: Techniques and Applications; Springer Berlin Heidelberg, 2007; pp 323–331. https://doi.org/10.1007/978-3-540-45456-4_19.

(85) Parkinson, C. R.; Sasov, A. High-Resolution Non-Destructive 3D Interrogation of Dentin Using X-Ray Nanotomography. Dent. Mater. 2008, 24 (6), 773–777. https://doi.org/10.1016/j.dental.2007.09.003.

(86) Sketchfab Community Blog - Take a Ride on a Root Canal: The VR Tooth Tour Story

https://sketchfab.com/blogs/community/take-a-ride-on-a-root-canal-the-vr-tooth-tour-story/ (accessed Dec 15, 2019).

(87) Heimel, P. et al. Iodine-Enhanced Micro-CT Imaging of Soft Tissue on the Example of Peripheral Nerve Regeneration. Contrast Media Mol. Imaging 2019, 2019. https://doi.org/10.1155/2019/7483745.

(88) Brisard, S.; Serdar, M.; Monteiro, P. J. M. Multiscale X-Ray Tomography of Cementitious Materials: A Review. Cement and Concrete Research. Elsevier Ltd February 1, 2020, p 105824. https://doi.org/10.1016/j.cemconres.2019.105824.

(89) How does a micro-CT scanner work? | Micro Photonics https://www.microphotonics.com/how-does-a-microct-scanner-work/ (accessed Dec 20, 2019).

(90) Nehlig, A.; Obenaus, A. Chapter 47 - Imaging Approaches in Small Animal Models. In Models of Seizures and Epilepsy; Elsevier Inc., 2006; pp 583–600. https://doi.org/10.1016/B978-012088554-1/50049-9.

(91) Sauer Jørgensen, J. X-Ray Computed Tomography (CT) Slides By; Springer, 2008.

(92) Russo, P. Handbook of X-Ray Imaging: Physics and Technology - Google Livros; 2018.

(93) Fernando A. Lasagi, A. F. L. Fabrication and Characterization in the Micro-Nano Range. Springer 2011, 10, 29–119. https://doi.org/10.1007/978-3-642-17782-8.

(94) Herman, G. T. Correction for Beam Hardening in Computed Tomography. Phys. Med. Biol. 1979, 24 (1), 81–106. https://doi.org/10.1088/0031-9155/24/1/008.

(95) Kyriakou, Y.; Prell, D.; Kalender, W. A. Ring Artifact Correction for High-Resolution Micro CT. Phys. Med. Biol. 2009, 54 (17). https://doi.org/10.1088/0031-9155/54/17/N02.

(96) Segura-Egea, J. J. et al. Diabetes Mellitus, Periapical Inflammation and Endodontic Treatment Outcome. 2012, 17 (2), 356–361. https://doi.org/10.4317/medoral.17452.

(97) Estrela, C.; Holland, R. et al. Characterization of Successful Root Canal Treatment. Braz. Dent. J. 2014, 25 (1), 3–11. https://doi.org/10.1590/0103-6440201302356.

(98) Chen, S.; Baker, I. Evolution of Individual Snowflakes during Metamorphism. J. Geophys. Res. Atmos. 2010, 115 (21). https://doi.org/10.1029/2010JD014132.

(99) Milutinović-Nikolić, A. D.; Medić, V. B.; Vuković, Z. M. Porosity of Different Dental Luting Cements. Dent. Mater. 2007, 23 (6), 674–678. https://doi.org/10.1016/j.dental.2006.06.006.

(100) Bukvic, G.; Sanchez, L. E. D. A. et al. Green Machining Oriented to Diminish Density Gradient for Minimization of Distortion in Advanced Ceramics. Mach. Sci. Technol. 2012, 16 (2), 228–246. https://doi.org/10.1080/10910344.2012.673968.

(101) Richerson, D. W.; Lee, W. E. Modern Ceramic Engineering: Properties, Processing, and Use in Design, 2nd ed.; 1992.

(102) Villat, C. et al. Impedance Methodology: A New Way to Characterize the Setting Reaction of Dental Cements. Dent. Mater. 2010, 26 (12), 1127–1132. https://doi.org/10.1016/j.dental.2010.07.013.

(103) Primus, C. M.; Tay, F. R.; Niu, L. na. Bioactive Tri/Dicalcium Silicate Cements for Treatment of Pulpal and Periapical Tissues. Acta Biomaterialia. Acta Materialia Inc September 15, 2019, pp 35–54. https://doi.org/10.1016/j.actbio.2019.05.050.

(104) Watson, T. F.; Atmeh, A. R. et al. Present and Future of Glass-Ionomers and Calcium-Silicate Cements as Bioactive Materials in Dentistry: Biophotonics-Based Interfacial Analyses in Health and Disease. 2014. https://doi.org/10.1016/j.dental.2013.08.202.

(105) Kim, Y.; Kim, S. et al. Failure of Setting of Mineral Trioxide Aggregate in the Presence of Fetal Bovine Serum and Its Prevention. J. Endod. 2012, 38 (4), 536–540. https://doi.org/10.1016/j.joen.2011.12.005.

(106) Remadnia, A.; Dheilly, R. M. et al. Use of Animal Proteins as Foaming Agent in Cementitious Concrete Composites Manufactured with Recycled PET Aggregates. Constr. Build. Mater. 2009, 23 (10), 3118–3123. https://doi.org/10.1016/j.conbuildmat.2009.06.027.

(107) Nekoofar, M. H.; Stone, D. F.; Dummer, P. M. H. The Effect of Blood Contamination on the Compressive Strength and Surface Microstructure of Mineral Trioxide Aggregate. Int. Endod. J. 2010, 43 (9), 782–791. https://doi.org/10.1111/j.1365-2591.2010.01745.x.

(108) Johnson, M. Fetal Bovine Serum. Mater. Methods 2012, 2. https://doi.org/10.13070/mm.en.2.117.

(109) Erickson, H. P. Size and Shape of Protein Molecules at the Nanometer Level Determined by Sedimentation, Gel Filtration, and Electron Microscopy. https://doi.org/10.1007/s12575-009-9008-x.

Annex A

- **Surface Porosity vs Base of the Bulk porosity**

The comparison of the total porosities of the surface and the base of the bulk was made taking into account the three different maturation periods of similar samples, to assess how the porosities behaved in these different parts of the samples.

As previously mentioned, the porosities of the surfaces have, in fact, shown to be relatively similar in most cases. The total porosities on the sample surfaces have shown to be, in general, higher than in the bulk base. The reason for this may be in the method of preparing these dental cements in which a macroscopically flat surface was used to facilitate the pressing of the cement materials and in this way the levels of porosity and the number of irregularities became higher due to a less fluid mixture of the compounds in each of the analyzed cements. This uncontrolled mixture resulted in a less effective homogenization of the materials and, consequently, a higher total porosity.

In the Fig. 24, we can see that the samples corresponding to 1 day of maturation present a very similar porosity in the base of the bulk in most of the different types of cements, not following the total porosities corresponding to the sample surfaces, which are higher in most of the dental cements analyzed. Only the Biodentine samples, revealed a much lower porosity on the base of the bulk when compared with the other types of samples. The Biodentine samples immersed in mQ water for 1 day, were the only samples which displayed a higher porosity on the base of the bulk when compared with its surface porosity. In the BG10 cements matured in mQ water and in the BG20 cements matured in FBS, the porosities of the surface and the base of the bulk are very similar. As stated before, it is possible to assume that the reason for this similarity is in the strength used by the producer of the samples in their manufacture. If the compression force used to create a flat surface is high, it can happen that both the sample surface and the base of the bulk exhibit the same microstructural characteristics i.e. similar degree of homogenization and porosities.

For the 7-day maturation period (Fig.25), in addition to observing an abrupt drop in the total porosity values that has already been commented on in a topic above, it is also possible to notice that the bases of the bulk continue, as in the 1-day period of maturation, less porous than surfaces, except for one type of samples. Samples BG10 immersed in FBS are the exception that present higher total porosities in the base of the bulk when compared to the porosities related to the surfaces of these

same samples. This superiority is not accentuated, which may not be explained by the assumption previously admitted, in which the force used in the production of the sample was, allegedly, higher, making the porosities related to the surface and the base of the bulk to be correlated. The samples of nAg0.50, nAg1.00FBS and nAg2.00FBS present uncommonly different porosity values when comparing the base of the bulk with the surface. This may be an indicator of increasing homogeneity throughout the content of the samples, which may explain the reduction in total porosity that are found on the bases of the bulk of these samples when compared to the total porosity found on the sample surfaces. Also, in the Biodentine samples, it is possible to observe after 7 days of immersion in both mediums, that the porosities on the base of the bulk are really reduced when compared with the one found on the surfaces. The porosity found on the base of the bulk of Biodentine samples immersed on both mediums, are both the lowest porosities found on the base of the bulk on samples immersed for 7 days.

In the Fig.26 corresponding to the period in which the samples are kept in the medium, whether it is FBS or mQ water, for 28 days it is noticeable, not only that the surface porosities are higher when compared with the base of the bulk of samples immersed during a period of 7 days, but it is also clear that the porosities at the bases of the bulk are also more unpredictable. Consequently, the presented values do not follow the surface porosities. One of these cements (nAg2.0FBS) revealed a much higher surface porosity compared with the porosity found in the base of its bulk, contrarily to what happens with nAg0.50FBS. There are two of these types of cements, that present a much higher total porosity at the base of the bulk (nAg1.0FBS and Biodentine_FBS), not presenting a logical reason that can be explained. Only the BG10FBS, nAg0.5FBS, nAg0.50W, nAg1.0_W and TCS_W cements present relatively similar values in the two different types of slices, revealing some homogeneity of these samples after 28 days of maturation.

The remaining cements (BG10_W, BG20_FBS, BG20_W, nAg2.0_W, TCS_FBS and Biodentine_W) on the other hand, have very disparate porosities, but with all the highest porosities being presented on the surface of them. This indicates different degrees of homogeneity from the sample surface until the middle of it, which we call bulk. This bulk will be the part of the cement that will be the cornerstone of root canal therapy and where the porosity should reach values low enough so that there is no penetration of a bacterial organisms.

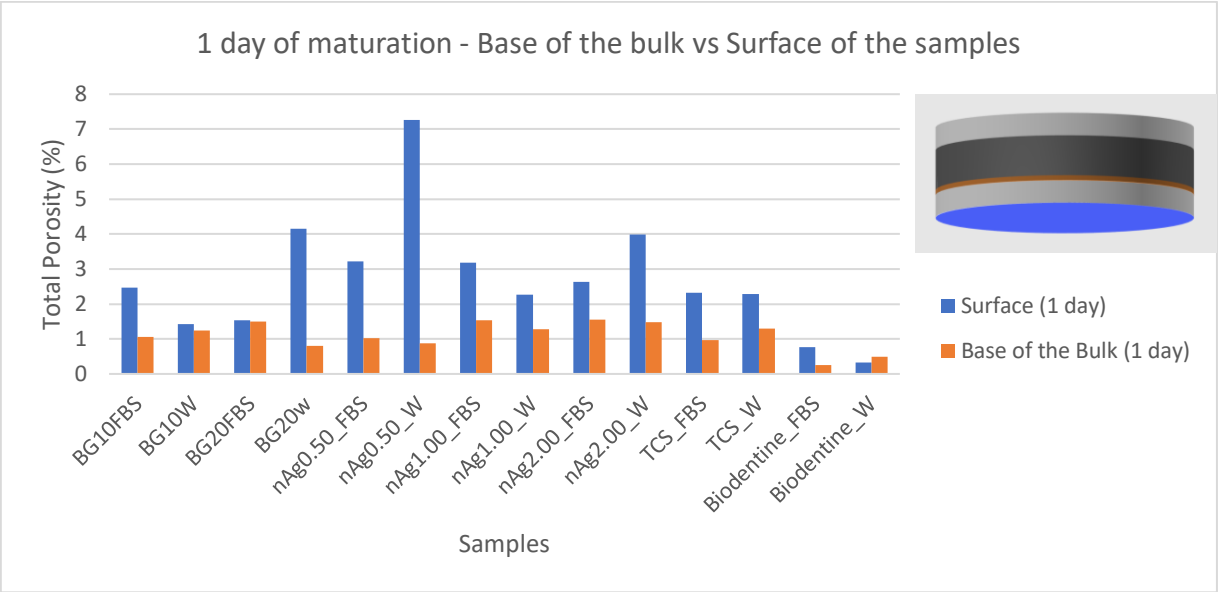

Fig.A-1 – Comparison of total porosities obtained on the base of the bulk and surfaces of every type of samples with 1 day of maturation

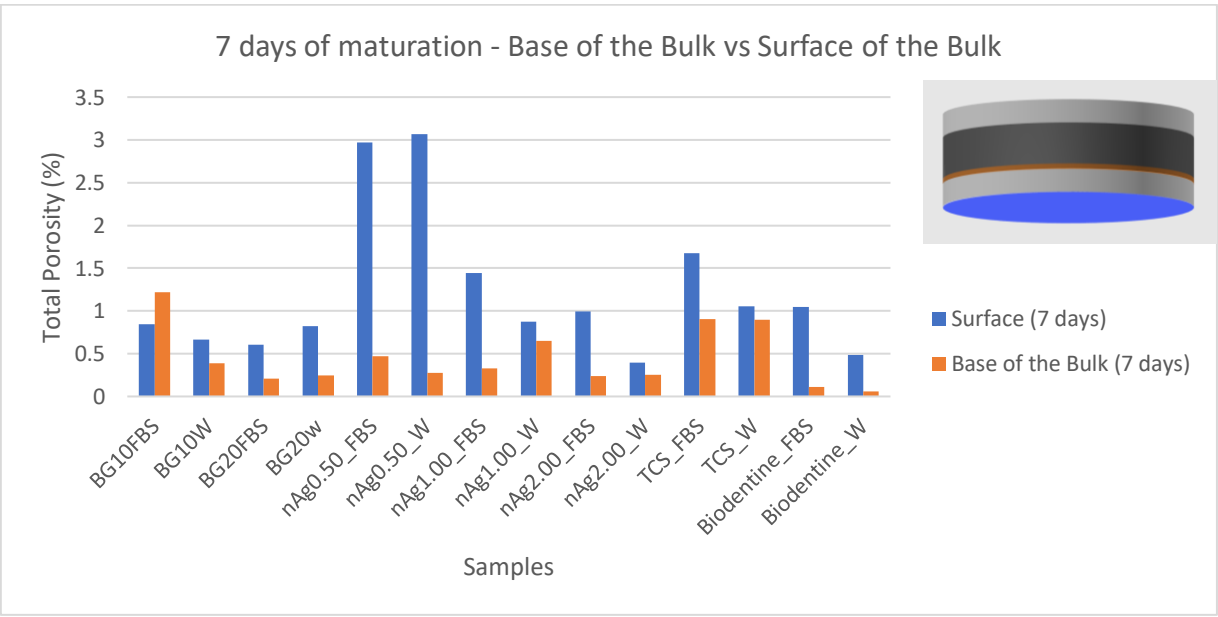

Fig.A-2 – Comparison of total porosities obtained on the base of the bulk and surfaces of every type of samples with 7 days of maturation

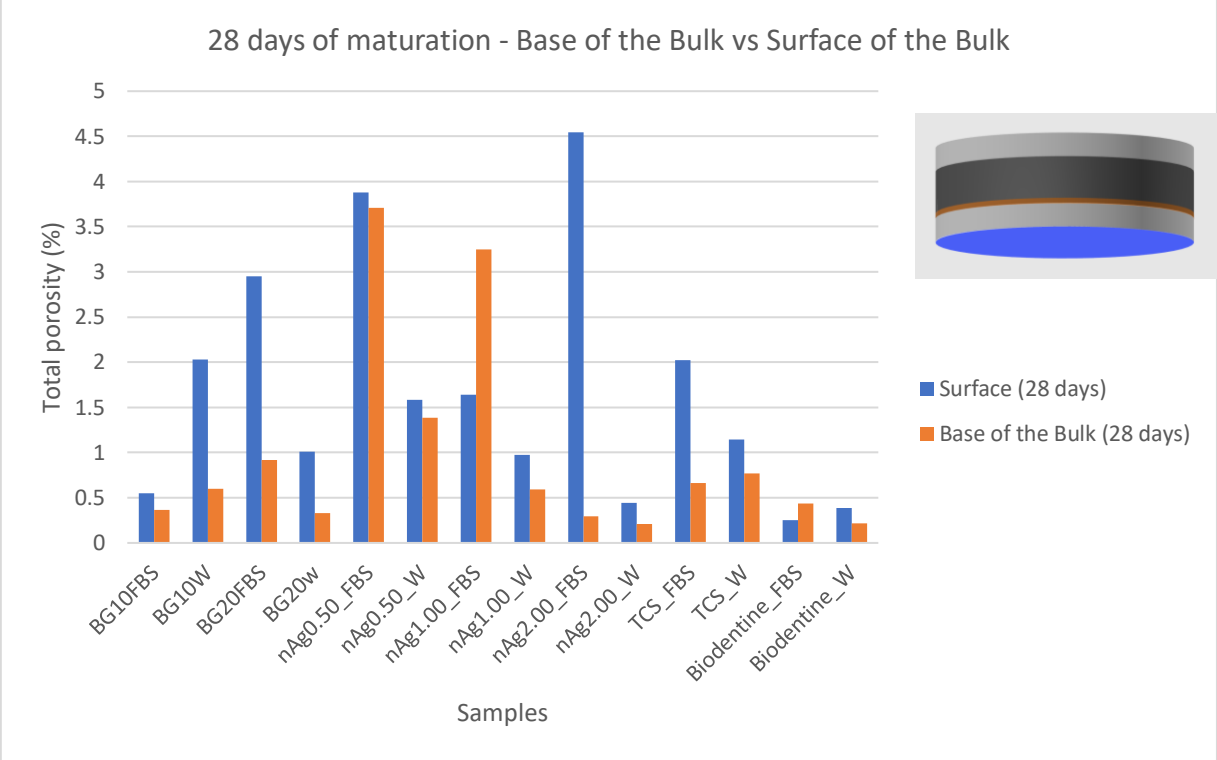

Fig.A-3 – Comparison of total porosities obtained on the base of the bulk and surfaces of every type of samples with 28 days of maturation

Annex B

- **Middle 20 slices and the Final 20 slices of the Bulk**

To better understand how the porosity behaves in all the samples volume, it was necessary not only to analyze the basis of the bulk used in each sample, but also the middle of each of these bulks as well as the final of each of them. Both volumes represent the 20 slices corresponding to each of the phases of the sample that were analyzed.

It has already been discussed and analyzed in this dissertation how the surface and the subsequent 20 slices (base of the bulk) are impacted by porosity. It was noticed that, in most cases, the porosity of the samples on the surface is higher than in the bases of the bulk and that this is due, especially to the way these samples were manufactured. Regarding the middle of the bulk, we analyzed the 20 slices that constitute it and represented the total porosities in the middles of all bulks over the different maturation times. As we can see through the analysis of the Fig.27, the porosity values are higher when

the samples are immersed (independently of the immersion fluid) for a period of 1 day. There are only two exceptions, for samples nAg0.50_FBS and nAg1.00 FBS, that present higher porosity values in the middle of the bulk after 28 days of maturation. In these, the total porosity after 28 days is significantly higher than the total porosity for 1 day and 7 days.

For the TCS samples, a considerable reduction of the total porosity in the middle of the bulk occurs over a period of 28 days when they are matured in water. However, when immersed in FBS, the decrease in porosity is clear from 7 to 28 days but does not change between 1 day and 7 days.

Biodentine samples showed the lowest porosities in almost all of the immersion periods. However, this commercial cement when immersed in FBS, showed to have a higher porosity at the end of 28 days of maturation, having prototype cements with lower porosities at the end of the same immersion period (n0.50_W and n2.00_W), although, none of the samples subjected to a FBS medium presented lower porosities than Biodentine_FBS.

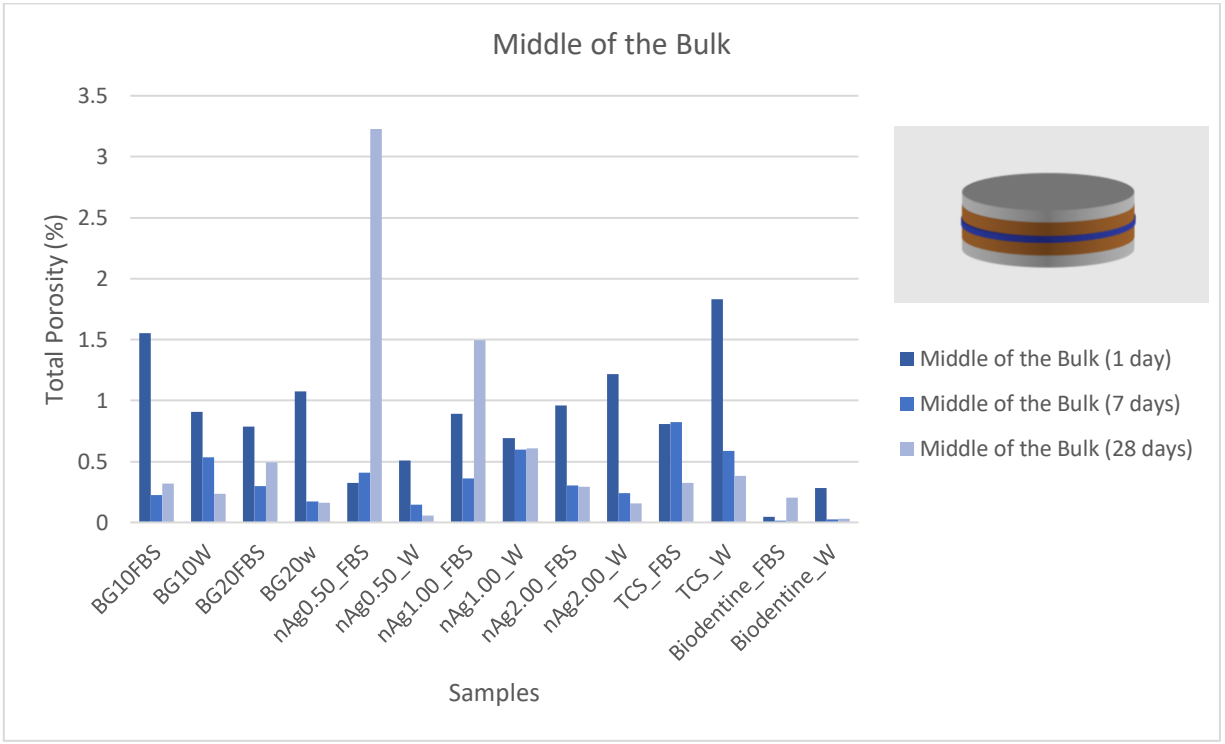

Fig.B-1 –Total porosities obtained on the middle of the bulk of every type of samples for different maturation periods (1 day, 7 days and 28 days)

The end of the bulk of each of the samples reveals the last part to be analyzed in the 100 samples that were subjected to a nano-CT analysis. In fact, in a generalized way, the total porosities relative to the 20 slices that make up the end of the defined bulk showed a higher number of pores when compared directly with the achieved value by the slices corresponding to the middle of the bulk.

Through a more careful analysis of the Fig.20, it is observed that the highest values of porosity are found, mostly, on the samples corresponding to the maturation period of 1 day. This condition is true for all types of samples matured in mQ water, except for nAg1.0. For the samples that were matured in FBS, a large increase in porosity in the nAg samples is notable for the maturation period of 28 days. These samples have the highest values of total porosity in maturation periods of 28 days revealing a noticeable discrepancy when compared to the same type of samples matured in mQ water.

Within all the sample types analyzed, the samples containing 45S5 bioglass proved to be the most consistent samples in terms of porosity on the final 20 slices of the bulk of all of the samples, with a. Although, BG20W samples are an exception due to the fact that the total porosity is higher in samples matured for 28 days when compared to them over 7 days of immersion on the mQ water, going against the porosity reductions evidenced by the other samples that include 45S5 bioglass.

Another conclusion that can be drawn from the Fig.28 is that only the TCS samples matured in mQ water, showed higher porosities at the end of 28 days of immersion when compared with the same samples maturated in FBS during the same time period. To finish, the Biodentine samples revealed the lowest total porosities in all of the immersion periods and in both maturation mediums.

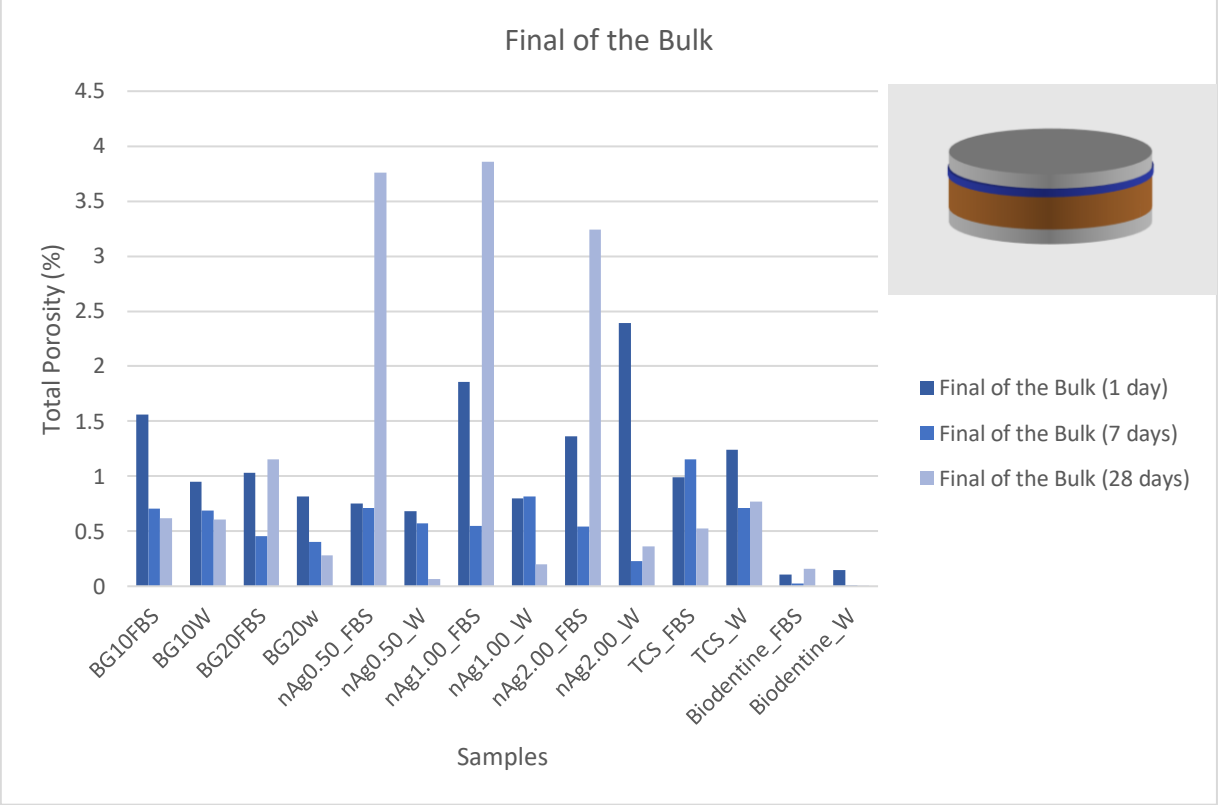

Fig.B-2 – Total porosities obtained on the final of the bulk of every type of samples between all the periods of maturation (1 day, 7 days and 28 days)

- **Middle of the Bulk porosity vs Final of the Bulk porosity**

The porosities found after the analysis of these different sample volumes confirmed the premise of the existence of a lower total porosity in the center of them. In the Fig.29 it is shown that, after 1 day of maturation, most types of samples have less porosity in the slices related to the middle of the bulk, and this evidence is notable, mainly, in samples containing silver nanoparticles (nAg).

Unlike samples that contain nAg in their composition, the types of samples that include only tricalcium silicate (TCS) present, at the end of 1 day of maturation, a higher total porosity in the middle of the bulks when compared to the average of the 20 slices that make up the end of the bulk.

The types of samples that in their composition contain 45S5 bioglass (BG), showed a slightly more regular behavior, and three of the four types of samples analyzed (BG10_FBS, BG10_W and BG20_FBS)

had a higher total porosity in the final of the bulk and only one type of sample presented a higher total porosity in the volumes corresponding to the middle of the bulk (BG20_W).

The commercial cement used for this analysis, the Biodentine, had shown the lowest porosities in both volumes (middle of the bulk and on the final of the bulk). However, it is possible to conclude that the Biodentine immersed in mQ water, presented higher porosities on the middle of the bulk when compared to the final of the bulk.

A point of interest was to understand the relationship between total porosity in the middle and at the final of the bulks with the maturation times (1-7-28 days). As already noted in the analyzes carried out previously, it will be unlikely that we will be able to reach any conclusions regarding the maturation means, since the results corresponding to the bases of the bulks and the surfaces of the samples revealed some irregularity in the values of total porosity acquired in all cases, and the clearest reason for that, must be the way of producing the prototype cements, since the hand-spatulate technique couldn't be really accurate, being used to get cements made out with different pressures with the spatula.

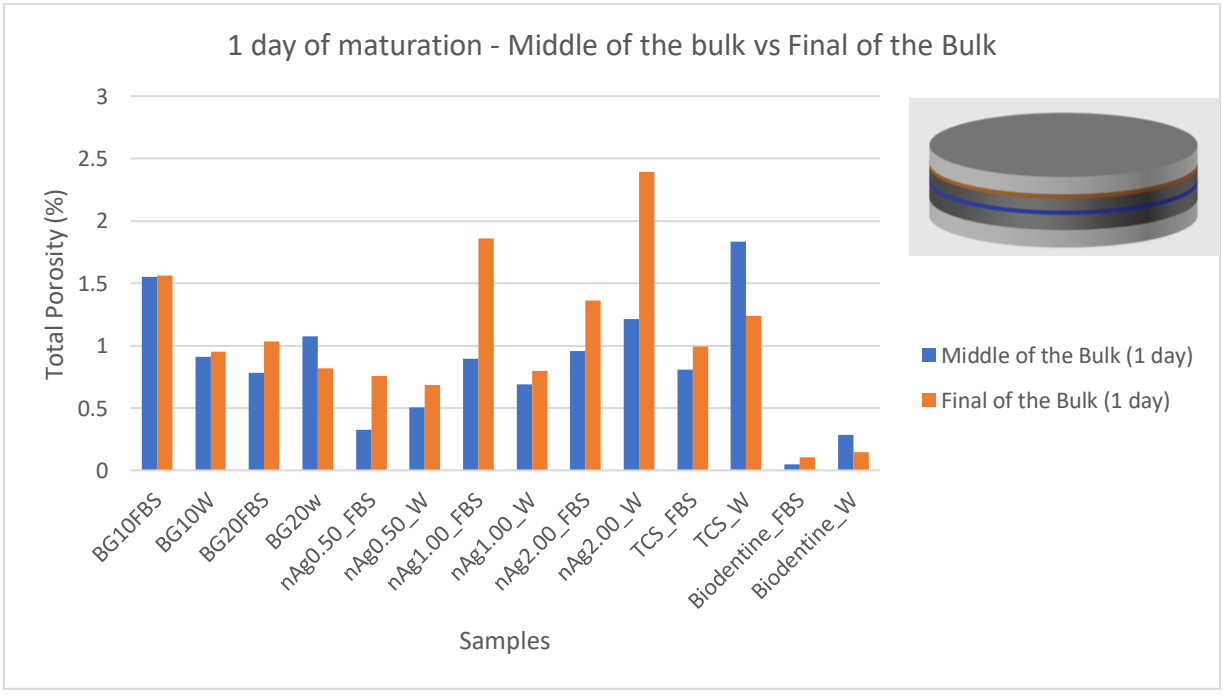

Fig.B-3 – Total porosities obtained on the middle of the bulk and the final of the bulk of every type of samples with 1 day of maturation

Regarding the Fig.30, corresponding to the total porosity of the samples matured in the respective media for seven days, it is possible to notice that there was a sharp decrease in the levels of total porosity in practically all types of samples analyzed, both in the average volumes relative to the middle of the bulks as in the average volumes at the final of bulks of all types of samples analyzed.

At the end of 7 days of maturation, it was already possible to identify a much more regularized inequality between the total porosities in the middle and at the final of the bulks. However, despite both total porosities showing an evident reduction in practically all types of samples compared with the samples immersed for 1 day, it is noticeable that there is a huge difference between the values of total porosity found in both volumes of the bulk in the prototype materials, when compared with the commercial cement (Biodentine). On both volumes, the total porosity identified on the Biodentine in both maturation mediums was below 0.03%, which reveals a truly small number of pores.

This decrease in total porosity, especially in middle of the bulks, reveals that the seven-day maturation period was effective in reducing total porosity, which shows a positive maturation of the materials in both medium used, making them less porous and, subsequently, less likely to incorporate bacterial biofilms which are the main cause of rejection of endodontic cements.

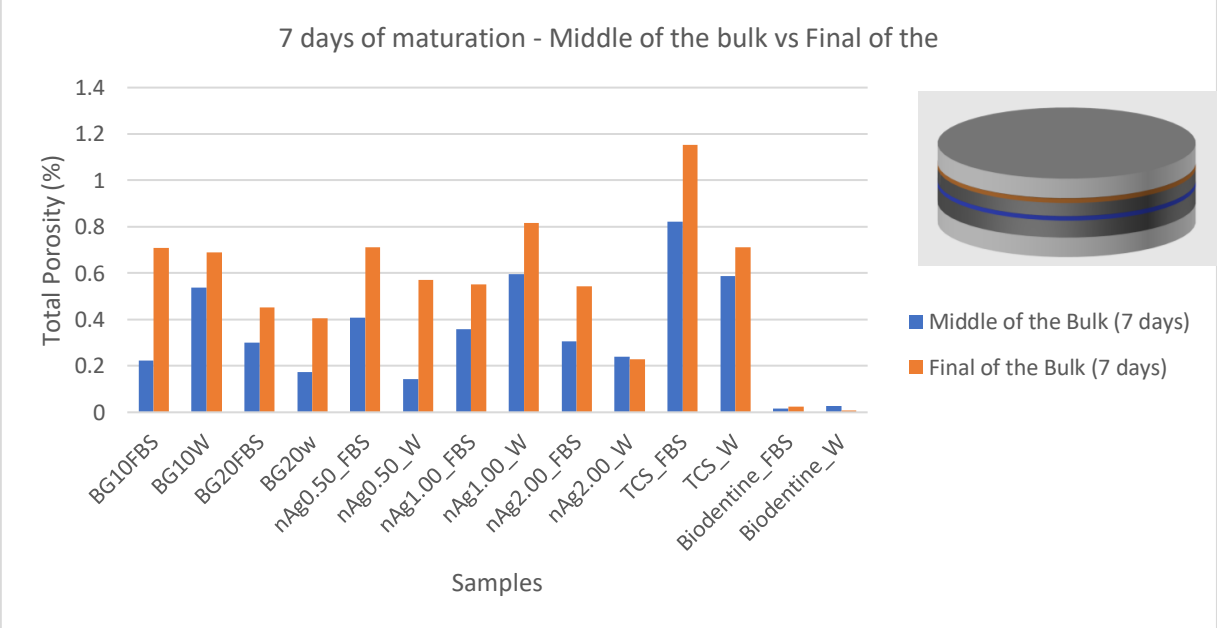

Fig.B-4 – Total porosities obtained on the middle of the bulk and the final of the bulk of every type of samples with 7 days of maturation

In the third and last maturation period, which is related to the samples kept in the respective medium for 28 days, a very high total porosity was expected in the sample types nAg0.50_FBS and nAg0.50_FBS, since these revealed extremely high total porosities in other analyzes referring to surface porosity, porosity at the base of the bulk and bulk porosity in general. This preposition proved to be true, since it is possible to see through the Fig.31 that the mentioned cements present the highest total porosities, both in the middle of the bulk and at the final of the bulk, being also notable the discrepancies between the samples nAg matured in FBS and matured samples mQ water, mainly in volumes relative to the final of the bulk.

The types of samples that include the silver nanoparticles as the main variable, revealed, as already discussed, a very sharp divergence between the different media in which the samples were matured. This divergence is notable in the slice volumes related to the bulks of these types of samples and indicates that samples matured in mQ water show better results in terms of total porosity after 28 days of maturation when compared with the same types of samples matured in FBS. This result is not scientifically favorable, since FBS is a means used to mimic the environment that is found in the oral cavity and, therefore, it would be important and profitable to obtain lower total porosities in samples matured in FBS.

Regarding the types of samples that include Bioglass in their composition, it is possible to conclude that the volume referring to the middle of the bulk have lower values of porosity in the samples that were matured in mQ water, although this difference is not sharp. In the BG10 samples, it is possible to identify that, the same types of samples in different maturation mediums, reveal very similar values of total porosity, showing that the medium used (mQ water or FBS) did not influence the total porosity present on these volumes of the bulk (middle of the bulk and final of the bulk).

In the samples constituted simply by TCS, the total porosities were found to be lower in the volumes corresponding to the middle of the bulk and show lower porosities in both volumes when compared with the TCS samples immersed in mQ water for 7 days. However, this reduction was not accompanied by the total porosities corresponding to the final of the bulks of the TCS samples maturated in mQ water, since they present a higher porosity when compared with the same volume after 7 days of maturation in the same maturation medium.

To conclude, the Biodentine samples revealed a sharp difference between both maturation mediums, however in both of them, the highest porosity can be found in the middle of the bulk. The Biodentine samples immersed in FBS for a period of 28 days, showed an increased value of total porosity when compared with the same type of samples maturated in mQ water. Interestingly, at the end of 28 days, the comparison between all cements analyzed, exhibit that the dental cement immersed in mQ water that showed the lowest porosity both in the middle and in the final of the bulk is the Biodentine, however the nAg0.5_W samples, showed also a really small value of total porosity liable to be compared with the Biodentine behavior on the same maturation medium.

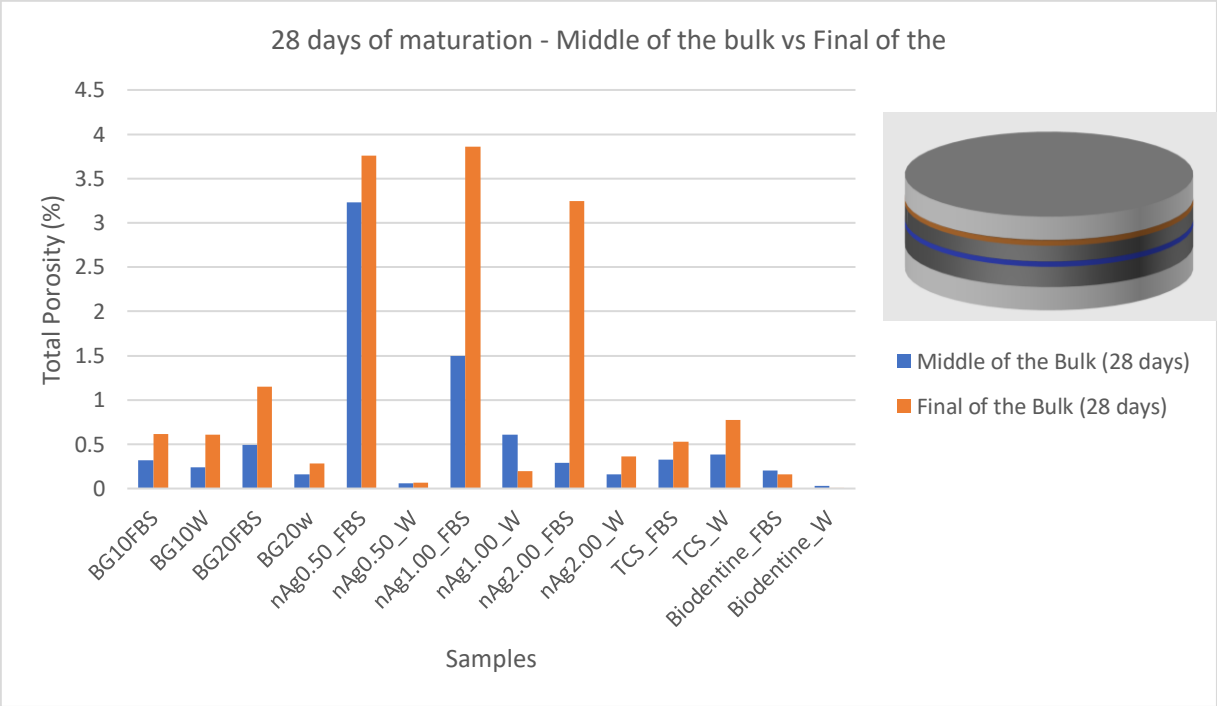

Fig.B-5 – Total porosities obtained on the middle of the bulk and the final of the bulk of every type of samples with 28 days of maturation

Annex C

SPSS - 1 day comparison between first, middle and last 20 slices

Descriptives								
					95% Confidence Interval for Mean		Minimum	Maximum
			Mean	N	Std. Deviation	Std. Error		
						Lower Bound		
						Upper Bound		
Base 20 slices		BG10_FBS	1.053537304	3	0.326245715	0.188358051	0.7737387	1.4118876
		BG10_W	1.24195902	3	0.576681926	0.332947465	0.65727082	1.8102865
		BG20_FBS	1.495277358	3	0.793127064	0.457912124	0.62703663	2.18172503
		BG20_W	0.804911592	3	0.199750802	0.11532618	0.64551654	1.02898812
							1.863976589	0.24309802
							2.67451634	-0.190598299
							3.465514207	-0.474959491
							1.301120093	0.308703091

1.44574139	1.44030947	3.08449063	1.50524896	2.26018614	1.75891734	1.78652623	1.88085278	3.08449063
0.48256155	0.26255919	0.61957755	1.03344571	0.7627048	1.11512213	0.54934687	0.92424159	0.26255919
2.260713679	2.336811352	4.890073126	4.266761725	3.40945612	2.293183647	2.729750855	2.574060965	1.420100316
-0.199424697	-0.593940784	-1.828862813	-1.728067054	-0.321132201	0.658971405	-0.794981206	0.002805123	1.005726961
0.285886235	0.340575027	0.780789941	0.235901629	0.433521894	0.189907523	0.409599877	0.298798904	0.10194968
0.495169484	0.58989325	1.352367847	0.333615282	0.750881947	0.328929478	0.709447798	0.517534884	0.60314244
1.030644491	0.871435284	1.530605156	1.269347336	1.544161959	1.476077526	0.967384824	1.288433044	1.212913639
3	3	3	2	3	3	3	3	35
nAg0.5_FBS	**nAg0.5_W**	**nAg1.0FBS**	**nAg1.0W**	**nAg2.0FBS**	**nAg2.0W**	**TCSFBS**	**TCSW**	**Total**

3.24842807	1.14939169	1.44827467	1.64704733	0.43679212	0.76985534	1.0380711	0.89939602	1.19771875
0.67029444	0.60509242	0.45287408	0.63128853	0.20950389	0.06119101	0.63755946	0.48497574	0.81215506
5.200956502	1.597764734	2.212295297	2.366435638	0.607908352	1.467250237	1.443713525	3.325040348	1.477921968
-2.094017352	0.219191456	-0.642946753	-0.218125822	0.042951698	-0.456129454	0.341928588	-1.940668589	0.437532372
0.847729797	0.160200389	0.331800197	0.300345115	0.065652133	0.223510914	0.128035541	0.207210141	0.120900949
1.46831108	0.277475212	0.5746948	0.520212999	0.113712829	0.387132259	0.221764062	0.293039391	0.209406586
1.553469575	0.908478095	0.784674272	1.074154908	0.325430025	0.505560391	0.892821057	0.69218588	0.95772717
3	3	3	3	3	3	3	2	3
BG10FBS	**BG10W**	**BG20FBS**	**BG20W**	**nAg0.5FBS**	**nAg0.5W**	**nAg1.0FBS**	**nAg1.0W**	**nAg2.0FBS**
Middle 20 Slices								

1.73639665	0.98602802	2.51162708	3.24842807	2.25815627	1.18873373	1.3601974	1.07948579	1.44006589
0.89312779	0.64325662	0.82880267	0.06119101	0.42628824	0.82061554	0.41108859	0.59132451	0.30358415
2.346779684	1.234608345	4.037217792	1.191024688	4.02198618	1.461865129	2.368156317	1.428594589	2.253529791
0.083733922	0.381122203	-0.37138328	0.749514526	-0.901009374	0.44313529	-0.304389996	0.205920796	-0.744046975
0.262982618	0.099181388	0.512311979	0.108626241	0.572088414	0.118383925	0.310569604	0.142083718	0.348340542
0.455499257	0.171787204	0.887350377	0.642641505	0.9908862	0.205046974	0.537922334	0.246096218	0.603343517
1.215256803	0.807865274	1.832917256	0.970269607	1.560488403	0.95250021	1.03188316	0.817257692	0.754741408
3	3	3	35	3	3	3	3	3
nAg2.0W	**TCSFBS**	**TCSW**	**Total**	**BG10FBS**	**BG10W**	**BG20FBS**	**BG20W**	**nAg0.5FBS**
				Final 20 Slices				

1.07198881	3.73993728	0.89475981	2.52773339	4.85194965	1.21184933	2.07289711	4.85194965
0.37072402	0.85120157	0.70201991	0.77505722	1.16082931	0.64669115	0.75439859	0.30358415
1.569612682	5.909929078	2.022886165	3.868628931	7.681289274	1.739403264	3.040529136	1.537913028
-0.202664396	-2.193862131	-0.426106452	-1.142397137	-2.892287144	0.24090216	-0.561746203	0.892566892
0.205951676	0.941720343	0.09636995	0.58231821	1.228727611	0.174136887	0.418610978	0.158776696
0.356718766	1.631107481	0.13628769	1.008604725	2.128218651	0.301613936	0.725055483	0.9393356
0.683474143	1.858033473	0.798389857	1.363115897	2.394501065	0.990152712	1.239391466	1.21523996
3	3	2	3	3	3	3	35
nAg0.5W	**nAg1.0FBS**	**nAg1.0W**	**nAg2.0FBS**	**nAg2.0W**	**TCSFBS**	**TCSW**	**Total**

ANOVA Test – 1 day Comparison between base, middle and final 20 slices

		Sum of Squares	df	Mean Square	F	Sig.
Base 20 Slices	Between Groups	2.311	11	0.21	0.48	0.897
	Within Groups	10.058	23	0.437		
	Total	12.369	34			
Middle 20 Slides	Between Groups	5.728	11	0.521	1.44	0.221
	Within Groups	8.314	23	0.361		
	Total	14.042	34			
Final 20 Slides	Between Groups	8.604	11	0.782	0.841	0.604
	Within Groups	21.396	23	0.93		
	Total	30	34			

Tukey HSDa,b – Base of the bulk (1 day)

Groups of samples	N	Subset for alpha = 0.05
BG20_W	3	0.804911592
nAg0.5_W	3	0.871435284
TCS_FBS	3	0.967384824
nAg0.5_FBS	3	1.030644491
BG10_FBS	3	1.053537304
BG10_W	3	1.24195902
nAg1.0_W	2	1.269347336
TCS_W	3	1.288433044
nAg2.0_W	3	1.476077526
BG20_FBS	3	1.495277358
nAg1.0_FBS	3	1.530605156
nAg2.0_FBS	3	1.544161959
Sig.		0.964

Means for groups in homogeneous subsets are displayed.

a) Uses Harmonic Mean Sample Size = 2.880.

b) The group sizes are unequal. The harmonic mean of the group sizes is used. Type I error levels are not guaranteed.

Tukey HSDa,b – Middle of the bulk (1 day)

Groups of samples	N	Subset for alpha = 0.05
nAg0.5_FBS	3	0.325430025
nAg0.5_W	3	0.505560391
nAg1.0_W	2	0.69218588
BG20_FBS	3	0.784674272
TCS_FBS	3	0.807865274
nAg1.0_FBS	3	0.892821057
BG10_W	3	0.908478095
nAg2.0_FBS	3	0.95772717
BG20_W	3	1.074154908
nAg2.0_W	3	1.215256803
BG10_FBS	3	1.553469575
TCS_W	3	1.832917256
Sig.		0.169

Means for groups in homogeneous subsets are displayed.

a) Uses Harmonic Mean Sample Size = 2.880.

b) The group sizes are unequal. The harmonic mean of the group sizes is used. Type I error levels are not guaranteed.

Tukey HSDa,b – Final of the bulk (1 day)

Groups of samples	N	Subset for alpha = 0.05
nAg0.5_W	3	0.683474143
nAg0.5_FBS	3	0.754741408
nAg1.0_W	2	0.798389857
BG20_W	3	0.817257692
BG10_W	3	0.95250021
TCS_FBS	3	0.990152712
BG20_FBS	3	1.03188316
TCS_W	3	1.239391466
nAg2.0_FBS	3	1.363115897
BG10_FBS	3	1.560488403
nAg1.0_FBS	3	1.858033473

nAg2.0W	3	2.394501065
Sig.		0.61

Means for groups in homogeneous subsets are displayed.

a) Uses Harmonic Mean Sample Size = 2.880.
b) The group sizes are unequal. The harmonic mean of the group sizes is used. Type I error levels are not guaranteed.